UNIVERSIDAD COMPLUTENSE DE MADRID

FACULTAD DE FARMACIA

TESIS DOCTORAL

Función de C3G en la regulación del crecimiento y progresión tumoral en hepatocarcinoma. Implicación en la ruta de señalización de HGF/Met.
Role of C3G in the regulation of tumor growth and progression in hepatocarcinoma. Implication in HGF/Met signaling pathway.

MEMORIA PARA OPTAR AL GRADO DE DOCTOR

PRESENTADA POR

Celia Sequera Hurtado

DIRECTOR

Almudena Porras Gallo

UNIVERSIDAD COMPLUTENSE DE MADRID
FACULTAD DE FARMACIA
DEPARTAMENTO DE BIOQUÍMICA Y BIOLOGÍA MOLECULAR

TESIS DOCTORAL

Función de C3G en la regulación del crecimiento y progresión tumoral en hepatocarcinoma. Implicación en la ruta de señalización de HGF/Met.

Role of C3G in the regulation of tumor growth and progression in hepatocarcinoma. Implication in HGF/Met signaling pathway.

MEMORIA PARA OPTAR AL GRADO DE DOCTOR
PRESENTADA POR
Celia Sequera Hurtado

Directora
Almudena Porras Gallo

Madrid 2020

UNIVERSIDAD COMPLUTENSE DE MADRID
FACULTAD DE FARMACIA
DEPARTAMENTO DE BIOQUÍMICA Y BIOLOGÍA MOLECULAR

TESIS DOCTORAL

Función de C3G en la regulación del crecimiento y progresión tumoral en hepatocarcinoma. Implicación en la ruta de señalización de HGF/Met.

Role of C3G in the regulation of tumor growth and progression in hepatocarcinoma. Implication in HGF/Met signaling pathway.

MEMORIA PARA OPTAR AL GRADO DE DOCTOR
PRESENTADA POR
Celia Sequera Hurtado

Directora
Almudena Porras Gallo

Madrid 2020

UNIVERSIDAD COMPLUTENSE DE MADRID
FACULTAD DE FARMACIA
DEPARTAMENTO DE BIOQUÍMICA Y BIOLOGÍA MOLECULAR

El presente trabajo ha sido realizado en el Departamento de Bioquímica y Biología Molecular de la Facultad de Farmacia de la Universidad Complutense de Madrid, bajo la dirección de la **Dra. Almudena Porras Gallo.**

Este trabajo ha sido posible gracias a la financiación de la Universidad Complutense de Madrid mediante la concesión de una beca pre-doctoral UCM para realizar la Tesis doctoral. Asimismo, el trabajo ha sido financiado a través de proyectos del Ministerio de Ciencia e Innovación SAF-2013-48210-C2-2-R y SAF2016-76588-C2-1-R. Además, la estancia breve de 3 meses en un laboratorio extranjero ha sido posible gracias a la "Short-Term Fellowship" otorgada por la FEBS.

OPTA AL GRADO DE DOCTOR CON MENCIÓN INTERNACIONAL:

Celia Sequera Hurtado

AGRADECIMIENTOS

Sin duda es una tarea casi imposible el intentar reflejar en tan sólo una página, agradecimientos y menciones a todas las personas que de una manera u otra han contribuido a que la escritura de esta tesis sea posible. Pero intentaré ser breve.

Empezaré dándole las gracias a mi directora de tesis, Almudena Porras, por todos estos años guiándome y ayudándome a construir mi carrera científica desde la primera piedra. Porque hay que decir que cuando entré en el lab. 15 en mi último año de Farmacia yo no sabía ni que era eso de C3G, y ahora van para ocho años… Pero también, quisiera agradecer a Almudena por su paciencia (porque no todos los días son fáciles), por ser una persona que trabaja tan duro y por su dedicación, que son todo una inspiración.

A continuación, le doy las gracias a toda la gente del lab. 15, pasadas (Dani, Neibla, Ana, y a María A. muchas gracias por tu ayuda allí dónde te encuentro) y presentes (Nere, Cris, Sara y Noelia). Gracias por todos los ratos que hemos pasado juntas, por todas las horas de poyata y cultivos, por compartir risas (discretas)… Me ha encantado estar ahí con vosotras en el labo, en conciertos, en el ballet, en el teatro, en restaurantes…

Por supuesto, gracias a las chicas de enfrente (Annalisa, Laura, Nerea L., María G.), por ser como un segundo laboratorio para nosotras a lo largo de todos estos años.

Gracias a todo el personal y profesores del departamento porque todos han ayudado en su medida a este trabajo. Gracias Arancha, Blanca, Pilar, César, Marga, Mª Jesús O., Óscar, Carlos, Almudena G., Fernando, Carmen A., Elisa… espero que no se me olvide nadie, y gracias a las nuevas incorporaciones en especial a Álvaro y Paloma por su *feedback* y por estar siempre dispuestos a ayudar. Y gracias a todos los compañeros del departamento, al lab.21…

Gracias a nuestros colaboradores en especial en España a Carmen Guerrero por su ayuda estos años, y en Francia, a Flavio Maina por abrirme las puertas de su laboratorio.

Por último, no quiero olvidarme de agradecer a mi familia y sobre todo a mis padres, por animarme y por estar ahí en los días buenos y en los malos también.

GRACIAS A TODOS.

INDEX

1. ABSTRACT

Role of C3G in the regulation of tumor growth and progression in hepatocarcinoma. Implication in HGF/Met signaling pathway.

Introduction

Hepatocarcinoma (HCC) is the most common liver cancer and the fourth in cancer-related mortality worldwide. HCC is characterized by a very heterogeneous pattern between patients that complicates its classification for prognosis and/or therapy purposes. HCC is initiated in livers predisposed by diverse determinants such as chronic inflammation, cirrhosis, hepatitis B or C virus, alcohol intake and non-alcoholic liver diseases, which frequently acquire a first mutation in the TERT promoter, and then, accumulate a series of genetic alterations progressing from early to advanced HCC, leading to lung metastasis, prevalently. EMT (epithelial-mesenchymal transition) enables epithelial cells to acquire pro-migratory and pro-invasive properties, which is necessary for driving carcinoma cells towards a metastatic phenotype.

As in other cancers, in HCC, the tumor microenvironment is also relevant for its development, which is comprised by myofibroblast, cancer-associated fibroblasts, hepatic stellate cells, immune system cells and other cell types that secrete several factors and cytokines. Thus, establishing a bidirectional communication between stroma and tumor cells that contributes to tumor growth and/or metastasis generation.

C3G is a guanine nucleotide exchange factor (GEF) for some members of the Ras superfamily of small GTPases, mainly Rap1 and R-Ras. However, it can act either dependently or independently of Rap1 activation, thanks to the presence in its structure of a proline rich domain that can bind to the SH3 domain of other proteins (Crk, Src, p130Cas…) and an E-cadherin-binding domain, in addition to its GEF catalytic domain. C3G is essential for embryonic development and is implicated in many biological functions, such as cell motility, adhesion, vesicle trafficking, cell death and survival, differentiation and platelet function. More recently, other functions of C3G related to its nuclear localization has been discovered.

The function of C3G in cancer is controversial as it can act as either a tumor suppressor (e.g. in breast cancer and cervical squamous carcinoma) or a tumor promoter (e.g. in chronic myeloid leukemia and non-small cell lung cancer) or both (e.g. in colorectal cancer). However, there are no data available in the literature about the role of C3G in HCC. There are just a few data about a potential function of Rap1 and Rap2, but they are controversial.

Met is a tyrosine kinase receptor for HGF, which is relevant in liver tumorigenesis, tumor progression and metastasis. In fact, Met is frequently overexpressed in HCC patients, being a marker of poor prognosis. According to a few data available from the literature, C3G has been involved in HGF/Met signaling pathway, but not in HCC cells.

Taking into account the above mentioned information, it is conceivable that C3G could play a role in HCC.

Aims

General Aim:

The main objective of this research project is to analyze the role played by C3G in HCC tumor growth, progression, dissemination and generation of metastasis using different human and mouse models to identify the mechanisms involved.

Specific Aims:

1. To determine whether C3G (RapGEF1) expression is altered in human and mouse HCC tumors and cell lines, as well as to identify the existence of potential genetic alterations in this gene.

2. To analyze the function of C3G, *in vitro* and *in vivo*, using human and mouse HCC cell lines and mouse models, characterizing its role in the regulation of the tumorigenic, migratory and invasive capacities of HCC cells.

3. To identify the molecular mechanisms involved in the actions of C3G in HCC.

Results

Using information from public databases, we found that C3G mRNA expression was higher in tumor samples from HCC patients as compared to control healthy livers. In agreement with this, C3G protein levels increased in human HCC cell lines and in two models of mouse HCC, induced by either DEN-treatment or Met overexpression in hepatocytes. Further analyses taking into account tumor stage and survival revealed that high C3G mRNA levels were positively correlated with HCC progression and poor prognosis. Moreover, several mutations identified in C3G gene correlated with lower survival in HCC patients.

To determine *in vitro* and *in vivo* the function of C3G in HCC cells, a permanent C3G knock-down in human (Hep3B and HLE) and mouse (mHCC1) HCC cell lines was performed, using these cells for functional assays. We discovered that C3G down-regulation decreased the pro-tumorigenic properties, according to anchorage dependent- and independent-growth assays. Moreover, foci generated by C3G silenced cells presented less cells, which displayed a more scattered phenotype. Additional assays revealed that non-silenced HCC cells showed a higher adhesion and survival under non-adherent conditions as compared to C3G silenced cells. Furthermore, in C3G silenced cells the pro-migratory and –invasive properties are enhanced, as shown by wound healing and invasion assays, respectively. To elucidate if the increased motility was due to the induction of an EMT-like process, we used TGF-β1 treatment as a positive control. In this way, we uncovered that C3G silenced

cells expressed high levels of mesenchymal markers, similar to those elicited by TGF-β1 treatment in non-silenced cells. However, the mechanism used by C3G to regulate this EMT-like process might be, at least, partially independent of TGF-β1, as the inhibition of its receptor had only a very limited effect reducing migration of C3G silenced HCC cells. Additionally, p38 MAPK activation could play a role as it is highly activated in C3G silenced HCC cells and its inhibition decreases migration.

Heterotopic xenografts generated by Hep3B cells with and without C3G silencing in nude mice also indicated that down-regulation of C3G decreased *in vivo* tumor growth by increasing apoptosis and reducing proliferation of HCC cells. Moreover, in tumors generated by non-silenced cells we detected more myo-fibroblasts and a higher expression of mouse HGF, TGF-β1 and IL6 mRNAs, not reaching statistically significance. This suggests a potential contribution of the tumor microenvironment to tumor growth. Moreover, a higher number of disseminated tumor cells were found in the bone marrow of mice with tumors generated by C3G knock-down HCC cells.

Next, heterotopic xenograft assays were performed with the mHCC cell lines (overexpressing Met) to generate lung metastasis. It was found that mice injected with mHCC cells expressing initially the lowest levels of C3G presented a higher frequency of lung metastasis, being macro- and micro-metastases of a bigger size. However, western-blot analysis revealed higher C3G protein levels in the lung metastases as compared to the primary tumor, in agreement with the increase in C3G mRNA levels found in public databases for HCC patients with lung metastasis. This suggests that C3G might also be necessary for the growth of lung metastasis.

Finally, as we found that C3G silencing decreased *in vitro* tumor growth of mHCC cells overexpressing Met, we evaluated the potential implication of C3G in HGF/Met signaling pathway in HCC cells. We detected that phosphorylation of Met and Gab1 in response to HGF was highly reduced in C3G silenced Hep3B cells, indicating a defective activation of HGF/Met signaling, corroborated by the reduced activation of downstream pathways (Abl, ERKs, p38 MAPK, etc). Moreover, immunoprecipitation and pull-down assays showed an interaction between activated Met, Gab1 and C3G that was independent of CrkL, and hence might be mediated by other potential adaptors. Abl and/or E-cadherin could facilitate Met activation.

Conclusions

1. C3G protein levels are increased in human and mouse HCC cell lines and in mouse liver tumors as compared to normal liver and adult hepatocytes, reaching similar levels to those expressed by liver progenitor cells and immature hepatocytes.

2. *C3G (RapGEF1)* mRNA levels are directly correlated with HCC progression, while inversely associated to patient survival according to public databases. Therefore, C3G can be proposed as a new potential prognostic biomarker for HCC patients.

3. *RapGEF1* mutations and other genetic alterations, such as deletions or amplifications are correlated with poor HCC patient survival, according to public genomic databases.

4. C3G enhances *in vitro* and *in vivo* tumor growth of HCC cells, through increasing proliferation, survival and cell adhesion.

5. C3G down-regulation enhances migration and invasion of HCC cells by promoting an EMT-like process, mimicking TGF-β-induced EMT. p38 MAPK contributes to the increased migration induced by C3G down-regulation.

6. C3G expression in HCC cells promotes the presence of active fibroblasts in HCC tumor stroma, favoring the expression of pro-tumorigenic and survival signals.

7. The expression of low levels of C3G in HCC cells favors their dissemination to bone marrow and the generation of lung metastasis.

8. C3G protein levels increases in lung metastatic samples generated by HCC xenograft tumors.

9. C3G is required for a full activation of Met receptor by HGF, as well as its downstream signaling pathways in HCC cells.

10. In response to HGF, C3G interacts with P-Met and Gab1 in HCC cells, independently of CrkL adaptor. Moreover, C3G proline rich domain binds to P-Gab1 and P-Met through a mechanism not mediated by CrkL.

In summary, C3G is a new key player in HCC that promotes tumor growth and progression and might be considered as a new potential bad prognosis biomarker for HCC patients.

2. RESUMEN

Función de C3G en la regulación del crecimiento y progresión tumoral en hepatocarcinoma. Implicación en la ruta de señalización de HGF/Met.

Introducción

El hepatocarcinoma (HCC) es el cáncer de hígado más común, y el cuarto en mortalidad dentro del conjunto de muertes relacionadas con cáncer. El HCC se caracteriza por un patrón muy heterogéneo entre pacientes que complica su clasificación de cara al pronóstico y/o tratamiento. El HCC se inicia en hígados predispuestos por diversos determinantes como la inflamación crónica, cirrosis, virus de la hepatitis B o C, consumo de alcohol y enfermedades no ligadas al alcohol, que frecuentemente dan lugar a la adquisición de una primera mutación en el promotor de TERT, y luego, se acumulan una serie de alteraciones genéticas progresando desde HCC temprano a avanzado, dando lugar a metástasis de pulmón, prevalentemente. La EMT (transición epitelio-mesénquima) permite a las células epiteliales adquirir propiedades pro-migratorias y pro-invasivas, que son necesarias para conducir a las células de carcinoma hacia un fenotipo metastásico.

Como en otros cánceres, en el HCC, el microambiente tumoral también es relevante para su desarrollo, el cual, está formado por miofibroblastos, fibroblastos asociados al cáncer, células hepáticas estrelladas, células del sistema inmunitario y otros tipos de células que secretan varios factores y citoquinas. Esto permite establecer una comunicación bidireccional entre el estroma y las células tumorales, que contribuye al crecimiento tumoral y/o a la generación de metástasis.

C3G es un factor que activa el intercambio de nucleótidos de guanina (GEF) de las GTPasas monoméricas de la superfamilia Ras, principalmente Rap1 y R-Ras. Sin embargo, puede actuar de forma dependiente o independiente de la activación de Rap1, gracias a la presencia en su estructura de un dominio rico en prolinas que puede unirse a dominios SH3 de otras proteínas (Crk, Src, p130Cas…) y un dominio de unión de E-cadherina, además de su dominio catalítico GEF. C3G es esencial para el desarrollo embrionario y está implicado en muchas funciones biológicas como motilidad, adhesión, tráfico de vesículas, muerte celular y supervivencia, diferenciación y función plaquetaria. Más recientemente, se han descubierto otras funciones de C3G relacionadas con su localización nuclear.

La función de C3G en cáncer es controvertida y puede actuar tanto como supresor tumoral (por ej. en cáncer de mama y carcinoma escamoso de cérvix), como promotor tumoral (por ej. en leucemia crónica mieloide y cáncer pulmonar de células no pequeñas) o ambos (por ej. en cáncer colorrectal). Sin embargo, no hay datos disponibles en la literatura sobre el papel de C3G en HCC. Sólo hay algunos datos sobre la función potencial de Rap1 y Rap2, pero son controvertidos.

Met es un receptor tirosina quinasa para HGF, que es relevante en la tumorigénesis, progresión tumoral y metástasis del hígado. De hecho, Met está frecuentemente sobre-expresado en pacientes de HCC, siendo un marcador de mal pronóstico. Algunos datos disponibles en la literatura, señalan la implicación de C3G en la vía de señalización HGF/Met, pero en ningún caso, en células de HCC.

Teniendo en cuenta la información mencionada anteriormente, es concebible que C3G pueda jugar un papel en el HCC.

Objetivos

Objetivo General:

El principal objetivo de este proyecto de investigación es analizar el papel que juega C3G en el crecimiento, progresión, diseminación y generación de metástasis en el hepatocarcinoma, usando diferentes modelos humanos y murinos para identificar los mecanismos implicados.

Objetivos específicos:

1. Determinar si la expresión de C3G (RapGEF1) se altera en tumores y líneas celulares de HCC humanas y murinas, así como identificar la potencial existencia de alteraciones genéticas en este gen.

2. Analizar la función de C3G, *in vitro* e *in vivo*, usando líneas celulares de HCC humanas y murinas, caracterizando su papel en la regulación de la capacidad tumorigénica, migratoria e invasiva de las células de HCC.

3. Identificar los mecanismos moleculares implicados en las acciones de C3G en HCC.

Resultados

Usando información de bases de datos públicas, hemos encontrado que la expresión del RNAm de C3G era más elevada en las muestras de tumores de pacientes de HCC en comparación con los hígados sanos control. De acuerdo con esto, los niveles proteicos de C3G aumentaban en las líneas celulares humanas de HCC y en dos modelos murinos de HCC, inducidos por tratamiento con DEN o por la sobreexpresión de Met en hepatocitos. Análisis más extensos teniendo en cuenta el estadio del tumor y la supervivencia, revelaron que altos niveles del RNAm de C3G se correlacionaban positivamente con la progresión del HCC y mal pronóstico. Además, se han identificado varias mutaciones en el gen de C3G que se correlacionan con una menor supervivencia en pacientes de HCC.

Para determinar *in vitro* e *in vivo* la función de C3G en células de HCC, se realizó un silenciamiento estable de C3G en líneas celulares de HCC humanas (Hep3B y HLE) y de

ratón (mHCC1), usando estas células para ensayos funcionales. Descubrimos que el silenciamiento de C3G disminuía las propiedades pro-tumorigénicas, de acuerdo a los ensayos de crecimiento dependiente e independiente de anclaje. Además, los focos generados por las células con silenciamiento de C3G presentaban menos células, las cuáles, exhibían un fenotipo más disperso. Ensayos adicionales, revelaron que las células no silenciadas de HCC mostraban una mayor adhesión y supervivencia en condiciones no adherentes en comparación con las células con silenciamiento de C3G. Además, en estas células con bajos niveles de C3G estaban aumentadas las propiedades pro-migratorias y pro-invasivas, como muestran los ensayos de cierre de herida e invasión, respectivamente. Para saber si el aumento de motilidad era debido a la inducción de un proceso de EMT, utilizamos el tratamiento con TGF-β1 como control positivo. De esta manera, descubrimos que las células con silenciamiento de C3G expresaban altos niveles de marcadores mesenquimales, similares a los inducidos por el tratamiento con TGF-β1 en las células no silenciadas. Sin embargo, los mecanismos utilizados por C3G para regular este proceso de tipo EMT podrían ser, al menos parcialmente, independientes de TGF-β1, ya que la inhibición de su receptor sólo tuvo un efecto muy limitado reduciendo la migración en las células de HCC con silenciamiento de C3G. Adicionalmente, la activación de p38 MAPK podría jugar un papel, ya que está altamente activada en células de HCC con silenciamiento de C3G y su inhibición disminuye la migración.

Los xenotransplantes heterotópicos generados por las células Hep3B con y sin silenciamiento de C3G en ratones desnudos también indicaron que la disminución en los niveles de C3G reducía el crecimiento tumoral *in vivo*, gracias al incremento de la apoptosis y a la disminución de la proliferación de las células de HCC. Además, en los tumores generados por las células no silenciadas detectamos más miofibroblastos y una mayor expresión de los RNAm murinos de HGF, TGF-β1 e IL6, no alcanzando significación estadística. Esto sugiere una potencial contribución del microambiente tumoral al crecimiento del tumor. Además, se encontró un mayor número de células tumorales diseminadas en la médula ósea en los ratones con tumores generados por las células de HCC con silenciamiento de C3G.

A continuación, se llevaron a cabo ensayos de xenotransplante con las líneas celulares mHCC (que sobreexpresan Met) para generar metástasis en pulmón. Encontramos que los ratones inyectados con la línea celular que expresaba inicialmente los niveles más bajos de C3G presentaban una mayor frecuencia de metástasis pulmonar, siendo las macro- y micro-metástasis de mayor tamaño. Sin embargo, el análisis por western-blot reveló que los niveles proteicos de C3G eran mayores en las metástasis de pulmón que en el tumor primario, en concordancia con el incremento de los niveles de RNAm de C3G de los pacientes de HCC con metástasis en pulmón encontrado en las bases de datos públicas. Esto sugiere que C3G también podría ser necesario para el crecimiento de las metástasis de pulmón.

Finalmente, dado que encontramos que el silenciamiento de C3G disminuía el crecimiento tumoral *in vitro* de las células mHCC que sobreexpresan Met, evaluamos la

potencial implicación de C3G en la ruta de señalización HGF/Met en las células de HCC. Detectamos que la fosforilación de Met y Gab1 en respuesta a HGF se reducía mucho en las células Hep3B con silenciamiento de C3G, indicando una activación defectiva de la ruta de señalización de HGF/Met, corroborado por la reducción en la activación de vías activadas por Met (Abl, ERKs, p38MAPK, etc.). Además, los ensayos de inmunoprecipitación y *pull-down* mostraron la existencia de una interacción entre Met activado, Gab1 y C3G, que era independiente de CrkL y, por tanto, podría ser mediada por otros posibles adaptadores. Abl y/o E-cadherina podrían facilitar la activación de Met.

Conclusiones

1. Los niveles proteicos de C3G están aumentados en líneas celulares de HCC humanas y murinas, y en tumores hepáticos de ratón en comparación con el hígado normal y los hepatocitos adultos, alcanzando niveles similares a los que presentan las células progenitoras hepáticas y los hepatocitos inmaduros.

2. Los niveles de RNAm de C3G (*RapGEF1*) se correlacionan directamente con la progresión del HCC e inversamente con la supervivencia de los pacientes, de acuerdo con las bases de datos públicas. Por tanto, C3G puede proponerse como un nuevo potencial biomarcador de pronóstico para pacientes de HCC.

3. Las mutaciones y otras alteraciones genéticas de *RapGEF1,* como deleciones o amplificaciones, se correlacionan con una menor supervivencia en los pacientes con HCC, de acuerdo con las bases de datos genómicas públicas.

4. C3G aumenta el crecimiento tumoral de las células de HCC *in vitro* e *in vivo* a través del incremento de la proliferación, supervivencia y adhesión celular.

5. La disminución de los niveles de C3G incrementa la migración e invasión de las células de HCC promoviendo un proceso de tipo EMT, semejante a la EMT inducida por TGF-β. p38 MAPK contribuye al aumento de la migración inducida por la disminución de los niveles de C3G.

6. La expresión de C3G en las células de HCC promueve la presencia de fibroblastos activados en el estroma tumoral del HCC, favoreciendo la expresión de señales pro-tumorigénicas y de supervivencia.

7. La expresión de bajos niveles de C3G en células de HCC favorece su diseminación a médula ósea y la generación de metástasis en pulmón.

8. Los niveles proteicos de C3G aumentan en las muestras de metástasis de pulmón generadas por los tumores de HCC de los xenotransplantes.

9. C3G se requiere para una completa activación del receptor Met por HGF, así como las rutas de señalización que éste activa en HCC.

10. En respuesta al HGF, C3G interacciona con P-Met y Gab1 en células de HCC, independientemente del adaptador CrkL. Además, el dominio rico en prolinas de C3G se une a P-Gab1 y P-Met a través de un mecanismo no mediado por CrkL.

En resumen, C3G es una nueva pieza clave en HCC que promueve el crecimiento y progresión tumoral, que podría considerarse como un nuevo potencial biomarcador de mal pronóstico en pacientes de HCC.

3. ABBREVIATIONS

α-SMA	Alfa-Smooth Muscle Actin
AA2	Adeno-associated virus 2
Abl	Abelson murine leukemia viral oncogene homolog (mammal)
ACRG	Asian Cancer Research Group
ADAMs	α-disintegrin and metalloproteinase
ADAMTS	α-disintegrin and metalloproteinase with thrombospondin motifs
AFP	Alpha-fetoprotein
AJCC	American Joint Committee on Cancer
AJs	Adherent Junctions
AKT	Akt strain Transforming
ALB	Albumin
AMC	Asian Medical Centre
ANOVA	Analysis of Variance
APES	3-(Aminopropyl)triethoxysilane
ATCC	American Type Culture Collection
AXIN1	Axis Inhition Protein 1
BCA	Bicinchoninin Acid
BCLC	Barcelona Clinic Liver Cancer
BM	Bone Marrow
BMDTCs	Bone Marrow Disseminated Tumor Cells
bp	base pair
BSA	Bovine Serum Albumin
C3G	Crk SH3-domain-binding guanine-nucleotide-releasing factor
CAFs	Cancer-associated fibroblasts
c-CBL	Casitas lineage lymphoma
CBP	CREB-binding protein
CCND1	Cyclin D1 gene
Cdc25H	Cell division cycle 25 homolog
cDNA	Complementary DNA
CML	Chronic Myeloid Leukemia
CO_2	Carbone Dioxide
CRC	Colorectal Carcinoma
CRK	v-crk sarcoma virus CT10 oncogene homolog
CSCs	Cancer Stem Cells
Ct	Cycle Threshold
CYP	Cytochrome
DAB	3, 3 -diaminobenzidine
DAPI	4’,6-diamidino-2-phenylindole
DEN	Diethylnitrosamine
DMEM	Dulbecco's Modified Eagle Medium
DMSO	Dimethyl Sulfoxide
DNA	Deoxyribonucleic acid
DNase	Deoxyribonuclease
dNTPs	Deoxynucleotide Triphosphates
DOCK180	Dedicator of Citokinesis 180

DPX	Dibutylphthalate Polystyrene Xylene
DTCs	Disseminated Tumor Cells
DTT	Dithiothreitol
ECM	Extracellular Matrix
ECOG	Eastern Cooperative Oncology Group
EDTA	Ethylenediaminetetraacetic Acid
EGF	Epidermic Growth Factor
EGTA	Ethylene Glycol-bis (β-aminoethylether)-N, N, N',N'-Tetraacetic Acid
EHM	Extrahepatic Metastasis
EMT	Epithelial to Mesenchymal Transition
EPCAM	Epithelial Cell Adhesion Molecule
ERKs	Extracellular Signal Regulated Kinases
EtOH	Ethanol
FAK	Focal Adhesion Kinase
FBS	Foetal Bovine Serum
FITC	Fluorescein-5-isothiocyanate
Foxo	Forkhead box protein O1
FPKM	Fragments per kilobase of transcript per million mapped read
Gab	Grb2-assossiated-binder
GATA-1	GATA-binding protein 1 (Globin transcription factor-1)
GCO	Global Cancer Observatory
GEF	Guanine Nucleotide Exchange Factor
GLUT4	Glucose transporter type 4
Grb2	Growth Factor Receptor-bound Protein 2
GST	Glutathione S-Transferase
GTEX	Genotype-Tissue Expression
GTPases	Guanosine Triphosphate Hydrolases
GUSB	Glucuronidase-β
H&E	Hematoxylin and Eosin
HBV	Hepatitis B Virus
HCA	Hepatocellular Adenoma
HCC	Hepatocellular carcinoma, Hepatocarcinoma
Hck	Hemopoietic cell kinase
HCV	Hepatitis C Virus
HEIH	Hepatocellular carcinoma up-regulated EZH2-associated long non-coding RNA
HEK293	Human Embrionary Kidney cells
Hep-A	Adult Hepatocyte
HEPES	4-(2-hydroxyethyl)-1-piperazineethanesulfonic acid
Hep-N	Neonatal Hepatocyte
HGF	Hepatocyte Growth Factor
HIF1α	Hypoxia-inducible factor 1 alpha
HOTAIR	HOX Transcript Antisense RNA
HPCs	Hepatic Progenitor Cells
HSC	Hepatic Stellate Cells
HULC	Hepatocellular Carcinoma Up-Regulated Long Non-Coding RNA
IARC	International Agency for Research on Cancer

IFNϒ	Inteferon ϒ
IGF2	Insulin Growth Factor 2
IHC	Immunohistochemical
IL	Interleukin
IP	Immunoprecipitation
IPT	Immunoglobulin-plexin-transcription
IPTG	Isopropil-β1-D1-thiogalactopiranoside
IRS1	Insulin receptor substrate 1
JAM	Junctional adhesion molecules
JCRB	Japanese Collection of Research Bioresources Cell Bank
JNK	c-Jun N-terminal Kinases
kDa	kilo Daltons
KLF8	Kruppel Like Factor 8
LEF	Lymphoid enhancer factor
LncRNA	Long non-coding RNA
MAGUK	Membrane-associated guanylate kinase
MAPK	Mitogen-Activated Protein Kinase
MBS	Met-binding site
MEFs	Mouse embryonic fibroblasts
MeOH	Methanol
Met	Met Tyrosin Receptor
MET	Mesemchymal-Epithelial Transition
mHCC	Mouse Hepatocarcinoma
MMPs	Metalloproteinases
mRNA	Messenger Ribonucleotic Acid
mTOR	Mammalian Target of Rapamycin
MVIH	Long non-coding RNA
MYC	V-Myc Avian Myelocytomatosis Viral Oncogene Homolog
NAFLD	Non-alcoholic fatty liver disease
NASH	Non-alcoholic Steatohepatitis
NGF	Neural Growth Factor
NP-40	Nonidet-40
NPCs	Non-parenchymal cells
NSCL	Non-Small Cell Lung Cancer
NTCs	No Template Controls
Oval-C	Oval cells
p130Cas	Crk-associated substrate p130Cas
PBS	Phosphate Buffered Saline
PCR	Polymerase Chain Reaction
PDGF	Platelet-derived Growth factor
PDXs	Patient Derived Xenografts
PFA	Paraformaldehyde
P-Gab1	Phosphorylated Gab1
PH	Pleckstrin homology
PI	Propidium Iodide
PI3K	Phosphatidylinositol 3-kinase
PKA	Protein Kinase A

PKC	Protein Kinase C
PLC	Phospholipase C
P-Met	Phosphorylated Met
PMSF	Phenylmethanesulfonylfluoride
Pro	Proline
PS	Performance Status
PSI	Plexin-semaphorin-integrin
PTB	Phosphotyrosine-binding domain
PTPB1	Protein Tyrosine Phosphatase B1
Rac	Ras-Related C3 botulinum toxin
Rap1	Ras-related protein 1
Ras	Rat Sarcoma virus
REM	Ras Exchange Motif
REX	ZFP42 Zinc Finger Protein
RhoA	Ras Homolog A
ROS	Reactive Oxygen Species
RPKM	Reads Per Kilobase Per Million
RPMI	Roswell Park Memorial Institute medium
RQ	Relative Quantification
RSEM	Accurate transcript quantification for RNA-Seq data
RT	Room Temperature
RTK	Receptor Tyrosine Kinase
RT-qPCR	Reverse transcription- quantitative polymerase chain reaction
S.E.M	Standard Error of the Mean
SDS	Sodium Dodecyl Sulphate
SDS-PAGE	SDS-Polyacrylamide gel electrophoresis
Ser	Serine
SF	Scatter Factor
SH2	Src Homology 2
SH3	Src Homology 3
SH3-b	Src Homology 3-binding
Shp2	Src homology -2(SH2)-containing protein tyrosine phosphatase 2
shRNA	Short hairpin RNA
Sos	Son of Sevenless
STAT3	Signal Transducer and activator of Transcription 3
TACE	Transcatheter arterial chemoembolization
TAMs	Tumor-associated macrophages
TBP	TATA-binding protein
TCF	T-cell factor
TCF4	Transcription factor 4
TCGA	The Cancer Genome Altlas
TECs	Tumor-associated endothelial cells
TEMED	Tetramethylethylenediamine
TERT	Telomerase Reverse Transcriptase
TERTp	Telomerase Reverse Transcriptase promoter
TGFβ	Tumor Growth Factor β
TIMPs	Tissue inhibitors of metalloproteinases

TJs	Tigh Junctions
TME	Tumor microenvironment
TNF-α	Tumor Necrosis Factor α
TNM	Tumor, Nodes, Metastasis
TP53	Tumoral Protein 53
TPM	Transcript Per Million
Tris	2-Amino-2-(hydroxymethyl)-1,3-propanediol
TRP	Translocated promoter region
TTBS	Tween-Tris-buffered saline
Tyr	Tyrosine
VEGF-A/C/D	Vascular Endothelial Growth Factor type A/C/D
WHO	World Health Organization
WNT	Wingless-related integration site
ZEB 1/2	Zinc finger E-box binding homeobox 1/2
ZO-1/2/3	Zona Occuldens proteins -1/2/3

4. INTRODUCTION

1. The Liver

1.1. Function and structure: generalities

The liver, the biggest internal organ in the body, plays relevant physiological functions, including energetic metabolism homeostasis (for glucose, lipids, including cholesterol, proteins and amino acids) by controlling nutrient synthesis and distribution, and detoxification of several substances by biliary excretion. In addition, it acts as an endocrine and paracrine gland (Michalopoulos, 2007; Hata et al., 2007; Trefts et al., 2017).

The liver has the property to regenerate in response to damage. Initially, the hepatocytes will try to restore liver mass, but in a more severe damage, the hepatoblasts (bipotential progenitor cells) will activate and expand from the portal area through the liver

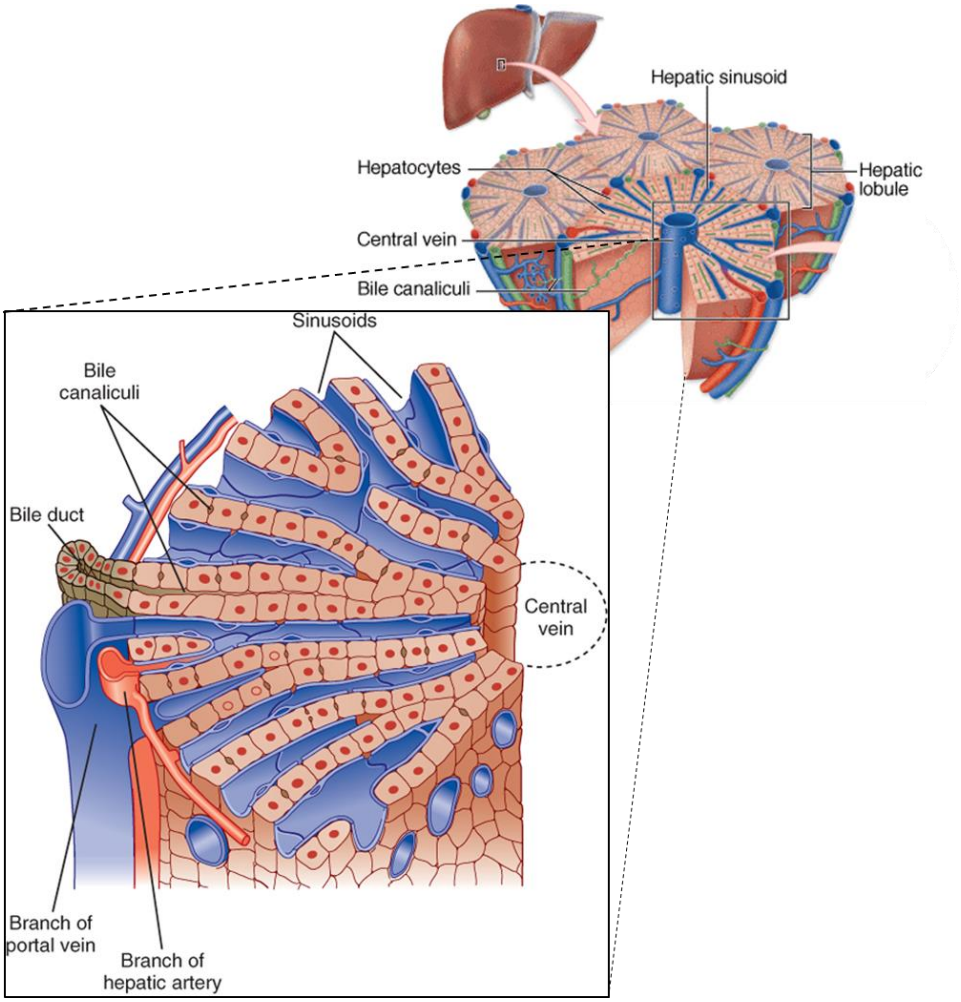

Figure I. Liver lobular structure. *Branches from the portal vein and the hepatic artery along with bile ducts constitute the portal tracts. Bile canaliculi, sinusoids and central vein are also indicated (modified from Koeppe and Stanton, 2008; Mescher, 2009).*

parenchyma, differentiating into hepatocytes and cholangiocytes, in order to regenerate the liver. However, malignant transformation of hepatoblasts could lead to liver cancer stem cells (CSCs), initiating liver cancer, but there is a lot of controversy on this issue on the literature (Machida, 2017; Castelli et al., 2017).

The liver has different lobar distribution in human and rodents. However, histologically, both human and rodent livers are identical, being constituted by lobules with randomly orientated units of hepatocytes rows (plates or cords). These lobules are delimited by the portal spaces, also called portal triads that contain portal vein small branches, hepatic artery and bile ducts. Through the terminal bile ductule, the Hering canal, the terminal segment of the biliary system connects to the hepatocytes in the liver parenchyma (Fausto and Campbell 2003). The one-cell thick rows of hepatocytes, extended from the periphery of the portal tracts to the central vein, are separated by spaces, the sinusoids, where the blood flows from portal space to central vein, while bile does so in the opposite direction (Figure I).

1.2. Hepatic cell types

Although the hepatocyte is the most abundant cell type in the liver, several other cell types constitute most of liver mass. In fact, there are, at least, 15 different cellular types in healthy liver: hepatocytes, biliary epithelial cells (or cholangiocytes), endothelial cells (sinudoidal endothelial cells, arterial and venous endothelial cells and lymphatic endothelial cells), Kupffer cells, hepatic stellate cells (or Ito cells), lymphocytes (or Pit cells), progenitor cells (fetal hepatoblasts, and adult oval cells in mice and human hepatic progenitor in humans), fibroblasts, smooth muscle cells from blood vessels, mesothelial cells, nerve unmyelinated cells, neuroendocrine cells, hematopoietic cells, blood cells (erythrocytes, leucocytes…) (Malarkey et al., 2005).

The most abundant cells are the hepatocytes (60% of total), accounting for 80% of liver volume and responsible for almost all the essential functions of the organ, including bile production and secretion from the apical membrane to the bile canaliculi and bile ducts formed by cholangiocytes. Both hepatocytes and cholangiocytes come from the same cell precursor, the hepatoblast (Kang et al., 2012). The rest of cells are non-parenchymal cells (NPCs) and immune cells infiltrated in the liver, such as Kupffer cells (15% of liver cells), which can proliferate in the liver, have phagocytic functions and are a major cytokine secretor source that enables crosstalk with other cells. Of special relevance are the HSCs (Hepatic Stellate Cells), a 5% of liver cells, which can produce ECM components, control blood vessel tone, store and metabolize vitamin A and lipids, when inactive. Upon activation, HSCs transform into myofibloblasts, expressing desmin and α-smooth muscle actin. HSCs are major players in hepatic regeneration, fibrosis and cirrhosis (Malarkey et al., 2005; Senoo et al., 2007) and promote the invasive capacity of hepatocarcinoma (HCC) cells (Liu et al., 2016).

Upon severe injury, the stem cell-like cells, located in the canals of Hering, expand and differentiate into hepatic progenitor cells (HPCs), a heterogeneous multipotent cell population, (specifically named oval cells in mouse, and intermediate hepatobiliary cells in humans) in order to regenerate the liver. These HPCs are bipotent, being able to differentiate into mature hepatocytes and cholangiocytes. However, their role in fibrogenesis and tumorigenesis, specially, in HCC, is controversial (Fausto and Campbell 2003; Esrefoglu, 2013; Cheng et al., 2017; Van Haele et al., 2017).

2. Hepatocarcinoma

2.1. Epidemiology and treatment

HCC is the most common liver cancer and accounts for around 80% of cases. According to the Global Cancer Observatory (GCO) from IARC institution (International Agency for Research on Cancer, from the WHO), in 2018 (the year of the most recent statistics), liver cancer was the sixth in number of new cases of cancer (incidence), accounting for a 4.7% (841 080 cases), and the fourth in number of cancer-related deaths (mortality), accounting for 8.2% (781 631 cases). The highest liver cancer incidence occurs in Asia (609 596 cases), followed by Europe (82 466 cases), Africa (64 779 cases) and North America (41 851 cases). Similarly, the highest rate of mortality is also registered in Asia (566 269 cases), followed by Europe (77 375 cases), Africa (63 562 cases) and Caribean/Latin American (36 436 cases). Regarding the distribution between sexes, the incidence cumulative risk (risk of new cases) is of 1.61% in males and 0.57% in females, and the mortality cumulative risk (risk of deaths) is of 1.46% in males and 0.53% in females. In fact, HCC has a powerful gender predilection as it is three-fold more common in men than in women (Llovet et al., 2016). These numbers indicate the existence of a sex-biased disparity that might be explained by the increasing evidence of a differentially gene expression pattern that can be responsible for an increased expression of certain proteins of CYP complexes (e.g. CYP3A4 in female hepatocytes). These proteins are implicated in the bioavailability, metabolism, distribution and secretion of chemo-drugs, increasing their effectiveness and reducing secondary effects (Shin, 2019). On the other hand, HCC is more prevalent in adults aged over 45 years (Llovet et al., 2016).

The main clinical algorithm for the classification of HCC patients in terms of prognosis and treatment allocation is the BCLC (Barcelona Clinic Liver Cancer) classification (Díaz and Barrera, 2015). This system takes into account how the liver is working through the Child-Pugh score (levels of plasmatic bilirubin and albumin, prothrombin time, ascites or encephalopathy), how big and where are the liver tumor nodules, and how is the performance status (PS) of the patient through the ECOG scale (Eastern Cooperative Oncology Group) (from PS 0, fully active, to PS 4, in bed all the time) (https://www.cancerresearchuk.org/about-cancer/liver-cancer/stages/bclc-staging-system-child-pugh-system). Hence, asymptomatic patients, with early tumors are treated radically with a curative treatment (30-40% of HCC patients) consisting in resection,

transplantation or local ablation and those with multinodular HCC are treated with transcatheter arterial chemoembolization (TACE). Patients with advanced symptomatology, tumors and/or metastasis (invasive pattern) are candidates for sorafenib treatment. Both TACE and sorafenib constitute palliative treatments, representing 50-60% of HCC patient treatments. Finally, end-stage patients with poor prognosis are given the best supportive care possible (10% of HCC patients).
On the other hand, the most used staging system in the United States for liver cancer is the AJCC (American Joint Committee on Cancer) with the TNM (Tumor, Nodes, Metastasis) system (more details can be consulted in the material and methods section or in the web: https://www.cancer.org/cancer/liver-cancer/detection-diagnosis-staging/staging.html. It is also useful to understand this HCC staging system, as it is found in many clinical histories from several public data bases.

Nowadays, the only preventive effective action against liver cancer is the immunization in the case of hepatitis B virus (HBV)-induced HCC (Llovet et al., 2018). Hence, the importance of following vaccination programs, as it has been demonstrated to reduce HCC incidence. Lifestyle modifications are also useful such as to moderate alcohol consumption or to control body weight, which can prevent liver diseases, such as cirrhosis or non-alcoholic fatty liver disease (NAFLD) that can lead to HCC.
In relation to treatments, only sorafenib, which inhibits multiples Receptor Tyrosine Kinases (RTKs), targeting both cancer cells and microenvironment, has demonstrated survival advantages (overall survival of 11 months). However, there are some limitations in its use. It is not indicated in patients with a poor liver function or in co-adjuvant treatment (with IFN-α), and generates drug resistance through different mechanisms (Llovet et al., 2016). On the other hand, most of the tested drugs, in this moment, in phase III trial, such as levantinib, regorafenib or cabozantinib, are cell cycle inhibitors, anti-angiogenic agents, RTKs inhibitors, checkpoint inhibitors, and more recently, epigenetic modifying therapies and microRNAs. In particular, many efforts are made in the direction of finding new Met inhibitors for the treatment of advanced HCC, taking into account the relevant function of HGF/Met pathway in tumorigenesis and progression of HCC (Okuma and Kondo, 2016; Matsumoto and Nakamura, 2006; Granito et al., 2015; García-Vilas and Medina, 2018).

2.2. Origin, development and progression of hepatocarcinoma. Generation of metastasis.

The etiology of HCC, and the implicated signaling mechanisms need to be fully characterized. In spite of the emergence of several hypotheses, the subject remains controversial (Lee, 2006) and complex, as multiple genetic aberrations are involved (Liu, 2016).

Etiology

Different environmental determinants and several risk factors involved in the development of HCC are well-known, which are frequently associated to chronic liver inflammation. For example, cirrhosis that is generated by chronic liver damage as a

consequence of persistent inflammation and fibrosis; viral infection by HBV and Hepatitis C Virus (HCV); alcohol abuse; fungal aflaxotin B1 intake; metabolic syndrome; obesity; autoimmune diseases; Wilson diseases, cholestatic liver disorders, α1-antitrypsin deficiency, NAFLD, non-alcoholic steato-hepatitis (NASH) (Anstee et al., 2019); and recently, adeno-associated virus 2 infection (AAV2) (Farazi and DePinho, 2006; Llovet et al., 2018; Lleo et al., 2019; Jindal et al., 2019). The prevalence of one over the other risks depends on the geographical situation, which is directly related to the environment and social patterns.

Development and progression

In livers with cirrhosis, HCC begins as precancerous low-grade dysplastic nodules, which later develop into high-grade dysplastic nodules and can transform into early-stage HCC that progress into advanced-stage HCC with metastasis (Figure II). Mature hepatocytes with excessive proliferation capability and longevity properties, and stem and progenitor cells, which has unlimited self-renewal capacity, are reported as the cellular origin of malignant transformation in HCC (Marquardt et al., 2015). As a matter of fact, after genetic and/or epigenetic alterations, all transformed murine hepatoblasts, hepatic progenitor cells and adult hepatocytes, can acquire stem cells like characteristics (Holczbauer, 2013). However, the origin of these Cancer Stem Cells (CSCs) or tumor-initiating cells, which are found in HCC solid tumors and are responsible for cancer relapses, metastasis and resistance to chemotherapy, is indeed a matter of controversy (Cheng, 2015).

On the other hand, 20-30% of HCCs develop without underlying cirrhosis, as a result of viral infections with HBV, HCV or AAV2, but also NASH and NAFLD are other exceptions to the pattern of HCC that is always associated with advanced liver fibrosis or cirrhosis (Llovet et al., 2018). Finally, the benign liver tumor, Hepatocellular Adenoma (HCA), can transform into HCC after a sequential accumulation of mutations, which is the case of woman taking oral contraception.

Metastasis

Metastasis develops when tumor cells disseminate from the primary site to adjacent or distant organs, representing a critical problem in cancer treatment and being the cause of 90% cancer mortality (Afify et al., 2019). Metastasis is a multistep process, involving migration, invasion, intra- and extravasation or immune system avoidance (Popper, 2016; Paolillo and Schinelli, 2019). This issue will be further developed in Section 4.

The most frequent place for HCC metastasis is the lung, where the communication between tumor cells and the microenvironment through macrophages or expression of MMP9 for example, is important for metastasis development (Zhuang et al., 2013).

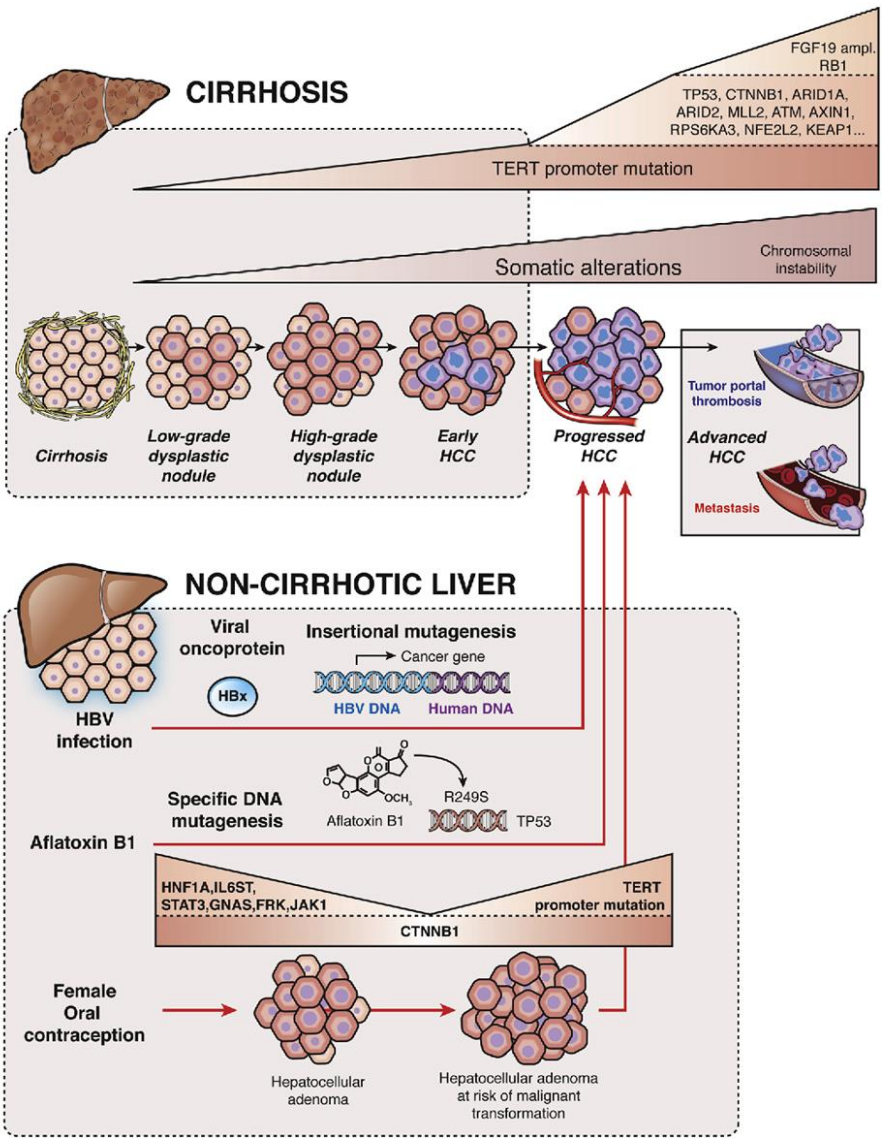

Figure II. HCC development and progression from cirrhotic and non-cirrhotic liver. *The accumulation of mutations in a predisposed liver by cirrhosis, fibrosis, viral infections or other circumstances leads to development and progression of HCC, finally leading to advanced HCC with metastasis (Zucman-Rossi et al., 2015).*

HCC extrahepatic metastasis (EHM) can be either simultaneous to intrahepatic disease or not, and can be produced at early stages of diagnostic, advanced HCC or after treatment as a recurrence. EHM is a consequence of direct extension to adjacent structures (adrenal gland, bowel and diaphragm), hematogenous spread, through systemic circulation to lungs and musculoskeletal system, or through lymphatic invasion to portal and abdominal lymph nodes, or induced by tumor rupturing (peritoneal dissemination). However, HCC has special predilection to directly invade veins in this order: portal, hepatic and vena cava. The most prevalent sites for metastasis are the lung (55%), lymph nodes (53%), bone (28%), musculoskeletal system (28%), adrenal glands (11%), peritoneum (11%) and brain (2%). Briefly, lymph nodes metastasis in HCC is the result of the lymphatic drainage of the liver, mainly in recurrence, leading to loco-regional dissemination of cancer cells, including porto-hepatic, para-aortic, peri-celiac and peri-pancreatic nodes, and is an indicator of poor prognosis. In the case of adrenal gland, metastases are solitary, facilitating a

successful surgical extirpation and is the result of direct extension of intrahepatic HCC tumors (exophytic growth) or systemic (through retroperitoneal venous system). Finally, metastasis to the lung is the most common EHM, resulting from systemic spread of tumor cells to the pulmonary capillary network, which results in non-calcified soft tissue nodules with lower lobe predominance and with a median survival of 35 months to 5 years using new advances in thoracic surgery (Chua et al., 2011; Becker et al., 2014).

2.3. Molecular mechanisms implicated in hepatocarcinoma pathogenesis

In livers predisposed by environmental and viral factors, both with and without cirrhosis, mutations in the TERT promoter are the first required step towards HCC tumor initiation in >90% of the cases, leading to dysplastic nodules and early HCC. Later, progression to advanced HCC is induced by a sequential accumulation of both genetic and epigenetic alterations that dysregulate different pathways, such as Wnt, p53, mTOR or Ras signaling and those involved in re-expression of fetal genes, folding machinery, telomere maintenance, chromatin remodeling, oxidative stress, metabolic reprogramming, immune system evasion, angiogenesis, sustained proliferation, apoptosis resistance, tissue invasion, etc (Figure II). If viral genome of HBV, HCV and AAV2 is inserted randomly in healthy hepatocytes, in cancerous cells, insertions occur in typical oncogenes. Some of these late genomic changes are mutations (TERTp, TP53, β-catenin or AXIN1), gene amplifications (MYC, MET, TERT or CCND1) and gene deletions (CDKN2A or PTEN), accompanied by epigenetic changes (Boon Toh et al., 2019), such as hypermethylation (CDKN2A, SOCS1 or HHIP), changes in microRNAs (miR122, miR17-96 or miR375) and long non coding RNAs (HOTAIR, HULC, MVIH or HEIH), among others (Dhanasekaran et al., 2018; Zucman-Rossi et al., 2015).

One of the main handicaps in HCC is the lack of a systematic classification for patients based on the molecular patterns, as happens in other types of cancer, such as breast cancer. The complexity of HCC pathogenesis lies not only on the diversity of the sequential accumulation of mutations and other genetic and epigenetic alterations in the genome, but also on the acquisition of different genome aberrations in tumor subclones. This leads to a diversified spatio-temporal heterogeneity. In fact, it is estimated that each HCC has 40 genomic alterations in average (Llovet et al., 2018). Moreover, a screen has discovered 275 genes that act as RTK cooperators to render the liver more vulnerable to other alterations, accelerating tumorigenesis. In fact, increased RTK levels were reported to be essential in tumor initiation (Fan et al., 2017).

Although it is difficult to classify HCC, a molecular classification of HCC has been proposed (Zucman-Rossi et al., 2015; Llovet et al., 2018):

A) Proliferative class: HBV-related, poor prognosis, vascular invasion, poor differentiation, with activation of Ras/MAPK, MET, AKT/mTOR or other pathways, which is divided in two subgroups:

-Progenitor-like: high levels of alpha-fetoprotein (AFP), epithelial cell adhesion proteins, NOTCH, IGF2 and EpCAM.

-Hepatocyte-like: alterations in Wnt and TGF-β pathways.

B) Non-proliferative class (hepatocyte-like): HCV and alcohol-related, well-differentiated, low AFP levels, low vascular invasion, better outcome, WNT, more heterogeneous, etc.

2.4. Tumor microenvironment in hepatocarcinoma

HCC tumor microenvironment (TME), enriched with cytokines, growth factors and enzymes, is constituted by stromal cells and extracellular matrix (ECM). Stromal cells include non-tumoral fibroblasts, cancer-associated fibroblasts (CAFs), myofibroblasts (or activated fibroblasts), HSCs, non-tumoral endothelial cells, tumor-associated endothelial cells (TECs), pericytes, adipose cells, immune cells (B and T cells, neutrophils, tumor-associated macrophages (TAMs)), etc (Tahmasebi Birgani and Carloni, 2017; Novikova et al., 2017) (Figure III). In addition, more recent studies highlight the relevant role of platelets, not only in the promotion of HCC cells proliferation, invasion, spread and survival in the blood stream, but also as mediators of pro-fibrogenic and immune response (Pavlovic et al., 2019; Lai et al., 2019). Exosomes are also emerging as important mediators between tumor cells, stroma and immune system (Wu et al., 2019). The bi-directional communication between tumor cells and TME results in the creation of a tumor-permissive niche.

HCC is an inflammation-associated disease, since in early stages, the immune system can eliminate tumor cells, but simultaneously, generates oxidative stress, DNA damage and inflammation. Chronic inflammation results in repetitive cycles of destruction-regeneration of hepatocytes, which contributes to HCC tumorigenesis and progression (Berasain et al., 2009; Tian et al., 2019; García-Vilas et al., 2018). Moreover, in early HCC, the hypoxic milieu leads to angiogenesis in the tumor induced by the release of VEGF-A by stromal and tumor cells, as well as inflammatory cytokines such as IL-1α, TNF-α or prostaglandin E2 secreted by the immune cells. In parallel, lymphangiogenesis occurs in response to VEGF-C and –D. Hypoxia in tumor stroma promotes the migration of tumor cells and the generation of metastasis. In fact, high blood and lymph vascularization is positively correlated to patient mortality (García-Vilas et al., 2018).

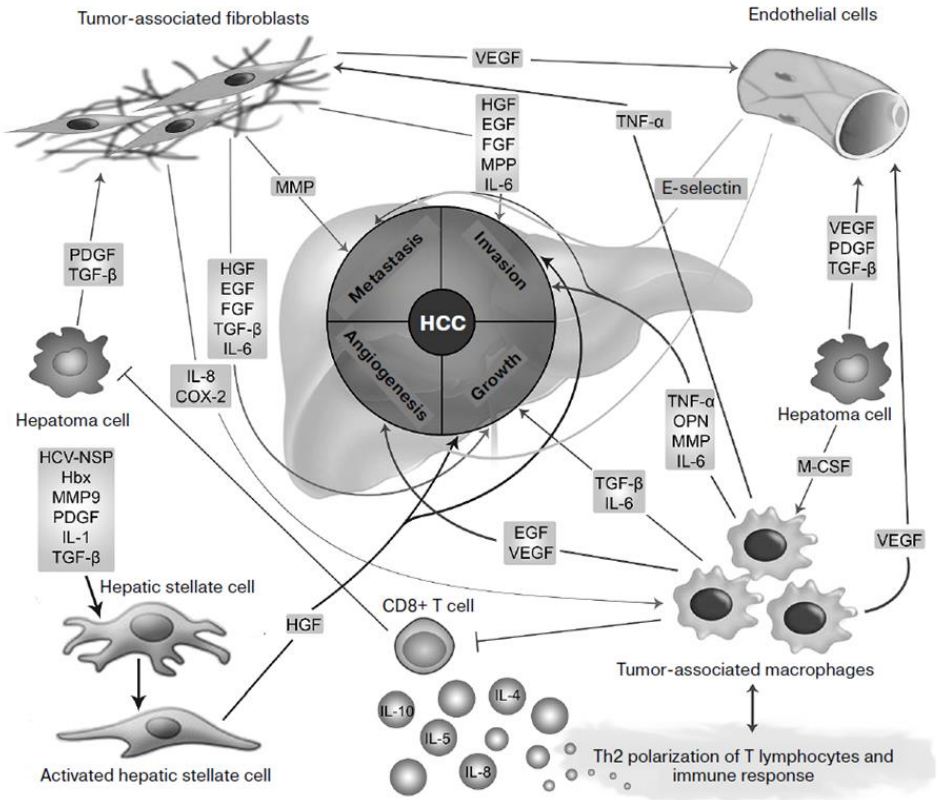

Figure III. Components of the tumor microenvironment in HCC. *Diverse cell types from the stroma establish a bidirectional communication with tumor cells, secreting growth factors, pro- and anti-inflammatory cytokines, interleukines, pro-angiogenic factors and other signals to promote tumor growth, invasion and metastasis of HCC cells, and angiogenesis (Novikova et al., 2017).*

Cancer-Associated Fibroblasts (CAFs)

Fibroblasts are implicated in wound healing, deposition of ECM, inflammatory response and tissue maturation. However, a sub-population of these cells, CAFs, expresses myofibroblast markers, such as α-SMA and are also involved in cancer initiation, progression and dissemination (Kalluri and Zeisberg, 2006). Depending on the type of liver injury, hepatic CAFs can be originated mostly from HSCs, or alternatively, from portal fibroblasts, although to a lesser extent. Other origins, such as bone marrow-derived cells, have a very small contribution to liver fibrosis (Baglieri et al., 2019). Resting fibroblasts are activated to myofibroblasts and CAFs, which have a rough endoplasmic reticulum and Golgi apparatus, suitable for the production and excretion of huge amounts of ECM constituents (Collagen type I, Fibronectin, Metalloproteinases (MMPs), etc), resulting in the remodeling of ECM that facilitates invasion of tumor cells. Moreover, they also secrete cytokines, which promotes the infiltration of monocytes and macrophages and the recruitment of endothelial progenitor cells to the site of liver injury, favoring angiogenesis. HGF is also secreted by CAFs at higher levels than normal fibroblasts. These CAFs remain in an active state, independently of stimuli removal, not undergoing apoptosis (Tahmasebi Birgani and Carloni, 2017; Baglieri et al., 2019; Affo et al., 2017). Moreover, they increase the proportion of ki67 positive proliferating malignant cells, preventing their necrosis.

Hence, the abundance of CAFs is positively correlated to tumor size (Jia et al., 2013, Plos one), metastasis (Coulouarn et al., 2012; Ji et al., 2015) and poor clinical outcome after curative resection (Ju et al., 2009).

Hepatic Stellate Cells

Hepatic Stellate Cells (HSCs) are located in the basolateral membrane of hepatocytes and the anti-luminal side of sinusoidal endothelial cells, to facilitate their contact with hepatocytes and endothelial cells. HSCs are non-proliferative cells, which can trans-differentiate into myofibroblast-like cells upon liver injury, becoming more contractile, proliferative and increasing their potential to produce ECM components. Stimuli from the stroma (sinusoidal endothelium, Kupffer cells, hepatocytes, platelets, etc) activate HSCs in a three step process: initiation, perpetuation and resolution, which induces its movement to the site of liver injury, where they secrete pro-inflammatory, pro-fibrogenic and pro-mitogenic factors, resulting in ECM deposition and remodeling (Forbes and Parola, 2011; Rombouts and Carloni, 2013). Thereby, promoting HCC progression and providing an immunosuppressive niche for HCC (Zhao et al., 2014).

Tumor-associated macrophages

In early HCC, M1 macrophages eliminate tumor cells by releasing ROS (reactive oxygen species). However, upon stimulation with IL-3/4, TGF-β or glucocorticoids, macrophages polarize to M2 activated macrophages with low antigen-presenting capacity, which decreases inflammation and favors repair. In advanced HCC, M2 macrophages replace M1 macrophages, resulting in suppression of adaptative immunity, cancer cell proliferation, angiogenesis and ECM remodeling, being M2 presence related to a more aggressive HCC (Noy and Pollard, 2014; Tahmasebi Birgani and Carloni, 2017; Tian et al., 2019).

Hence, the efforts of researchers in the recent years to develop, not only drug agents against tumor cells, but also therapeutic strategies to target the different components of the tumor microenvironment, such as CAFs or immune system, to reach a more successfully treatment for HCC patients (Yin et al., 2019; Fu et al., 2019).

3. C3G

C3G (Crk SH3-domain-binding guanine-nucleotide-releasing factor) or RapGEF1 is a guanine nucleotide exchange factor (GEF) for some members of the Ras superfamily of small GTPases, mainly Rap1 (Gotoh et al. 1995) and R-Ras (Gotoh et al. 1997), although it can also activate TC21, or TC10 (Ehrhardt et al. 2002). On the other hand, C3G can also act through GEF independent mechanisms, which involves protein-protein interactions (Guerrero et al. 1998; Guerrero et al. 2004; Shivakrupa et al. 2003).

In 1994, C3G was identified as the first RapGEF, originally isolated as a Crk interactor (Tanaka et al. 1994). The nucleotide sequence of the 4.1 kb C3G c-DNA contains a 3.2 kb open reading frame that encodes a 121 kDa protein. However, antibodies raised against C3G detect a protein of 130-140 kDa (Tanaka et al. 1994). The human C3G gene, *RapGEF1*, located on chromosome 9q34.13, comprises 24 exons spanning 163 kb (Takai et al. 1994).

Despite C3G ubiquity, tissue-specific expression has been detected. For instance, in humans, C3G levels are higher in skeletal muscle, brain, heart, kidney, lung and liver, as well as in placenta, fetal heart and brain (Tanaka et al. 1994; Guerrero et al. 1998). In mouse, C3G expression is high in brain, heart, liver and muscle, but low in adipose tissue, kidney and spleen (Radha et al. 2011).

3.1. Structure and isoforms

Mouse and human C3G cDNA nucleotide sequence comparison revealed an 88% identity shared (Zhai et al. 2001). Protein databases account for the existence of, at least, seven different isoforms, although most of them have not yet been studied. In humans, there are two predominant isoforms, a and b, which result from alternative splicing and differ in their N-terminus, so that three amino acids from isoform a are replaced by 21 amino acids in isoform b (Radha et al. 2011). There is a non-predominant isoform in humans that has been associated with chronic myeloid leukemia (CML), p87C3G, a truncated C3G isoform that lacks 305 amino acids in the N-terminal region (Gutierrez-Berzal et al. 2006). It is abundantly expressed in CML cell lines and primary cells from patients and interacts with Bcr-Abl. p87C3G expression levels correlates with the disease stages, as its levels decrease during disease remission upon treatment. This suggests that p87C3G plays a key a role in CML (Gutierrez-Berzal et al. 2006). In mice, two transcripts with or without a 144 bp N-terminus insertion are expressed in most tissues (Zhai et al. 2001).

C3G is structured into three distinct domains (Figure IV) with different functions. In the C-terminus, the CDC25 homologous domain together with the REM (Ras-Exchange-Motif) domain are responsible for its GEF activity. The central region contains five proline-rich sequences that bind to SH3 (Src Homology-3) domains present in proteins such as Crk, p130Cas, Grb2, c-Abl and Hck (Radha et al. 2011) and harbors a tyrosine residue (Tyr504), able to be phosphorylated by different kinases, resulting in C3G activation (Shivakrupa et al. 2003). Finally, in the N-terminus, there is a negative regulatory domain for C3G GEF activity, so that, its deletion results in constitutive catalytic activity (Ichiba et al. 1999). In addition, there is a binding site for the cytoplasmic domain of E-cadherin (amino acids 144 to 230) (Hogan et al. 2004) (Figure IV).

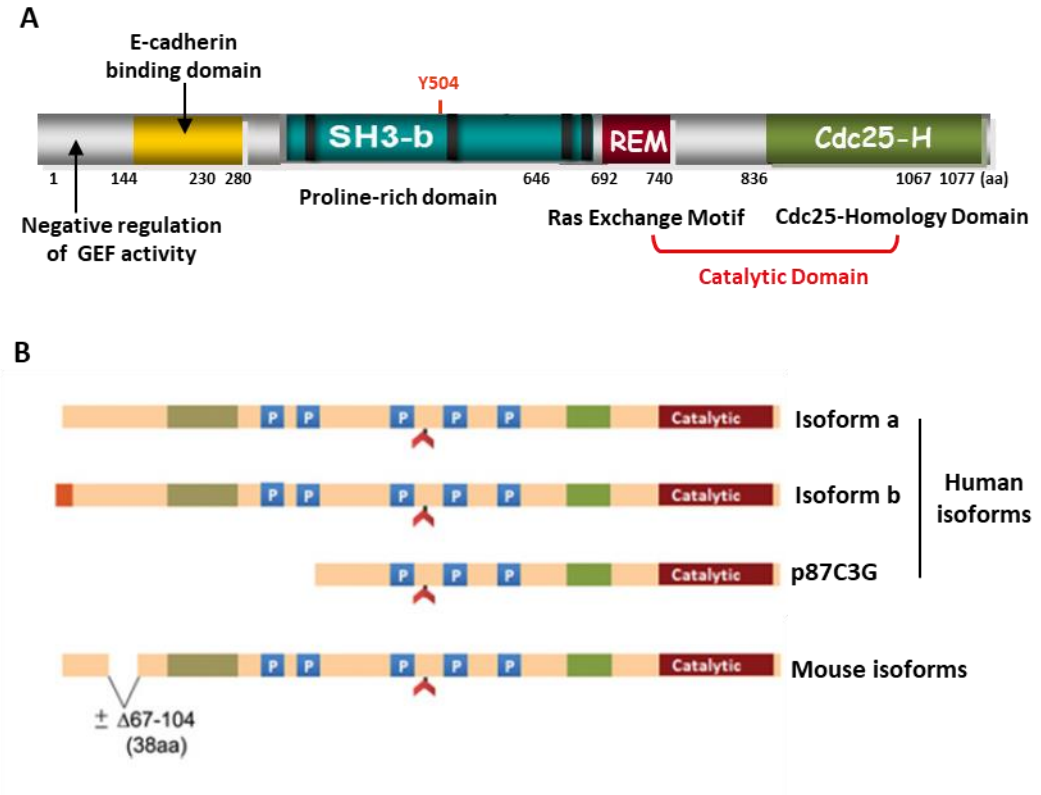

Figure IV. Structure of C3G human and mouse isoforms. ***(A)*** *C3G domains from C-terminal to N-terminal: REM together with Cdc25-H are responsible for the GEF activity; the proline rich domain or SH3-biding domain; the E-cadherin binding domain and the GEF activity negative regulatory domain. Red pin indicates residue Tyr504, whose phosphorylation activates C3G.* ***(B)*** *Comparison of the C3G mouse and human a, b and p87C3G isoforms (modified from Radha et al., 2011).*

3.2. Functions of C3G

In the last two decades, several studies have demonstrated C3G involvement in multiple signaling pathways and cellular functions, mediated either by its GEF activity or by protein-protein interactions (Figure V) (Guerrero et al. 1998; Shivakrupa et al. 2003).

C3G is essential for embryonic development. Hence, C3G knock-out mice die before embryonic day 7.5 due to a defect in integrin-mediated cellular adhesion (Ohba et al. 2001). Furthermore, the use of MEFs (Mouse embryonic fibroblasts) from C3G knock-out mice revealed that Rap1 activation by C3G is necessary for adhesion and spreading (Ohba et al. 2001). C3G is not only relevant for cell adhesion and spreading, but also for the regulation of migration and cell-cell junction assembly and disassembly in different cell types (Radha et al. 2011). Moreover, C3G is implicated in adipocyte differentiation (Jin et al. 2000) and skeletal muscle differentiation (Sasi Kumar et al. 2015).

C3G also controls proliferation, differentiation and survival of neuroblastoma cells (Radha et al. 2008), as well as brain development. Hence, C3G-deficient mice present an over-proliferation of the cortical neuroepithelium, resulting in a defective cortex development

(Voss et al. 2006). It is also required for neuron transition from multi- to bipolar, during cortical development (Shah et al., 2016).

Additionally, C3G can induce apoptosis through Hck (Shivakrupa et al. 2003) or c-Abl (Radha et al. 2008). Depending on the cell type and the stimulus, C3G promotes cell death or survival through the downregulation of p38α activity (Maia et al. 2009; Gutierrez-Uzquiza et al. 2010).

C3G-mediated TC10 activation is also involved in insulin-induced GLUT4 (glucose transporter type 4) membrane translocation in muscle and adipose tissue, through the cytoskeletal rearrangement implicated in vesicle trafficking (Chiang et al. 2001).

C3G also plays an important function in platelets, where it promotes clotting through a mechanism mediated by Rap1 (Gutiérrez-Herrero et al. 2012). In addition, C3G is involved in megakaryocytic differentiation and pro-platelet formation, acting through a mechanism dependent on its GEF activity (Ortiz-Rivero et al., 2018). In this context, the hematopoietic transcription factor, GATA-1, induces C3G expression. Moreover, C3G regulates platelet secretion through both Rap1 dependent and independent mechanisms, which leads to a net pro-angiogenic effect in tumors and other contexts (Martín-Granado et al., 2017).

The role of C3G in cancer is controversial. It has been reported to act as both a tumor suppressor and promoter. As a tumor suppressor, it prevents malignant transformation induced by several oncogenes (Guerrero et al. 1998; Guerrero et al. 2004; Martín-Encabo et al. 2007). In agreement with this, C3G expression decreases in cervical squamous cell carcinoma, likely as consequence of the methylation of C3G regulatory sequences (Okino et al. 2006). In contrast, C3G levels are increased in human non-small-cell lung cancer (Hirata et al. 2004) and RET/PTC1-CrkII/Gab1/C3G-Rap1 pathway is involved in the process of transformation of papillary thyroid carcinoma (De Falco et al. 2007). The expression of p87C3G isoform is also associated with the development of CML (Gutierrez-Berzal et al. 2006). In contrast, C3G decreases migration in highly invasive breast cancer cells (Dayma and Radha, 2011). Different from this, other data indicate that C3G-mediated Rap1 activation promotes migration and invasion of epithelial ovarian cancer cells (Che et al. 2015). Our group, reported a dual role for C3G in colon carcinoma cells, as it inhibits migration and invasion through p38α activity downregulation, while it favors tumor growth in a p38α-independent manner (Priego et al., 2016).

More recent studies, have uncovered new functions for C3G as a repressor of histone modifications associated with euchromatin, thanks to its nucleo-cytoplasmatic exchange (Shakyawar et al., 2017). Nuclear C3G also binds to nuclear speckles in order to regulate mRNA splicing (Shakyawar et al., 2018). Moreover, C3G can localize into the mother centriole to control its division and therefore, the primary cilia dynamic (Nayak and Radha, 2019).

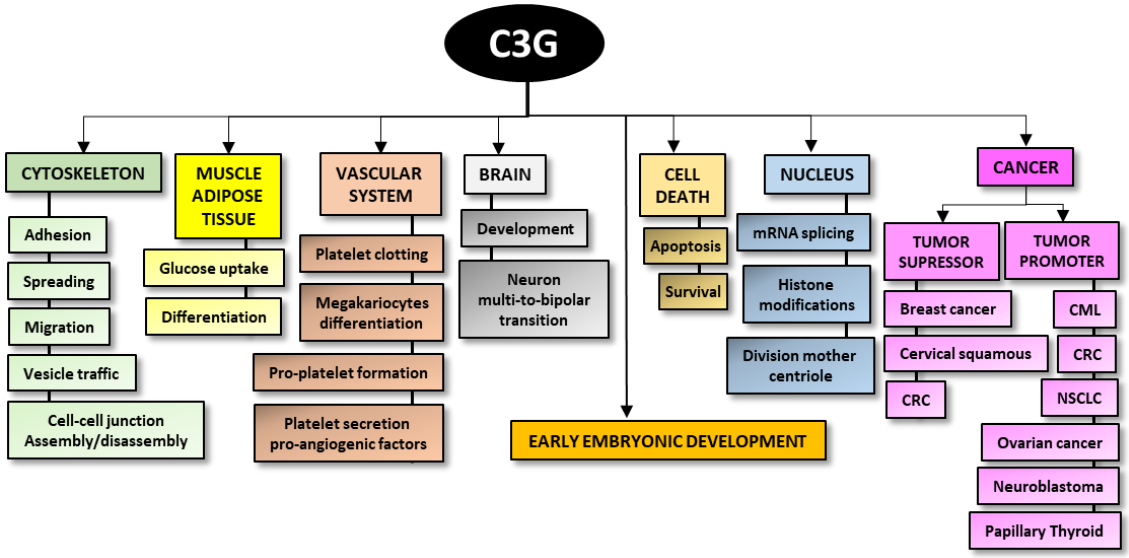

Figure V. C3G functions in different physiopathological contexts. *C3G is essential for early embryonic development. Moreover, C3G regulates several cellular functions in different organs and tissues, acting in different subcellular compartments, including the nucleus. In cancer, C3G acts as a tumor promoter and/or suppressor depending on the cancer type and stage.*

3.3. C3G in cell signaling pathways.

So far, there is little literature available about the mechanisms that regulate C3G activation. C3G is a mediator of the signalling induced by different stimuli and receptors, such as T cell receptor stimulation (Reedquist et al. 1996), hepatocyte growth factor (HGF) (Sakkab et al. 2000), growth hormone (Ling et al. 2003), platelet-derived growth (PDGF) (Yokote et al. 1998), nerve growth factor (NGF) (York et al. 1998), interferon-ϒ (Alsayed et al. 2000), integrins (Buensuceso and O'Toole 2000) or interleukin-3 (Arai et al. 2001).

The formation of multiprotein complexes plays a key role in the activation of C3G in response to different stimuli (Radha et al. 2011), being relevant for the signalling elicited by tyrosine kinase receptors. Several proteins can interact with C3G directly or indirectly, depending on specific contexts, leading to the regulation of a huge number of cellular functions. C3G can be activated by phosphorylation in Tyrosine residue 504 (Y504) (Ichiba et al. 1999; Radha et al. 2004) by kinases, such as c-Src, Hck, Fyn and c-Abl. C3G can also be phosphorylated in other tyrosines (Radha et al. 2011) and serine (Utreras et al. 2013) residues, but their function remains unknown. The interaction between Crk and C3G is important for C3G-mediated Rap1 activation (Gotoh et al. 1995; Van den Berghe et al.

1997), which is dependent on Crk phosphorylation (Radha et al. 2011). In addition, Crk SH2 domain enables the translocation of Crk-C3G complex to the membrane through its binding to tyrosine-phosphorylated molecules (Ichiba et al. 1997), such as receptor tyrosine kinases (Yokote er al. 1998) or adaptors, like Gab1 (Sakkab et al. 2000) and p130Cas (Lamorte et al. 2002). In particular, in HEK293 cells overexpressing Gab1, once Met is activated in response to HGF, CrkL-C3G complex binds to phosphorylated Gab1 through CrkL SH2 domain, leading to Rap1 activation (Sakkab et al., 2000). Other Crk isoforms, such as CrkI and CrkII interact with C3G leading to Rap1 activation (Huang et al., 2008). However, alternative adaptors to Crk proteins containing SH3 domains, such as p130Cas (Lamorte et al., 2002) or Grb2 (Smit et al., 1996) can also mediate the interaction between C3G and tyrosine kinase receptors through its binding to C3G proline rich domain.

Furthermore, C3G through its SH3-binding domain can interact with Abl in chronic myeloid leukemia (CML) cells, where C3G also form complexes with proteins present in focal adhesions, such as p130Cas, Cbl, CrkL or Abi1, to regulate CML cell adhesion (Maia et al., 2013). In relation with this, C3G was previously found to interact with Abl, leading to filopodia formation through a mechanism that requires Abl tyrosine Kinase activity (Radha et al., 2007). Moreover, Abl can phosphorylate CrkII, leading to the dissociation of CrkII-C3G complex, decreasing Rap1 activation (Huang et al., 2008). On the other hand, oxidative stress-induced Abl activation induces C3G phosphorylation in Y504 leading to cell apoptosis (Mitra and Radha, 2010).

C3G also binds to E-cadherin, facilitating its membrane localization and Rap1 activation (Asuri et al., 2008; Radha et al., 2011; Sciarratta et al., 2006). In relation with this, C3G can also interact with β-catenin through its proline rich domain, leading to β-catenin degradation, avoiding its accumulation in the nucleus (Dayma et al., 2012). However, C3G interaction with E-cadherin does not require β-catenin association (Asuri et al., 2008).

3.4. C3G in liver patho-physiology

Rap small GTPase family and its GEFs are relevant players in hepatic physiology through modulation of metabolism, proliferation, survival and other cellular functions. In HCC, the function of Rap is controversial (Sequera et al., 2018). Rap1 was reported to impair tumorigenesis in Hep3B cells by inhibiting Ras pathway and proliferation (Lin et al., 2000). In contrast, other studies suggest that Rap1 participates in HCC induction by promoting tumor growth and migration (Su et al., 2009; Sheng et al., 2014). More recently, it was found in some human HCC samples and cell lines, either an up-regulation of Rap2B (Zhang et al., 2017) or Rap1B expression (Tang et al., 2018), inducing proliferation and migration. RapGEFs, Epac1 and 2, have been proved to be relevant for liver physiopathology (Sequera et al., 2018). However, there is no information about C3G role in liver (Sequera et al. 2018). Based on C3G RapGEF catalytic function (Maia et al., 2009; Gutiérrez-Herrero et al., 2012; Ortiz-Rivero et al., 2018), C3G could be an alternative GEF for Rap in the liver,

regulating its physiology and/or HCC. C3G is expressed in E16.5 mouse embryonic liver, although the isoform expression profile is different, according to proteomic data. Hence, the liver is enriched in smaller isoforms, in contrast to embryonic brain, where full-length isoform predominates (Cheerathodi et al., 2015). These shorter liver isoforms contain the C-terminal catalytic domain, but lacks the N-terminal E-cadherin binding domain. This suggests that differences in C3G RNA processing might confer tissue-specific functional abilities. In this case, liver embryonic C3G isoforms would be implicated in Rap1 signaling regulation and might interact with CrkL and/or other proteins containing SH3 domains, whereas embryonic brain C3G would be more relevant in focal adhesion formation and E-cadherin interaction (Cheerathodi et al. 2015).

4. Cell adhesion, migration, invasion and epithelial to mesenchymal transition

4.1. Adhesion

Cell adhesion plays an important role during embryonic development and in different adult physio-pathological processes, including cancer, due to its implication in cell organization, proliferation and survival. Within the tissues, it is important not only cell-cell interaction, but also cell binding to the extracellular matrix, which provides attachment, protection against external aggressions and leads to the activation of different signaling pathways (Maruthamuthu et al. 2011).

Epithelial cells are connected by three types of structures: tight junctions (TJs or zonula occcludens), adherens junctions (AJs or zonula adherens) and desmosomes (or macula adherens) (Le Bras et al. 2012). The adherens junctions are dynamic structures, remodeled by endocytosis and recycling of their components that are generally constituted by calcium-dependent homophilic binding of cadherins or nectins.

Cadherins have important roles in cell to cell adhesion, tissue morphogenesis and cancer (Gloushankova et al., 2017). Specifically, E-cadherin accumulates, forming macro-complexes, in AJs that bind to actin through mediators, such as catenins, being one of the most relevant modulators of epithelial phenotype. Its expression is regulated by mechanical forces, recycling, binding and/or phosphorylation of proteins such as catenins, etc (Kourtidis et al., 2017). In fact, E-cadherin-mediated nuclear signaling requires a mediator, such as β-catenin (Van Veelen et al., 2011; Piedra et al., 2001). β-catenin is a component of the Wnt signaling pathway, present in the cell surface of normal adult liver, but can change its localization and signaling upon liver injury and in cancer (Monga, 2015). β-Catenin phosphorylation by RTKs induces its dissociation from E-cadherin, leading to β-catenin activation and nuclear translocation (Van Veelen et al., 2011; Piedra et al., 2001),

which in turn activates several transcription factors, leading to epithelial-mesenchymal-transition (EMT), dissemination or tumor cell proliferation (Perugorria et al., 2019).

On the other hand, TJs are not only the barriers that selectively allow passage to ions and solutes, but they also establish cell polarity (Campbell et al., 2017). They are constituted by diverse families of proteins, such as claudins, MARVEL or JAM (junctional adhesion molecules) that associate to scaffolding proteins from MAGUK (membrane-associated guanylate kinase) family (e.g. Zonula occludens proteins), linking the TJs to cell signaling and cytoskeleton (Zihni et al., 2016). In fact, TJs are not only involved in cell attachment, but also regulate cell proliferation (Díaz-Coránguez et al., 2019) being involved in cancer and metastasis control (Soini, 2012; Odero-Marah et al., 2018). Specially, occludin is one of the major components of TJs, whose dysregulation is implicated in many diseases, including cancer (Cummins et al., 2012). Thus, during the EMT process, occludin and E-cadherin are down-regulated, so cells lose their epithelial phenotype (Odero-Marah et al., 2018).

During cell migration and adhesion, new adhesions can turn over rapidly or mature to form larger focal complexes in the lamellipodium-lamellum interface, and then into larger focal adhesions in the actin bundles or stress fibers. In order for the cell body to move forward by traction forces, focal adhesions need to assemble and disassemble constantly. Therefore, contraction is coupled to de-adhesion (Gardel et al. 2010; Parsons et al. 2010), while cell adhesion requires the maintenance of focal adhesion complexes. They are constituted by integrins that bind to talin, kindlin, vinculin, α-actinin, paxilin, FAK and other proteins, enriched in phosphotyrosines, forming active signaling complexes (Parsons et al. 2010).

4.2. Migration

Cell migration is a complex process involved, both in physiological and pathological situations. For instance, skin and intestine cell turnover requires new epithelial cell migration from basal layer or the crypts, respectively, to the top layer. Migration is also required for tissue repair and immune response (Ridley et al. 2003). On the other hand, migration is important in vascular diseases, osteoporosis, chronic inflammatory diseases or cancer, where it allows cancer cell dissemination and generation of metastasis (Franz et al. 2002; Ridley et al. 2003).

Cells can not only migrate individually, either directionally by a mesenchymal movement through proteolysis at the leading edge or by a non-orientated amoeboid movement without direction or polarity (Le Bras et al. 2012); but also they can migrate collectively in solid cell strands, sheets, files or clusters (Friedl and Wolf 2003; Rorth 2009).

Migration is accomplished through the continuous cycle of coordinated and interdependent steps involving the cytoskeletal machinery (Friedl and Brocker 2000). Cell body movement is achieved thanks to the contractibility generated by actin and myosin II

filaments. When migrating cells are polarized, we find extensions, called filopodia, at the front, as well as lamellipodia, formed by dynamic actin polymerization (Franz et al. 2002). This is regulated by the Rho GTPases, Rac and Cdc42 (Parsons et al. 2010). Maturation of focal complexes to focal adhesion requires Rho activation, which involves Rho GEF recruitment and Rho-mediated Rac inhibition (Sanz-Moreno et al. 2008; Tomar and Schlaepfer 2009). Rho activity promotes the assembly of contractile actomyosin structures, which regulate changes mediated by traction and tension (Gardel et al., 2010). Other proteins such as FAK, Src, paxillin, talin or p130Cas also regulate cell protrusion, adhesion and contraction, modulating F-actin cytoskeleton and integrin-mediated adhesion interaction (Gardel et al. 2010).

4.3. Invasion

Invasion is one of the hallmarks of cancer, constituting one of the first steps to undergo metastasis, and therefore, it is of great interest to identify invasive markers. However, the task is not simple, as there is a diversity of cancer cell invasion patterns and mechanisms, due to the different phenotypic transitions generated by cellular plasticity (epithelial-mesenchymal, collective-amoeboid, etc) (Gerashchenko et al., 2019), even determined by the nature of the EMT undergone, with initiating capabilities (trailblazer-type EMT) or dependent on extrinsic factors (opportunist-type EMT) (Pearson, 2019; Wu et al., 2017). In fact, invasion process is not a single-cell process, so most invasive solid tumors undergo a collective invasion, where a group of invading cells do not loose cell-cell interaction. According to this, patterns of cancer cell invasion have been classified into individual-cell migration (single-cell migration with either amoeboid or mesenchymal phenotype), multicellular migration (collective migration that maintains cell-cell junctions and supra-cellular contractility), and multicellular streaming (something in between the two previous types), among others (Friedl et al., 2012).

Stromal cells are involved in tumor cell migration and invasion (Sameni et al. 2003). In particular, the production of matrix-metalloproteases (MMPs) by fibroblasts and macrophages present in tumors, contribute to ECM degradation, favoring cancer cell migration and invasion (Wells et al. 2008).

During cell migration and invasion, ECM is modified and degraded by secreted endopeptidases such as MMPs, to create a path for cells to migrate, invade and disseminate to adjacent and/or distant organs (Sternlicht and Werb 2001). Within all tissues and organs, the ECM is a non-cellular component that constitute not only a physical scaffolding for cells through its interaction with integrins (Gout and Huot 2008; Halper and Kjaer 2014; Arriazu 2014), but also generate bio-chemical and –mechanical signals, necessary for tissue morphogenesis and organization, differentiation, homeostasis and protection through a buffering action and water retention (Frantz et al. 2010). ECM is a complex structural macromolecular tridimensional network that surrounds cells. Distinct molecules such as collagens, laminins, fibronectin, elastin,

fibrillins, tenascin, nidogen, entactin, fibulins, fibrinogen, trombospondins, hyaluronans or proteoglycans are components of the ECM. However, ECM composition varies in the different tissues. A particular type of ECM is the basal lamina, a layer under epithelial cell sheets and tubes, produced by epithelial and stromal cells, which is relevant in cancer (Gout and Huot 2008). In fact, ECM can determine the preference of cancer cells to generate metastasis into specific tissues (Tse and Kalluri 2007). Hence, the ECM constitute a naturally complex and dynamic microenvironment under constant remodeling.

In the liver, ECM regulates its development, regeneration and the maintenance of its architecture and differentiated state through different mechanisms. It acts as a solid phase agonist or as polypeptides that bind to cell surface receptors. In addition, ECM can facilitate the exchange of nutrients and cytokines between circulating blood and hepatocytes during liver regeneration (Kim et al. 1997; Michalopoulos 2010). In healthy liver, ECM components are mainly expressed in the liver capsule, portal tracts and biliary ducts and ductules, while in the sinusoidal space (or Space of Disse), space between hepatocytes and sinusoidal endothelial cells, the basement-like matrix is formed mainly by collagens, elastin, structural glycoproteins and proteoglycans (Karsdall 2014; Friedman 2003). In liver pathologies, such as fibrosis and cirrhosis, the balance between formation and degradation of ECM is lost, resulting in an aberrant deposition of ECM (Schuppan et al. 2001; Wells 2008; Morten A. Karsdal 2014), achieved by a change in the secretion profile of the different MMPs, among other mechanisms (Duarte et al. 2015).

ECM is degraded by different proteases, being particularly relevant, the MMPs that belong to the Metzincins heterogeneous family of Zinc proteolytic proteins, which share a consensus motif with three histidines that enables their binding to zinc at the catalytic site and their active site holds a conserved motif (HEXXHXXGXXH). This family is constituted by MMPs, ADAMs (α-disintegrin and metalloproteinases) and ADAMTS (α-disintegrin and metalloproteinase with thrombospondin motifs) (Bergers and Coussens, 2000; Gardel et al., 2010). Specifically, MMPs are synthetized as pro-MMPs (inactive zymogens) and then, activated by limited proteolysis, being either secreted or expressed as transmembrane proteins. Their activity is negatively controlled by TIMPs (tissue inhibitors of metalloproteinases) and their transcription can be modulated by several signals, such as cytokines, growth factors, hormones and other signals from the ECM (Gardel et al., 2010). The expression and activation of MMPs by tumor cells and tumor microenvironment cells allows ECM remodeling, facilitating migration, invasion, intra- and extra-vasation and spread of cancer cells, leading to metastasis (Radisky and Radisky, 2010; Shay et al., 2019). In particular, MMPs have important roles during EMT in HCC, not only enabling tumor cell invasion and metastasis, but also angiogenesis (Scheau et al., 2019).

4.4. Epithelial-mesenchymal transition

EMT (epithelial-mesenchymal transition) is a process that enables epithelial cells to acquire pro-migratory and pro-invasive properties and a fibroblastic like phenotype. It is relevant for embryogenesis, organogenesis and tissue repair in adult life. In addition, it is necessary for driving carcinoma cells towards an invasive phenotype (Grünert et al. 2003).

EMT and the reverse mechanism, mesenchymal-epithelial transition (MET), allow the spreading of tumor cells from primary localization to distant organs and its proliferation in the new place (Pereira et al. 2015). For the metastasis to take place, cells need to undergo an EMT process in the primary tumor as the first step. In fact, metastasis comprises different steps: local infiltration of primary tumor cells to adjacent tissues, intravasation (trans-endotelial migration of cancer cells) into vessels, survival in the blood system and extravasation, which results in the formation of a secondary tumor (Tse and Kalluri 2007; Van Zijl et al. 2009). For the last step, cells need recognition, adhesion to endothelial cells and degrading the ECM to invade the secondary location (Tse and Kalluri 2007), where tumor cells re-differentiate through MET and proliferate, recapitulating the organization and characteristics of the primary tumor (Pereira et al. 2015).

EMT involves several changes such as loss of polarity, decrease in the expression of epithelial-specific proteins (E-cadherin, ZO-1, etc), while increases that of mesenchymal-specific proteins (N-cadherin, Vimentin, etc) and MMPs. EMT can be accompanied by the expression of stemness markers (Zeisberg and Neilson 2009). However, recent works have demonstrated that EMT is not necessarily associated to the acquisition of stemness properties (Fabregat et al., 2016). In contrast to classical reports, the new ones support the idea that EMT does not consist in a binary change from a full epithelial to a full mesenchymal phenotype, but rather it is a process that allows the existence of multiple transitional states, where the cell undergo a partial EMT program (Nieto et al., 2016) (Figure VI).

During the EMT process, several markers change, not only their expression, but also their localization or both. An example is the switch from E-cadherin (present in adherent junctions) to N-cadherin expression (Tsanou et al. 2008). In the cytoplasm, β-catenin bound to E-cadherin to stabilize cell junctions. When it is released and translocates to the nucleus, where it contributes to induce EMT via its transcripcional activity, specially increasing Snail1 expression (Zeisberg and Neilson 2009). E-cadherin loss can promote tumor cells detachment from primary focus, favoring invasion and dissemination to adjacent organs (Tse and Kalluri 2007).

Tight junction components, including claudins, occludins or JAMs and connectors (zona occluden proteins (ZO-1/2/3)) to the actin cytoskeleton are downregulated during EMT (Wendt, Tian & Schiemann, 2012). ZO-1, ZO-2 and ZO-3 proteins belong to MAGUK family. In particular, ZO-1 plays a key role modulating cadherin-mediated cell-cell junctions and F-actin cytoskeletal distribution (Gonzalez-Mariscal et al. 2000; Bazzoni et al. 2000;

Fanning and Anderson 2009; Fanning et al. 2012). Therefore, its down-regulation during EMT contributes to cytoskeleton re-organization.

Most of the signaling pathways that trigger EMT converge at the induction of EMT regulators that control the expression of different genes (review by Thiery et al., 2009). Among the great variety of signals that can induce EMT, different members of TGF-β family, Wnt ligands, Notch, EGF or HGF are of special relevance (review by Thiery et al., 2009).

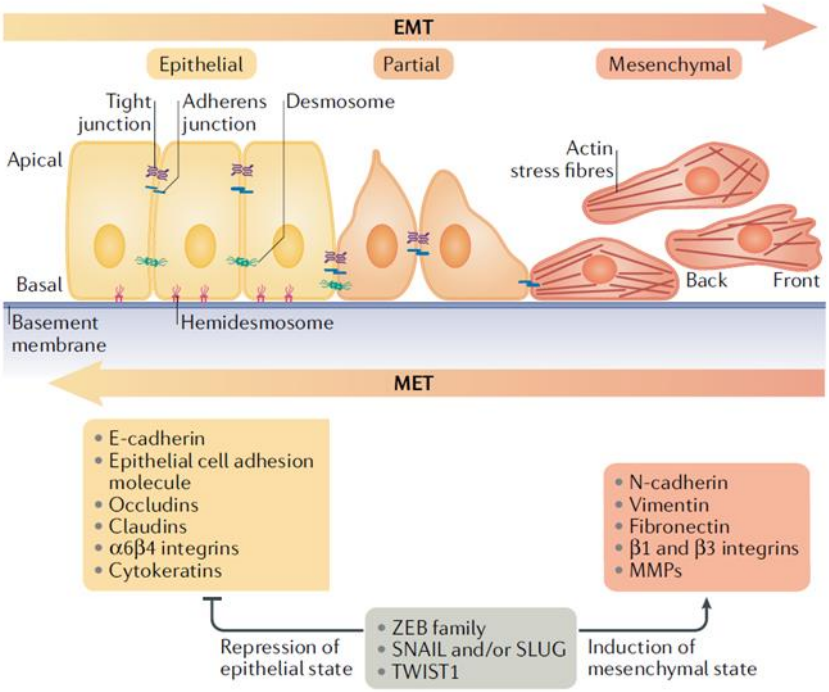

Figure VI. EMT process. *During EMT, epithelial cells loose cell-cell and cell-basement membrane contacts and reorganize the cytoskeleton to acquire a more mesenchymal phenotype, which promotes cell motility. Throughout EMT, epithelial markers (E-cadherin, occludins, claudins, etc) are down-regulated, whereas mesenchymal proteins are up-regulated (N-cadherin, Vimentin, etc). Snail (and/or Slug), Zeb and Twist1 transcription factors regulate it (Dongre et al., 2018).*

Several transcription factors are involved in the induction of EMT. Snail1/2 and Zeb1/2 transcription factors are the most important ones, although KLF8, Twist or FoxC2 play also a relevant function. Snail1 is usually expressed at the beginning of the EMT process, whereas Snail2, Zeb1/2 or Twist are usually induced to maintain the mesenchymal state (review in Thiery et al., 2009). Snail and Zeb directly bind to the E-cadherin promoter, repressing its activity, and enhance Wnt signaling by increasing β-catenin levels in the cytosol, due to the loss of E-cadherin (review by Thiery et al., 2009). Snail (1/2) also inhibits the expression of other epithelial markers, apart from E-cadherin, and promotes that of mesenchymal ones, such as fibronectin or vitronectin (De Herreros et al. 2010). Twist can also decrease E-cadherin expression and increase Fibronectin and N-cadherin expression through Snail-independent mechanisms (Zeisberg and Neilson 2009). Finally, Zeb family of proteins also increase the expression of genes encoding MMPs (Miyoshi et al. 2004), being important for cancer progression, cancer cell stemness maintenance,

aggressiveness, metastasis and angiogenesis (Sánchez-Trillo et al. 2011). To explore *in vitro* the mechanisms involved in EMT, several stablished models have been used, using TGF-β1 as the triggering signal, as it is a well-known inducer of EMT (Nieto et al., 2011; O'Connor and Gomez, 2014), also for HCC cells (Bertran et al., 2013). In fact, TGF-β is sufficient to induce *in vitro* EMT in epithelial cells (Brown et al., 2004) through both canonical (Smad-dependent) and/or non-canonical (p38 MAPK and JNK) signaling pathways (Derynck et al., 2014; Moustakas and Heldin, 2005; Lamouille et al., 2014).

4.5. Role of C3G in adhesion, migration and invasion

C3G plays a key role in integrin-mediated cell adhesion and spreading. Hence, C3G-deficient MEFs presented an impaired cell adhesion and spreading, while cell migration was enhanced (Ohba et al. 2001; Voss et al. 2003). C3G mediated adhesion was dependent on Rap1, while Rap1 activation by C3G was not sufficient for cell spreading (Ohba et al. 2001). In agreement with this, C3G overexpression promoted cell spreading and filopodia formation by a mechanism that involves C3G-c-Abl interaction and requires c-Abl catalytic activity (Radha et al. 2007).

In mammal cells, during integrin-mediated focal adhesion, multiprotein complexes are formed by association of proteins, such as C3G, Dock, Crk, p130Cas and/or Rap1 (Bos, 2005). Rap1 and its GEFs and GAPs are responsible for the spatio-temporal modulation of actin dynamics at focal adhesions through regulation of their localization and interactions with other intracellular proteins such as cadherins (Bos, 2005). Other protein complexes are also relevant for adhesion in specific contexts. For example, C3G/p38α promotes cell adhesion in CML K562 cells, although C3G and p38α also play antagonistic roles in the regulation of the expression of focal adhesion proteins, so that, while C3G knock-down impairs it, p38α silencing increases it (Maia et al. 2013).

C3G function in migration is context- and cell type-dependent. Thus, C3G-deficiency in MEFs enhanced migration (Ohba et al. 2001; Priego et al., 2016). C3G is also a negative regulator of migration in highly invasive breast carcinoma cells (Dayma and Radha 2011) or in colorectal cancer cells (Priego et al., 2016). In contrast, sympathetic preganglionic neurons migration is defective in a C3G mutant mouse model (Yip et al. 2012). Cortical neurons from C3G knock-out mouse embryos also failed to migrate (Voss et al. 2008). Moreover, C3G/Rap1 is required for migration of this type of neurons and for cortical development (Shah et al., 2016). C3G overexpression increases cell migration of glomerular epithelial cells in glomerulonephritis (Rufanova et al. 2009), too.

Finally, C3G can also regulate cell-cell interactions. For instance, it can bind intracellular E-cadherin to activate Rap1 and mediates E-Cadherin translocation to the plasma membrane (Pannekoek et al. 2009), so that, C3G can compete with β-catenin for the binding of E-cadherin cytoplasmic domain (Kooistra et al. 2007). Therefore, both β-catenin and E-cadherin can be regulated by C3G.

Our group described that C3G inhibits invasion in colorectal cancer HCT116 cells by down-regulating p38α activity through mechanisms that include MMP2/9 activities decrease (Priego et al., 2016).

5. HGF/Met signaling pathway

5.1. Generalities

HGF structure and function

HGF was initially identified as a strong mitogen for hepatocytes *in vitro* (Nakamura 1989). It is also known as scatter factor (SF), as it induces epithelial cell motility and scattering. It is secreted mainly by fibroblasts and smooth muscle cells (Stocker et al. 1987), but other cell types can contribute to its secretion.

HGF is a heterodimeric glycoprotein constituted by a heavy α and a light β chain (Nakamura 1989; Zarnegar et al. 1992). Its primary structure is 90% homologous in humans and rodents. HGF is secreted as an inactive protein (pro-HGF), which is cleaved by serine proteases, leading to an active disulfide-linked heterodimer (αβ-HGF) that binds to the Met receptor with high affinity (Patthy et al. 1984; Nakamura and Mizuno, 2010; Naldini et al. 1995; Nakamura et al. 2011).

HGF is produced during development and adulthood (Nakamura and Mizuno 2010). Specifically, in the liver, HGF is secreted by HSCs (Maher 1993), acting as either a paracrine or autocrine signal (Sonneberg et al. 1993; del Castillo et al. 2008).

HGF promotes bone remodeling, angiogenesis (Birchmeier et al. 2003; Nakamura et al. 2011), epithelial cells growth, motility (Bladt et al. 1995), cell invasion and polarization, and survival (Comoglio and Trusolino 2002; Zhang and Vande Woude 2003; Tulasne and Foveau 2008).

Met structure

Met was originally identified as a proto-oncogene (*TRP-MET*) in a human osteosarcoma-derived cell line (Cooper et al. 1984), generated by a chromosomal re-arrangement that leads to a truncated MET protein fused to TPR (*translocated promoter region*). Later, Met proto-oncogene was identified as the HGF receptor (Bottaro et al. 1991). Met receptor is synthesized as a precursor, which is cleaved, leading to a disulphide-linked α/β heterodimer. It is a tyrosine kinase receptor from the same heterodimeric family of receptors as Ron, Ryk and Sea (Huff et al. 1993; Ronsin et al. 1993; Gaudino et al. 1994; Maestrini et al. 1996).

The α chain together with N-terminal residues of β chain constitute the semaphorin (Sema) domain. The rest of the β chain includes the extracellular PSI (plexin-semaphorin-integrin) and IPT (immunoglobulin-plexin-transcription) domains, and the intracellular region, which includes: the juxtamembrane sequence, the catalytic region juxtamembrane sequence and the multifunctional docking site (Faria et al. 2011; Benvenuti and Comoglio 2007; Organ and Tsao 2011). The juxtamembrane sequence contains the negative regulator, Y1003 that once is phosphorylated, recruits the ubiquitin ligase c-CBL (casitas lineage lymphoma). The catalytic region contains the activating tyrosines Y1234/1235, which are phosphorylated in response to HGF. Finally, the multifunctional docking site bears Y1349/1356, which, upon phosphorylation, recruit several transducers and adaptors (Faria et al. 2011; Benvenuti and Comoglio 2007; Organ and Tsao 2011).

5.2. Function of HGF/Met pathway in the liver and hepatocarcinoma

In the liver, HGF/Met pathway plays an important role, not only during embryonic development (Schmidt et al. 1995; Uehara et al. 1995), but also during regeneration (Huh et al., 2004) and in pathological processes (Giebeler et al., 2009; Marquardt et al., 2012). HGF or Met knock-out mice show a defective embryonic development (Bladt et al. 1995), including liver organogenesis (Schmidt et al. 1995; Uehara et al. 1995). In the embryonic period, HGF/Met signaling induces hepatocyte growth (Nakamura et al., 2011), motility and differentiation, and liver morphogenesis (Fausto et al. 1995). In addition, sustained activation of HGF/Met pathway is implicated in liver tumorigenesis, tumor progression and metastasis (Bouattour et al., 2018; Hu et al., 2017; García-Vilas et al., 2018; Xie et al., 2001).

In the healthy liver, HGF is mainly secreted by HSCs. However, after liver injury, HGF is produced by proliferating liver sinusoidal endothelial cells in order to promote hepatocyte proliferation to allow liver regeneration (Kinoshita et al. 1989; Maher 1993).

Although in adult liver tissue, the loss of Met is not critical for hepatocyte functions, upon liver injury Met is essential to promote proliferation and survival of hepatocytes (Huh et al., 2004). Thus, the lack of this receptor can disrupt tissue remodeling, transforming acute into chronic injury (Borowiak et al. 2004; Huh et al. 2004; Phaneuf et al. 2004; Shiota et al. 1994). The HGF/Met axis is also hepatoprotective in the context of liver fibrosis. It inhibits pro-fibrotic signals such as TGF-β (Xia et al., 2006; Inagaki et al. 2008; Ueki et al., 1999), promotes ECM resolution (Kanemura et al., 2008), induces myofibroblasts apoptosis (Kim et al., 2005) and survival of hepatocytes (Marquardt et al. 2012; Gieveler et al. 2009).

Finally, HGF/Met pathway is also involved in HCC tumorigenesis (Goyal et al. 2013), and Met overexpression is found in 20-50% of human HCC (Boix et al. 1994; Kiss et al. 1997), which is associated to poorly differentiated HCC. Thus, Met overexpression constitutes a signature found in a subclass of human HCC with poor prognosis and aggressive

phenotype (Daveau et al. 2003; Kaposi-Novak et al. 2006). HGF/Met activation is required for acquisition and maintenance of mesenchymal features and cancer stem cell properties (You et al. 2011). Moreover, Met crosstalk with other RTKs such as EGFR or VEGFR favors tumor survival (Venepally and Goff 2013). Hence, much effort has been put to develop Met inhibitors and combinatorial therapies for the treatment of HCC that can overcome resistance to already used drugs in clinical practice such as sorafenib (García-Vilas and Medina, 2018; Okuma and Kondo, 2016; Granito et al., 2015).

5.3. Effectors of HGF/Met signaling

In response to HGF, Met receptor is activated, leading to its autophosphorylation, which allows its interaction with several proteins through its multidocking site (Y1349/1356), present in the C-terminal region, below the catalytic domain. The main Met-binding substrates are the following (Furge et al., 2000; Trusolino et al., 2010; Bolanos-García, 2005) (Figure VII):

-Gab1 (Grb2-assossiated-binder-1) that binds through its PH (Pleckstrin homology) domain (see below for details).

-Grb2, which can either interact directly through its SH2 domain or indirectly through Shc adaptor.

-Shc that associates directly through its PTB (Phosphotyrosine binding) or SH2 domain.

-Src tyrosine kinase that contains both SH2 and SH3 domains, binds through the SH2 domain.

-STAT3 transcription factor can bind Met directly through its SH2 domain or through Gab1 adaptor.

-PLCγ (phospholipase C) interacts directly or through Gab1 adaptor.

-PI3K (phosphatidylinositol 3-kinase), through its p85 subunit adaptor subunit, binds directly or through Gab1 adaptor.

-SHP2 (Src homology -2(SH2)-containing protein tyrosine phosphatase 2), a tyrosine phosphatase that interacts directly or indirectly through Gab1.

-CrkI and CrkL bind indirectly through Gab1.

The spatio-temporal interaction with the mentioned specific adaptors and/or effectors allows the activation of a great variety of biological responses by HGF/Met. For example, PI3K-mediated Akt activation promotes cell survival and liver regeneration, cell growth, protein translation and proliferation. Sos recruitment by Grb2 activates Ras and subsequently, ERKs, which impairs TGF-β pro-fibrotic activity and leads to proliferation and transformation. PI3K/Rac/JNK cascade induces cell transformation, apoptosis and anchorage-independent growth and PI3K/Rac/p38 MAPK pathway leads to proliferation,

transformation, differentiation, migration, survival or apoptosis. Additionally, Src can act as either an adaptor to recruit other proteins or as an activator of other protein kinases, such as FAK, resulting in cell invasion, motility or transformation (Trusolino et al., 2010; Furge et al. 2000; Bolanos-García, 2005). Also, Crk and CrkL can activate downstream pathways such as C3G/Rap1 or Dock180/Rac/JNK, implicated in cell motility (Furge et al., 2000; Feller et al., 1998; Rodrigues et al., 1997). Other proteins, such as Shc can lead to either migration (through its PTB domain) or mitogenesis (through its SH2 domain), SHP2 promotes liver regeneration, and STAT3 activates cell proliferation, and transformation. On the other hand, PLCϒ can inhibit Met pathway in a PKC-dependent manner (Trusolino et al., 2010; Furge et al. 2000; Bolanos-García, 2005) (Figure VII).

Grb2-associated-binder (Gab) proteins, Gab1, Gab2 and Gab3, belongs to a family of scaffolding proteins that act as RTKs adaptors through their binding to the docking sites created by tyrosine phosphorylation, leading to activation of different signaling pathways. Gab proteins are members of the insulin receptor substrate 1 (IRS1)-like multi-substrate docking adaptor protein family (Wang et al., 2015). Gab1 and Gab2 are ubiquitous, while Gab3 levels are particularly high in lymphoid tissue.

Structurally, Gab proteins contain a PH domain at the N-terminal region, two proline-rich sequences (PXXP), or three, in the case of Gab1, which are potential docking sites for proteins containing SH3 domains and tyrosine-based motifs that allow multiple tyrosine phosphorylation. Gab1 (100-120 kDa) also contains serine and threonine residues that can be phosphorylated by PKC-α and PKC-β1, leading to a negative modulation of HGF signaling. In addition, Gab1 contains a Met-binding sequence (MBS) (from amino acid 487 to 499), which allows the direct interaction with tyrosine phosphorylated Met, while most RTKs recruit Gab1 indirectly through Grb2 SH2 domain (Wang et al., 2016). Gab1 is an adaptor for various receptors, such as those for VEGF, HGF, NGF, PDGF or EGF cytokines, etc (Nishida and Hirano, 2003; Sármay et al., 2005). Gab1 transduces the activation of several RTKs into important and diversified biological responses through the association, upon phosphorylation, to SH2 domain-containing proteins, such as SHP2, PI3K through p85 regulatory subunit, PLC, Crk, Shc or GC-GAP (Wang et al., 2015). Moreover, in HEK293 cells overexpressing Gab-1, it has been described that HGF-induced Met activation binds to and phosphorylates Gab1 protein, which in turn leads to the interaction with Crk and CrkL SH2 domain through its Tyr-X-X-Pro motif at the multisite docking site. Crk uses its first SH3 domain to recruit C3G leading to Rap1, a mechanism possibly linked to cell migration (Furge et al., 2000; Sakkab et al., 2000). Previously, it was reported that the formation of the P-Met/P-Gab1/Crk complex upon HGF stimulation leaded to Rac1-mediated JNK activation that could be involved in Met-dependent tumorigenesis, and it was suggested that C3G, DOCK180 or Sos might be potential mediators for the interaction between Crk and Rac1, although it was not demonstrated (García-Guzman et al., 1999). It was also found in MDCK cells that, in response to HGF, a complex containing P-Met and CrkII/CrkL-C3G activated Rac1 and Rap1, promoting an EMT process, cell dissemination, loss of tight junctions, showing that CrkII overexpression induced β-catenin internalization (Lamorte et al., 2002).

Abl family comprises Abl (*ABL1*) and Arg (*ABL2*), which are non-receptor tyrosine kinases that can link activated Met to the RhoA signaling, resulting in the regulation of Met-dependent functions such as cell scattering, tubulogenesis, migration and invasion (Li et al., 2015). Moreover, Abl mediates the interaction between Met and p53 pathways in gastric cancer and HCC, including Hep3B cells (Furlan et al., 2011). Additionally, during liver development, both Abl and p38 MAPK pathways are required downstream of Met receptor to allow embryonic hepatocytes survival through p53 regulation (Furlan et al., 2012).

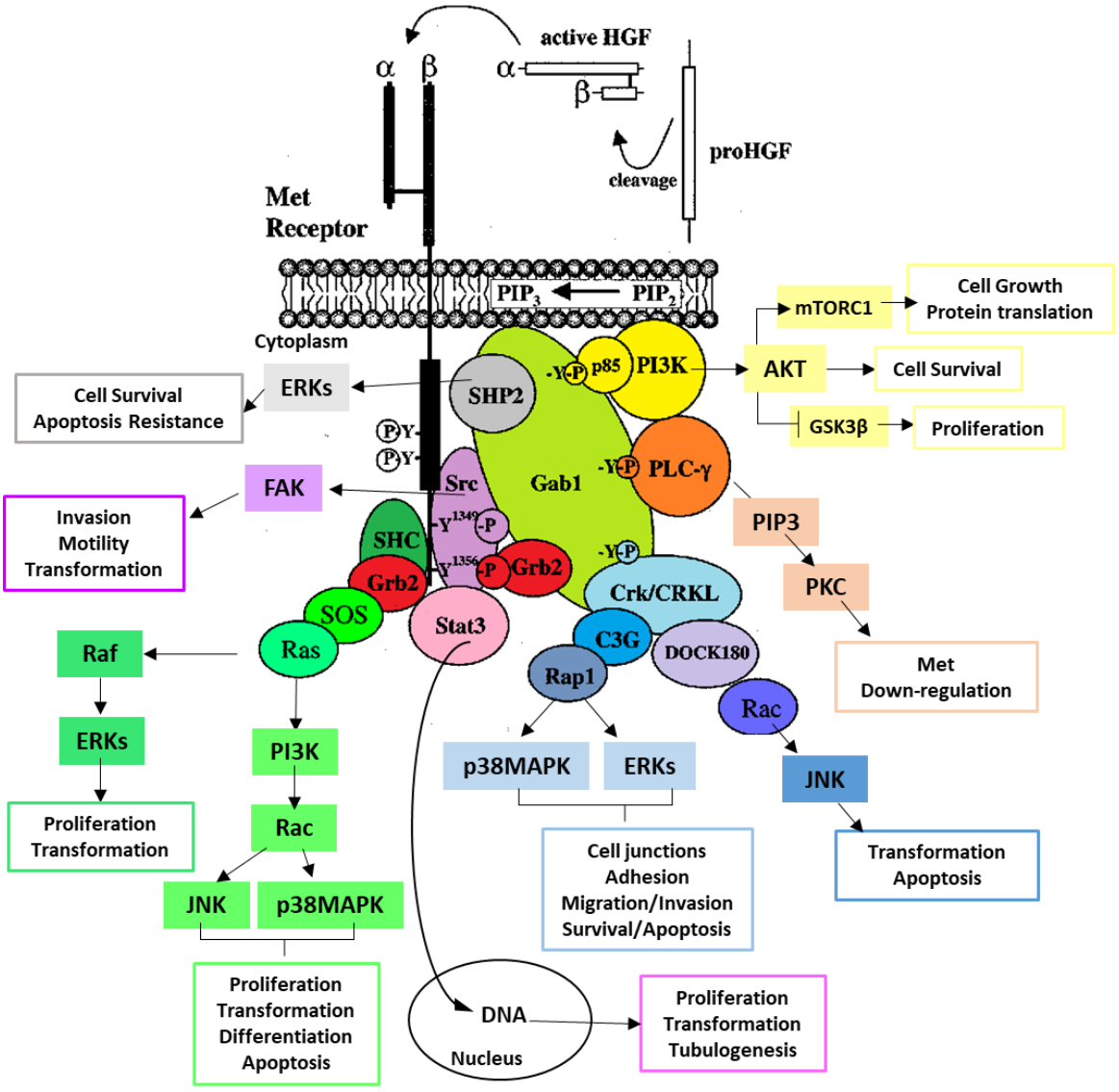

Figure VII. HGF/Met signaling pathway. *Met activated by HGF is autophosphorylated, enabling the binding of adaptors and other proteins to the multidocking site, either directly or indirectly. This results in the activation of several downstream signaling pathways, which allows the regulation of multiple biological functions depending on the cell-type, context, etc (modified from Furge et al., 2000).*

Due to the plethora of downstream pathways activated by Gab1 adaptor, once Met is activated, important physio- and pathological biological functions are mediated by Gab1, being essential for embryonic development in a similar way than Met (Sachs et al., 2000).

In colorectal cancer, when Met is overexpressed, Gab1 promotes tumor progression in a Grb2-independent manner (Seiden-Long et al., 2008). In hepatocytes maintained in culture, Gab1 acts as a signal amplifier for low-intensity stimulation by HGF (Aasrum et al., 2015).

Taking into account the previously described data from the literature, it seems that the determinant point that makes Met-mediated human tumorigenicity, tissue- or cell-specific, is the selectivity towards particular adaptor proteins downstream of Met (Seiden-Long et al., 2008) and other RTKs. Therefore, this explains the increasing interest in developing anti-cancer treatments targeting Gab1, using inhibitors of protein-protein interactions, among other therapies (Simister and Feller, 2012; Yart et al., 2003).

5. BACKGROUND AND PREVIOUS RESULTS FROM THE GROUP

1. Function of C3G in the regulation of cell death and survival through the control of p38α MAPK activity.

p38 MAPKs can mediate either cell death or survival (Nebreda and Porras, 2000), depending on cell type, stimulus or the p38 isoform implicated (Wagner and Nebreda, 2009). Our group, using cells deficient in p38α MAPK isoform, contributed to characterize the role played by p38α MAPK in cell death/survival balance and its crosstalk with other signaling pathways. Thus, in both embryonic cardiomyocytes and MEFs generated from p38α knock-out mice, our group reported that p38α plays a key role promoting apoptosis in response to various stimuli, mediated by both up-regulation of pro-apoptotic proteins and down-regulation of survival pathways, such as ERKs (Porras et al., 2004) and Akt (Zuluaga et al., 2007).

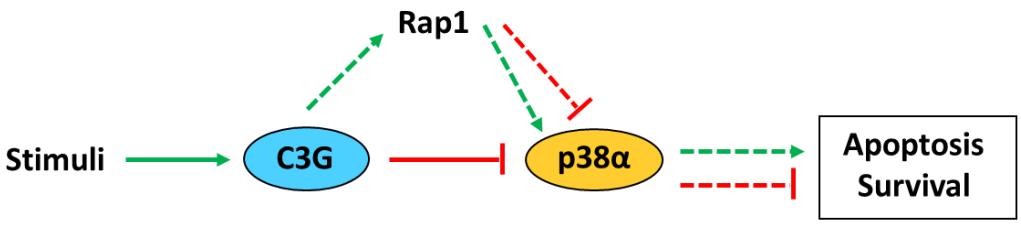

Figure A. C3G regulates cell death/survival balance through down-regulation of p38α activity via Rap1 dependent or independent mechanisms. *Model showing the negative regulation of p38α activity by C3G through a Rap1 dependent or independent mechanism, leading to different outcomes, either cell apoptosis or survival, depending on the stimuli and/or cell type.*

p38α acting through p53 also induces cell death in colorectal cancer HCT116 cells in response to cisplatin (Bragado et al., 2007). Based on these studies on p38α, in collaboration with Dr. Guerrero's group, a crosstalk between p38α and C3G in the control of apoptosis and survival was uncovered. Thus, in CML K562 cells, C3G down-regulation enhances Imatinib-induced apoptosis through the up-regulation of p38α activity mediated by a Rap1-dependent mechanism (Maia et al. 2009). In MEFs, C3G knock-down also increases p38α activation, inducing either survival in response to oxidative stress or cell death upon serum-deprivation, but through a Rap1-independent mechanism (Gutiérrez-Uzquiza et al., 2010) (Figure A). More recently, our group also found that p38α mediates survival in response to oxidative stress in different cellular contexts (Gutiérrez-Uzquiza et al., 2012; Arechederra et al., 2013).

2. C3G as a regulator of cell adhesion and migration in non-tumor and tumor cells. Cross-talk with p38α MAPK.

Our group has also found that the functional interaction between C3G and p38α also takes place in the control of cell adhesion and migration. Hence, in collaboration with Dr. Guerrero's laboratory, our group reported that in CML K562 cell line, C3G and p38α interact and collaborate to promote cell adhesion through a common regulatory pathway, although they display antagonistic effects in the regulation of the expression and activation of focal adhesion proteins (Maia et al., 2013).

Based on these data, it was explored whether C3G might also be acting through p38α to regulate cell migration and invasion in MEFs and colorectal cancer cells. It was demonstrated that in MEFs C3G through down-regulation of p38α activity, leads to inhibition of cell migration and invasion through a mechanism not mediated by Rap1. In fact, Rap1 exhibits opposite effects (Priego et al., 2016) (Figure B). Similarly, in CRC HCT116 cell line, C3G knock-down highly decreases adhesion, while promotes cell migration and invasion through the up-regulation of p38α activity via Rap1, which it is likely activated by other RapGEFs as a compensatory mechanism (Priego et al., 2016). These effects of C3G down-regulation in migration involves ZO-1 internalization, E-cadherin loss and re-organization of F-actin cytoskeleton. Moreover, the inverse correlation between C3G protein levels with the invasive capacity of different human CRC cell lines also supports the role of C3G as a negative regulator of migration in CRC cells (Figure B).

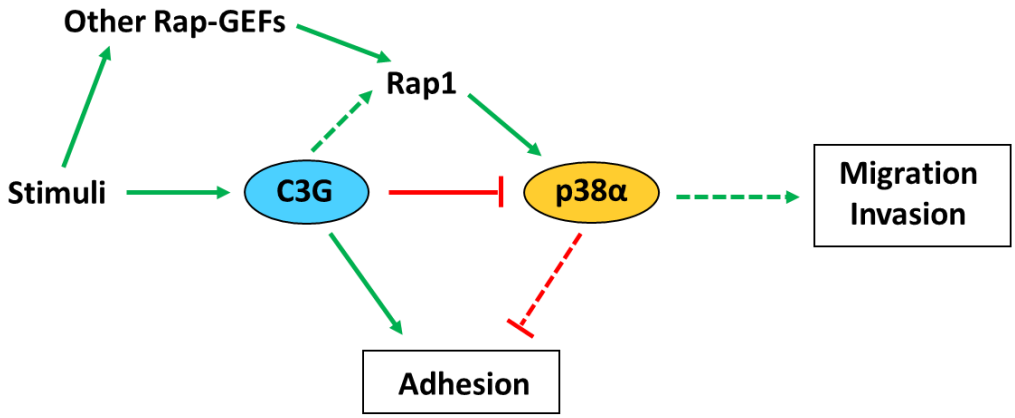

Figure B. C3G decreases cell migration and invasion in MEFs and CRC cells through down-regulation of p38α activity. *The scheme shows that C3G inhibits migration and invasion through down-regulation of p38α activity, while favors adhesion. Rap1 mediates p38α hyperactivation in C3G silenced CRC cells.*

3. Role of C3G in tumor growth of colorectal cancer cells.

Our group has also uncovered a pro-tumorigenic function of C3G in colorectal cancer using HCT116 cells as a model (Priego et al. 2016). In these CRC cells, *in vitro* and *in vivo* studies revealed that both C3G and p38α promote tumor growth through independent mechanisms, so that the silencing of both C3G and p38α have an additive effect in xenograft tumors. This pro-tumorigenic action of C3G is most likely dependent on an increased survival, and adhesion. Moreover, Rap1 does not mediate C3G pro-tumorigenic effect, but rather decreases *in vitro* tumor growth (Priego et al., 2016) (Figure C).

Taking into account the inhibitory effect of C3G on migration and invasion described above, and its tumorigenic function in CRC, C3G plays a dual role in colorectal cancer through different mechanisms. Thus, while down-regulation of p38α activity mediates the inhibition of migration and invasion elicited by C3G, both p38α and C3G promotes tumor growth through independent mechanisms.

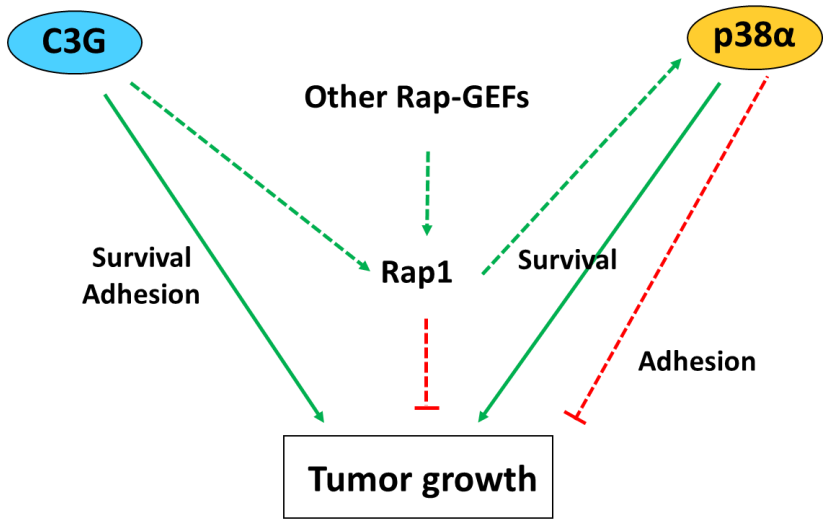

Figure C. C3G and p38α promote tumor growth through independent pathways in CRC. *Schematic representation shows that C3G promotes cell survival and adhesion, favoring tumor growth through mechanisms independent of p38α or Rap1. p38α also induces tumor growth by increasing survival.*

6. AIMS

General Aim:

The main objective of this research project is to analyze the role played by C3G in hepatocarcinoma (HCC) tumor growth, progression, dissemination and generation of metastasis using different human and mouse models to identify the mechanisms involved.

Specific Aims:

1. To determine whether C3G (RapGEF1) expression is altered in human and mouse HCC tumors and cell lines, as well as to identify the existence of potential genetic alterations in this gene.

2. To analyze the function of C3G, *in vitro* and *in vivo*, using human and mouse HCC cell lines and mouse models, characterizing its role in the regulation of the tumorigenic, migratory and invasive capacities of HCC cells.

3. To identify the molecular mechanisms involved in the actions of C3G in HCC.

7. MATERIALS AND METHODS

1. Cell Culture

1.1. Cell lines

1.1.1. Human and Mouse Cell lines

For experimental research the following human and mouse cell lines were used:

Human cell lines:

- **Hep3B** (ATCC HB-8064), human hepatocarcinoma cell line from an 8-year-old black male, adherent cells with epithelial phenotype, containing an integrated Hepatitis B Virus genome and have tumorigenic properties.

- **HLE** (JCRB0404), human hepatoma non-differentiated cell line from a 68-year-old male, adherent cells with mesenchymal phenotype.

- **Huh7** (JCRB0403), human well differentiated hepatocyte derived cellular carcinoma cell line, from a 57-year-old Japanese male, adherent cells with intermediate phenotype between epithelial and mesenchymal, and tumorigenic properties.

Mouse cell lines:

- **mHCC1, 13 and 14** cells derived from a mouse genetic model that overexpresses Met receptor in hepatocytes under the Albumin promoter (mouse *Alb-R26*^{Met} HCC cells) and were selected by their ability to grow as tumor spheres (Fan, 2017; Arechederra, 2018).

1.1.2. Permanent C3G gene silencing of human hepatocarcinoma cells

C3G was stably knocked-down in Hep3B, HLE and Huh7 cells by infection with human C3G shRNAs lentiviral particles containing a mixture of different shRNAs (Santa Cruz Biotechnology sc-29863-V) or a control shRNA (Santa Cruz Biotechnology sc-108080) for non-silenced cells. Cells were seeded 24 h prior to the viral infection at a density that guaranteed 50-60% confluence the next day. Then, the medium was replaced and 75.000 infectious units of lentiviral particles were added in the presence of 10 μg/ml Polybrene (Santa Cruz Biotechnology sc-134220). Cells were incubated overnight and the medium was replaced by a fresh one. After 48 h cells were selected with 2 μg/ml puromycin (Panreac A2856).

Permanent silencing of C3G was verified by western-blot analysis of C3G using C3G H300 antibody (Santa Cruz Biotechnologies sc-15359).

1.1.3. Generation of mouse hepatocarcinoma cell lines with Met overexpression and C3G silencing

Mouse HCC cell lines were originated in Dr. Maina's group from a genetic model that overexpresses Met receptor in the liver, specifically in the hepatocytes under the control of Albumin promoter (mouse *Alb-R26^{Met}* HCC cells) (Fan, 2017; Arechederra, 2018). This overexpression leads to the spontaneous formation of liver tumors that recapitulate human HCC (proliferative subtype, progenitor subclass). Different cell lines were established from those tumors and used as an *in vitro* mouse HCC model. Three of these cell lines (mHCC1, mHCC13, and mHCC14) were kindly provided by Dr. Maina to perform *in vitro* and *in vivo* assays. A permanent C3G knock-down was carried out in mHCC1 cells through transfection with a mouse PRSshC3G (PRetroSuper vector), selecting the cells with puromycin as previously mentioned in section 1.1.2. We worked with the most efficient selected clones.

1.2. Cell culture conditions and cryopreservation

1.2.1. Culture conditions

Hep3B and Huh7 cell lines were grown in DMEM (4.5 g/l glucose) medium (Lonza 12-604F) and HLE cell line in RPMI-1640 medium (Lonza BE-12-702F), both supplemented with 10% fetal bovine serum (FBS) (Gibco 10270106), 20 mM Hepes (pH 7.4), 12 µg/ml penicillin G (Sigma 13752), 10 µg/ml streptomycin (Sigma S9137) and 0.25 µg/ml amphotericin B (Sigma A2942). mHCC cell lines were grown in Williams E (-) L-Glutamine culture medium (Lonza BE-12-761F) with 10% FBS, 1% Glutamine, 0.5% Glucose, 0.5% sodium pyruvate, 1% antibiotics (12 µg/ml penicillin and 10 µg/ml streptomycin), Dexamethasone (Sigma D4902; 0.4 µg/ml), and in the moment of use Insulin (Sigma I0516; 10 µg/ml), HGF (R&D 2207-HG-025; 10 ng/ml) and EGF (R&D 236-EG-200; 20 ng/ml) were added to the culture medium.

Cells were grown in the presence of puromycin (1 µg/ml) when selection of knock-down cells was required, but it was removed 48h prior to the experiments. All cell lines were maintained at 37ºC with 5% CO_2 in a humidified atmosphere.

Cells were split for maintenance or for doing experiments by trypsinization with 0.25% Trysin-0.02% EDTA (Hyclone SH30042.02), stopping trypsin action with 10% FBS culture medium.

1.2.2. Cryopreservation and thawing of cells

Cells were centrifuged and resuspended in 10% DMSO-FBS and transferred to a cryopreservation vial that was progressively frozen at -20ºC for 30 min, -80ºC overnight and finally stored in liquid nitrogen (-170ºC).

Thawing of cells was performed quickly in a 37ºC water bath, and cells were seeded in a plate with complete culture medium.

1.3. Cell treatments

1.3.1. Inhibitors

Chemical Inhibitor	Inhibits	Final Concentration	Reference
SB203580	p38α and p38β	5µM to inhibit p38α 10µM to inhibit p38α/β	Calbiochem 559389
SU11274	Met	5 µM	Sigma S9820
SB431542	TGF-β receptor type I	10 µM	Sigma 616464
PD98059	MEK	10 µM and 20 µM	Calbiochem 513000
Mitomycin C	Proliferation	25 µg/ml	Sigma M0503
Imatinib	Abl	10µM	Sigma SML 1027

1.3.2. Treatment with growth factors

Growth Factor	Final Concentration	Reference
mHGF	40 ng/ml	R&D, 2207-HG-025
hTGF-β1	5 ng/ml for EMT induction 2.5 ng/ml for EMT maintenance	Preprotech, AF-100-21C

2. Protein analysis

2.1. Protein extraction and preservation

Culture dishes were kept on ice along this process. First, culture medium was either discarded or stocked in Eppendorf tubes and immediately stored at -80ºC, when necessary for future determinations. Cells were washed twice with cold Phosphate Buffer Solution (PBS) and IP lysis buffer was added:

IP Lysis Buffer Composition	
Tris pH 7.5	50 mM
NaCl	150 mM
Nonidet NP-40	1%
EGTA	5 mM
EDTA	50 mM
PMSF	1 mM
Aprotinin	10 µg/ml
Leupeptin	10 µg/ml
Na_3VO_4	1 mM
NaF	20 mM

Cells were detached from the plate with the help of a scraper, recovered in a pre-chilled Eppendorf tube, and maintained on ice for 20 min, vortexing every 5 min. Cells lysates were, then, centrifuged at 13000 rpm for 10 min at 4ºC and the supernatant containing the total protein extract was transferred to a new tube for storage at -80ºC and the pellet was discarded.

For frozen tissue protein extraction, the samples were reduced to powder with the help of a porcelain mortar kept on dry ice. Sample powder was collected into an Eppendorf tube with RIPA lysis buffer:

RIPA Lysis Buffer Composition	
Sodium Deoxycholate	1%
Tris pH 7.5	10 mM
SDS	0.1%
NaCl	150 mM
EDTA	2 mM
NP-40	1%
Triton X-100	1 mM
PMSF	1 mM
Aprotinin	10 µg/ml
Leupeptin	10 µg/ml
Na_3VO_4	100 µM
NaF	50 mM

Samples were then maintained on ice for at least 20 min, vortexing every 5 min. Cell lysates were then treated as previously explained for IP lysis buffer.

2.2. Protein quantification

Proteins were quantified using either Bradford or Bicinchoninic acid (BCA) method. In both cases, a blank and a standard curve of known concentrations of Bovine Serum Albumin (BSA) was prepared (0 to 10 μg) for each experiment.

Samples extracted with IP Buffer were quantified using the method described by Bradford in 1976. 5 min after the addition of Bradford reagent (Sigma S6916), absorbance was measured at 595 nm.

Samples extracted with RIPA buffer, were quantified with BCA method using the Thermo-Fisher kit (10341664, 10495944 and 10753505). In a 96-multiwell plate, 10 µl of each sample was pipetted in duplicate and 200 µl/well of the BCA reactive was added that was prepared as follows: Reactive A and B were mixed in a 1:1 proportion; then, Reactive A+B was mixed with Reactive C in a 50:1 proportion. Absorbance was measured at 562 nm.

2.3. Western-blot analysis

2.3.1. Protein electrophoresis

Protein electrophoresis was either performed with SDS-polyacrylamide gels (SDS-PAGE) or with non-SDS-polyacrylamide gels (Anderson gels). The latter allows a better separation of phosphorylated proteins with similar electrophoretic mobility. The concentration of acrylamide in the separation gel was determined by the target protein size. So that, for proteins with small molecular weights (25-80 KDa), higher percentages of acrylamide were used (12-15%), while for higher molecular weights (>80 KDa), a lower percentage of acrylamide were used (8-10%).

SDS-PAGE gels composition (Vf = 10ml)				
Composition	**Separating Gel 10%**	**Separating Gel 12%**	**Separating Gel 15%**	**Stacking gel (Vf = 5ml)**
30% Acrylamide/ Bisacrilamide	3.3 ml	4 ml	5 ml	0.83 ml
H_2O	4 ml	3.3 ml	2.3 ml	3.4 ml
1.5 M Tris pH 8.8	2.5 ml	2.5 ml	2.5 ml	-
Tris 1 M pH 6.8	-	-	-	0.63 ml
10% SDS (w/v)	100 µl	100 µl	100 µl	50 µl
10% Ammonium Persulfate	100 µl	100 µl	100 µl	50 µl
TEMED	4 µl	4 µl	4 µl	5 µl

Anderson gels composition (Vf = 10ml)				
Composition	**Separating Gel 7.5%**	**Separating Gel 10%**	**Separating Gel 15%**	**Stacking gel (Vf = 5ml)**
30% Acrylamide	2.52 ml	3.36 ml	5.03 ml	0.833 ml
1% Bisacrilamide	1.95 ml	1.31 ml	0.87 ml	0.667 ml
H_2O	3.02 ml	2.82 ml	1.59 ml	2.875 ml
1.5 M Tris pH 8.8	2.52 ml	2.52 ml	2.52 ml	-
Tris 1 M pH 6.8	-	-	-	0.625 ml
10% Ammonium Persulfate	50 µl	50 µl	50 µl	50 µl
TEMED	5 µl	5 µl	5 µl	5 µl

For protein sample preparation, Laemmli buffer 4x (Tris-HCl pH 7.6, 10% glycerol, 1% SDS, 0.002% Bromophenol blue and 2 mM β-mercaptoethanol and DTT) was added to the samples. Then, they were boiled 5 min at 95ºC. Samples were then loaded into the gel, as well as a molecular weight marker. Electrophoresis was developed at 90-120 V using the following running buffers:

-For SDS-PAGE gels: 25 mM Tris-HCl (pH 8.3), 200 mM Glycine and 0.1% SDS.

-For Anderson gels: 50 mM Tris-HCl (pH 8.3), 400 mM Glycine and 0.1% SDS.

2.3.2. Protein transfer

Proteins from the gels were transferred to a nitrocellulose membrane (Amersham 15259794) activated with distilled water, using a semi-dry equipment (BioRad 1703940). Transfer was assembled as follows (from bottom to top): Whatmann papers (3 layers), nitrocellulose membrane (GE Healthcare Amersham 15259794), acrylamide gel and Whatmann papers (3 layers), all previously soaked in semi-dry transfer buffer (20% methanol, 50 mM Tris, 400mM Glycine and 0.1% SDS). Then, an electrical current of 15 V was applied for 30-45 min/gel depending on the size of the gel and the proteins of interest. The resulting membrane was stained with Ponceau S (0.5% in 1% Tricloroacetic acid) to confirm a correct protein transfer.

2.3.3. Immunodetection

Membranes were washed with TTBS (Tween-Tris-buffered saline: 10 mM Tris-HCl, 150 mM NaCl, 0.05% Tween-20, pH 7.5), and incubated in blocking solution (5% skimmed milk in TTBS) for 1h at RT or o/n at 4ºC for P-Met. After washing with TTBS, membranes were incubated with the primary antibody in 0.5% BSA-TTBS or skimmed milk-TTBS) at a 1/500-1/1000 dilution (depending on the antibody) for 1h at RT for total proteins or o/n at 4ºC

for phosphorylated proteins. After washing with TTBS (10 min, 3 times), membranes were incubated with the secondary antibody, anti-rabbit (Cell Signaling 7074) or anti-mouse antibody (Cell Signaling 7076) conjugated with HRP (Horseradish Peroxidase) at a dilution of 1/2000-1/5000 in 0.5% BSA-TTBS for 1h at RT. Membranes were washed as previously and proteins were visualized by incubating with a chemiluminescent- HRP substrate (Thermo Fisher 32106 and BioRad 170-5061) and developed using X-Ray films (Thermo Fisher 34089) or digitally (VWR Imager Chemi Premium).

Primary Antibodies				
Antibody	**Laboratory**	**Isotype**	**Molecular Weight (kDa)**	**Reference**
Met (D1C2) XP	Cell Signaling Technology	Rabbit	140	8198
P-Met (Tyr 1234/1235)	Cell Signaling Technology	Rabbit	145	3126
c-Abl (8E9)	Santa Cruz Biotechnology	Rabbit	135	sc-56887
P-Abl (Tyr 412)	Cell Signaling Technology	Rabbit	135	2865
C3G H300	Santa Cruz Biotechnology	Rabbit	130	sc-15359
C3G G-4	Santa Cruz Biotechnology	Mouse	130	sc-17840
C3G Custom prepared (N-terminal region)	Genosphere Biotechnologies	Rabbit	130	Polyclonal raised against amino acids 4-245
Gab1	Cell Signaling Technology	Rabbit	110	3232
P-Gab1 (Tyr627)	Cell Signaling Technology	Rabbit	110	3231
P-Akt (Ser 473)	Cell Signaling Technology	Rabbit	60	9271
ERKs	Cell Signaling Technology	Rabbit	42, 44	9102
P-ERKs (Thr202/Tyr204)	Cell Signaling Technology	Rabbit	42, 44	9101
p38α (C-20)	Santa Cruz Biotechnology	Rabbit	38	sc-535
P-p38 MAPK (Thr180/Tyr182)	Cell Signaling Technology	Rabbit	38	9211
β-Actin	Cell Signaling Technology	Mouse	45	3700
β-Tubulin	Cell Signaling Technology	Mouse	55	2146
N-Cadherin	BD Biosciences	Mouse	130	610920
Vimentin	BD Biosciences	Mouse	57	550513
Occludin	Invitrogen	Rabbit	65	71-1500
CrkL (C-20)	Santa Cruz Biotechnologies	Rabbit	39	sc-319

3. Protein-protein interaction analysis

3.1. Immunoprecipitation

Total protein extracts (1000-2000 µg) diluted to a final volume of 400-500 µl in lysis buffer were used for immunoprecipitation assays. Proteins were incubated with a specific antibody in a 1:25 or 1:50 dilution for 3h on ice, gently shaking the samples from time to time. Then, 40 µl of 50% v/v Protein A Sepharose (GE healthcare 17-0780-01) or Protein G agarose beads (Roche 11 719 416 001), for rabbit or mouse IgGs, respectively, were added, which were previously rinsed with lysis buffer. Samples were rotated for 2-4 h at 4ºC and the immune complexes were collected by centrifugation at 14 000 rpm for 1-2 min at 4ºC. The supernatants were removed and the beads resuspended in fresh lysis buffer. This was performed three times to rinse the immunoprecipitates. Finally, the bead pellets with the immune complexes were resuspended in 20 µl of Laemmli buffer 4x and boiled for 5 min. Samples were analyzed by western-blot.

3.2. Expression of GST-fused proteins and pull-down assay

An alternative method to immunoprecipitation to study protein-protein interactions is the pull-down of proteins that interact with a specific substrate (protein or domain) bound to a solid base (beads). Specifically, we used as substrates, fusion proteins constitute by the enzyme Glutathione S- transferase (GST) and either C3G SH3-b domain, CrkL SH3 domains or E-cadherin C3G-binding domain. For control purposes, GST alone was used. All these substrates were bound to glutathione sepharose beads.

cDNAs encoding the mentioned GST-fused proteins were inserted into an expression vector to transform BL21 competent E. coli cells, which were grown in LB (Luria-Bertani broth) medium supplemented with ampicillin (100 µg/ml) at 37ºC and shaking (200 rpm) until a 0.4-0.6 O.D at 600 nm was reached, corresponding to logarithmic growth phase. Then, IPTG (Isopropil thiogalactopiranoside; Sigma I6758) was added to the culture at a final concentration of 0.2 mM and incubated for 2-3 additional hours. Then, bacteria pellet was lysed and GST-fused proteins were purified and bound to Glutathione Sepahrose 4B beads (Healthcare 4510) and stored at 4ºC in a concentration of 50% v/v in PBS-0.2% PMSF.

For pull-down assays, first, a pre-clearing of cell lysates was performed, incubating cell lysates with 40 µl of pre-rinsed glutathione beads 10 min at 4ºC to eliminate potential non-specific binding. Supernatants were recovered after a 10 sec spin down at 13000 rpm at 4ºC. Then, the lysates (1000-2000 µg of protein in a final volume of 400-500 µl) were incubated with rotation with 40 µl beads bound to GST-fused protein for 2 h at 4ºC.

Samples were centrifuged at 13000 rpm for 1 min at 4ºC, the supernatant was discarded and the beads were washed three times with lysis buffer. Finally, the beads were resuspended in 20 µl of sample buffer, boiled 5 min and loaded in an SDS-PAGE gel for their analysis by western-blot.

4. β-catenin analysis by immunofluorescence

Cells were seeded in circular glass coverslips pre-coated with gelatin 2% (Sigma G9391) and were allowed to grow until desired confluence in culture medium supplemented with 10% FBS, and then, were serum- starved for 24h). Cells were washed with PBS twice, fixed with 4% paraformaldehyde (PFA) (Sigma 158127) in PBS for 20 min at RT and washed with PBS. Cells were permeabilized by incubation with PBS containing 0.1% Triton TX-100 (Sigma X-100) and 0.1% BSA (Panreac A1391) for 20 min at RT. Then, cells were incubated with blocking solution (5% BSA in PBS) for 1h at RT. Next, cells were incubated with β-catenin antibody (BD Bioscience 610154) at a dilution 1/50 in 1% BSA PBS for 1h to o/n at 4ºC. Then, cells were washed with PBS and coverslips were incubated with anti-mouse FITC secondary antibody diluted 1/200 (Sigma F0257) and DAPI (dilution 1/1000, Panreac A4099) in 0.1% BSA-PBS. After washing with PBS, cells were mounted with mounting medium (Ibidi 50001) and images were captured using an immunofluorescence microscope (Nikon Eclipse TE300) coupled to a camera.

5. Analysis of mRNA expression

5.1. RNA extraction and quantification

Cells were washed twice with cold PBS and total RNA was isolated using RNA isolation kit from Mackerey-Nagel (MN 22740955) following manufacturer instructions. This kit includes a step of DNase treatment to avoid genomic DNA contamination. RNA was collected in a clean Eppendorf by elution from the isolation column with ultrapure autoclaved water and stored at -80ºC until use. RNA quantification was performed by measuring the absorbance of the samples at 260 nm in a spectrophotometer (one unit of absorbance at 260 nm corresponds to 40 µg of RNA per ml). RNA purity was estimated by calculating the ratio A_{260}/A_{280}. RNA was accepted as pure when A_{260}/A_{280} = 1.8-2.

5.2. Retro-transcription

SuperScript III RT Kit (Invitrogen 18080-040) was used to reverse-transcribe 1-3 µg of total RNA into cDNA, following instructions from the manufacturer. Briefly, RNA was incubated

with oligo(dT) (0.5mM) and dNTPs, 5 min at 65ºC, to ensure RNA denaturation and then, placed on ice for 1 min. Samples were incubated with cDNA synthesis mix (5X RT buffer, 20 Units of RNase inhibitor (Promega N2115), 5mM DTT and 200 Units of SuperScript III) 1h at 50ºC. In order to stop the reaction, enzyme was inactivated by heating at 70ºC for 15 min. cDNA was stored at -80ºC until use.

5.3. Real Time PCR

Real time PCR (or quantitative PCR, qPCR) reactions were performed in triplicate using specific primers (see Table below) and Fast Start Universal SYBR Green Master (Rox) (Roche 04913850001) to detect DNA in the 7900 Fast Real Time System (Life Technologies 4329001). GUSB was used as the housekeeping normalizing gene, as its expression was constant under the experimental conditions. Negative controls were prepared using RNA or ultrapure water (NTCs), instead of cDNAs.

During the exponential phase of real time PCR, a fluorescence signal threshold was determined that was significantly higher than background fluorescence. The fractional number of PCR cycles required to reach this threshold is defined as the cycle threshold, or Ct. In order to quantify RNA levels: first, ΔCt value for each sample and specific gene primer was calculated (ΔCt= specific gene primer Ct – GUSB Ct) and this value was, then, referred to ΔCt for the control condition values, obtaining the ΔΔCt value (ΔΔCt=Sample ΔCt - control ΔCt) and finally, we obtained the relative quantification (RQ) using the formula $RQ=2^{(-\Delta\Delta Ct)}$. We consider a significant difference when there is a minimum of two-fold change: RQ more than 2 or less than 0.5.

Gene (mouse/human)	Forward (5'-3')	Reverse (3'-5')
Human Zeb 2	AATGCACAGAGTGTGGCAAGGC	ATCTGGCGTTCCAGGGACTCAT
Human Twist 1	CAAAGAAACAGGGCGTGGGG	CAGAGGTGTGAGGATGGTGCC
Human HGF	AGGACGCAGCTACAAGGGAACA	ACCCCGATAGCTCGAAGGCA
Human IL-6	TCTCGAGAGCCCAGCTATGAACTC	ATAGCGGCCGCTTACTACATTTGCCG AAGA
Human TGF-β1	GAGCCTGAGGCCGACTACTA	CGGAGCTCTGATGTGTTGAA
Human Gusb	ATCACCGTCACCACCAGCGT	GTCCCATTCGCCACGACTTTGT
Human C3G	GGTGCAGAACGATCCTCGAA	AGACCAGCGAATGAGGTTGG
Mouse HGF	TGACCTGCAACGGTGAAAGC	TGTGGGGTACTGCGAATCC
Mouse IL-6	AGACAAAGCCAGAGTCCTTCA	GGAGAGCATTGGAAATTGGGG
Mouse TGF-β1	ATGAACCGGCCCTTCCTGCT	TTGGTATCCAGGGCTCTCCGGT
Mouse Gusb	AAAATGGAGTGCGTGTTGGGTCG	CCACAGTCCGTCCAGCGCCTT

6. Adhesion, migration and invasion assays

6.1. Adhesion assay

50 000 cells were seeded in a 12 multiwell plate with complete medium and maintained at 37ºC and 5% CO_2 for 15 min, 30 min or 1 h. Then, culture medium was carefully removed, and wells were washed twice with PBS. Cells were stained for 20 min at RT with a solution of 0.2% crystal violet in 2% ethanol. After removal of crystal violet, cells were washed with distilled water and left to air dry before taking images with a camera coupled to a phase-contrast microscope to quantify the number of cells per well using ImageJ version 1.47v software.

6.2. Wound healing

Cell migratory capacity was evaluated using wound healing assays. Confluent cells were pre-treated with Mitomycin C (25 µg/ml, Sigma-Aldrich M0503) for 30 min in order to inhibit cell growth. Cells were then washed with PBS, and one scratch was performed with a disposable plastic tip. Cells were washed with PBS, and a serum-free culture medium was added. Cells were allowed to migrate at 37ºC and 5% CO_2. Migration was followed over time by a phase-contrast microscope coupled to a digital camera. Photographs were taken at different time points (0 h, 6-8 h, 12h and 24 h) and the percentage of wound healing closure was quantified using TScratch program (Gebäck, 2009) and referred to 0 h value.

6.3. Invasion assay

To study the invasive capacity of the cells through matrigel, Boyden chambers with transwells inserts (8 µm filter; BD 353097) coated with matrigel (444ug/cm^2) (Corning 4132053) were used. 50 000 cells were seeded in the upper chamber in serum-free medium. In the lower Boyden chamber 10% FBS culture medium was added to act as chemoattractant. Cells were left in the incubator at 37ºC and 5% CO_2 for 24 h. Then, the medium and matrigel from the upper chamber were removed and cells adhered to the lower part of the insert were fixed with 4% PFA in PBS for 15min, washed twice with PBS for 5 min and stained with 0.2% crystal violet for 20min. Inserts were then washed with distilled water to remove excess of staining and left to air dry. To count the cells, images taken by a digital camera coupled to a phase-contrast microscope were analyzed with ImageJ version 1.47v software.

7. Analysis of apoptosis by flow cytometric cell cycle analysis

In order to analyze apoptosis in attached cells and anoikis, HCC cells were maintained attached or detached (in suspension under soft shaking to prevent adhesion) for 6 h, in either complete or serum-free medium. Cells in suspension were directly pelleted by centrifugation at 2500 rpm for 5 min at 4ºC. Attached cells were first trypsinized and then, the medium and cell suspension were also centrifuged. The pellet of cells was washed with PBS (37ºC) and centrifuged again. The supernatant was removed, cells were resuspended in 300 µl of cold PBS and fixed with cold ethanol (700 µl) by incubation for 1 min on ice. After centrifugation at 2500 rpm for 5 min at 4ºC, the supernatant was removed and cells were washed with cold PBS. Then, cells were resuspended in 500 µl of PBS, transferred to a cytometer tube and incubated with 5 µl of RNAse (stock 10 mg/ml) for 30 min at 37ºC to eliminate RNA. Finally, propidium iodide (0.25µg/ml in PBS) was added to stain DNA and cell cycle was analyzed in the cytometer. Cells with a DNA content less than 2N were considered apoptotic.

8. *In vitro* analysis of tumorigenesis

8.1. Anchorage-dependent growth assay

To measure anchorage-dependent growth, HCC cells (100) were seeded in a 6 cm dish in triplicate with complete medium. Cells were grown at 37ºC and 5% CO_2 for 15 days. Then, the medium was removed and cells were washed twice with PBS. Cell foci were stained for 20 min with a 0.2% w/v crystal violet (Sigma-Aldrich C-0775) in 2% ethanol solution. Excess of staining was removed by washing with distilled water and left to air dry. Images taken by a digital camera coupled to a phase-contrast microscope were used to quantify the total number of foci, the number of cells per foci and foci diameter using ImageJ version 1.47v software.

8.2 Anchorage-independent growth assay

To measure anchorage-independent growth, cells were cultured in 24 multiwell dishes containing two agar layers. Plates were coated with 0.5% soft agar (Sigma-Aldrich A9414) diluted in complete medium and cells resuspended in a 0.7% soft agar diluted in complete medium (3000 cells/well) were seeded on the top. Cells were grown at 37ºC and 5% CO_2 for 15 days. Fresh complete medium was added to the top every two days to prevent agar drying. Then, images taken by a digital camera coupled to a phase-contrast microscope were analyzed quantifying the number of foci and the number of cells per foci using ImageJ version 1.47v software.

9. *In vivo* analysis of tumor growth and metastasis generation

All animal experiments were carried out in compliance with the institution's guidelines.

9.1. Tumor xenografts and metastasis generation and analysis

9.1.1. Tumor xenografts assays

Hep3B cells ($1x10^6$/100 µl) with and without C3G knock-down resuspended in PBS were injected subcutaneously into the flank of eight-week-old-male nude mice (Envigo). In controls, only the vehicle, PBS, was injected. Tumor growth was monitored twice a week till the end of experiment (22 days). Tumor size progression was measured using a caliper and tumor volume was calculated by applying the formula developed by Feldman et al., 2009, V= π/6*1.69*(L*W)^(3/2), where L is length and W is width. At end point, mice were sacrificed and tumors were resected, measured and weighed, and documented macroscopically with photographs. Then, tumors were cut in different pieces. A part was frozen down in liquid nitrogen and kept at -80ºC for protein and RNA analysis. Those pieces for tissue immunostaining were fixed with 4% PFA for later paraffin-embedding. Lung, blood and bone marrow were also obtained for additional analyses.

9.1.2. Bone marrow disseminated tumor cells isolation and analysis

Tibiae and femur from mice were cut and the muscle was removed. Then, the bone marrow (BM) was flushed with a 26G needle in 1 ml of PBS and centrifuged at 1200 rpm at RT. BM suspension (5 ml) was slowly poured onto the surface of 5 ml of Percoll and centrifuged without brake at 1500 rpm for 30 min. Cells were recovered with a 1 ml pipet, washed with 10 ml PBS++ and centrifuged at 1500 rpm 5min at RT. BM flushing was fixed with 4% PFA in PBS for 20 min at 4ºC, cells were stored in PBS at 4ºC or directly centrifuged at 1200 rpm for 5 min for cytospin preparation. Pre-treated slides (charged) were mounted with the paper pad and the cuvette in the metal holder. Then, 100 µl of the cell suspension ($1x10^6$ cells/ml in 1% BSA-PBS) was loaded in each cuvette. Samples were cyto-spun at 500 rpm for 3 min and slide was extracted carefully without damaging the fresh cytospin, which was allowed to dry for 5 min and stored in PBS at 4ºC.

9.1.3. Generation and analysis of lung metastasis in xenograft assays

mHCC1, 13 and 14 cell lines ($5x10^6$ cells in 100 µl PBS plus 100 µl matrigel) were subcutaneously injected into the flank of wild type mice (from the same genetic background of mice used to obtain mHCC cells) in Dr. F. Maina's lab. Tumor growth was followed up by measuring the size using a caliper. Tumors were resected before they reached a 10 mm diameter for analysis after anesthetizing the mice. Then, the wound was sewn and the mice were put back in their cages and monitored for a correct recovery. The mice were followed up to the end point (134 ± 6.4 days). Mice were sacrificed at different time points for ethical and compassionate reasons. Lungs were removed for metastasis analysis. Macro metastases (tumor big enough to be seen with a naked eye), were kept in two parts, one fixed in 4% PFA and embedded in paraffin and another kept at -80ºC for protein extraction. The rest of the whole lung was also fixed for paraffin embedding. Samples were analyzed to determine the size and morphology of metastasis and C3G protein expression.

9.2. Tissue paraffin-embedding, samples processing and slide preparation

Tissue samples were maintained in 4% PFA o/n and then, they were washed in cold PBS twice for 5 min. Samples were dehydrated by incubations in a rocker at 4ºC of 20 min/each and 3 times, as follows: 30% ethanol (EtOH), 50% EtOH and 70% EtOH. Finally, samples were incubated with 95% EtOH o/n and then, they were allowed to warm up to RT, washed 3 times with 100% EtOH for 20 min at RT and finally, incubated with xylene for 15 min at RT 3 times. Afterwards, samples were embedded in paraffin wax through successive incubations steps at 62ºC with the following mixtures: paraffin: xylene (1:1) for 30 min; paraffin for 1 h (3 times); and finally, samples were placed in the correct orientation in molds with fresh paraffin, placing a plastic cassette on the top, removing air bubbles and allowing them to harden o/n at RT. The paraffin blocks can be stored at RT or 4ºC.

In order to perform samples sections, the paraffin blocks were removed from the mold and assembled in the microtome, where they were cut in 8 µm slices. Then, slices were mounted in APES ((3-Aminopropyl) triethoxysilane) pre-coated slides to ensure correct adhesion and left in a 40ºC surface to allow paraffin stretching and drying and then, stored at RT. APES pre-treatment consist in an incubation with 3% APES (from Sigma A3648) diluted in acetone for 10 seconds, followed by 1 min of acetone treatment, 5 min in H_2O and then, slides were left to air dry o/n. APES is used to prepare positively charged slides suitable for immunohistochemistry, immunofluorescence or other *in situ* hybridations.

9.3. Immunofluorescence and immunohistochemistry analysis of paraffin-embedded tissues

9.3.1. Preparation of paraffin-embedded tissue samples for immunostaining

Prior to either immunofluorescence or immunochemistry, slides were dewaxed at 50ºC for 30 min and re-hydrated through subsequent incubations in: Xylene 5 min (2 times); 100% EtOH 5 min (2 times); 90% EtOH 3 min; 80% EtOH 3 min; 70% EtOH 3 min; H_2O 3min (2 times). For antigen retrieval, slides were heated in 10 mM citrate buffer pH 6 in a microwave at 800 W for 20 min and left them to cool down at RT. Then, they were washed with water and with PBS for 5 min.

After dewaxing and re-hydration of sections, endogenous peroxidase activity was blocked, in the case of immunofluorescence, by incubating slides with 3% H_2O_2 in PBS for 15 min, followed by a 5 min wash with PBS; and in the case of immunohistochemistry, by incubating slides as follows: 90% EtOH 3 min; 100% EtOH 3 min; 100% MeOH (methanol) 3 min; 3% H_2O_2 in 100% MeOH 20 min; 100% EtOH 3 min; 90% EtOH 3 min; H_2O 5 min; PBS 5 min (3 times).

Samples were permeabilized by a 5 min incubation with 0.5% Triton X-100 in PBS. Then, samples were washed with PBS for 5 min, blocked with 3% BSA in PBS containing 15 µl/ml of NGS (Normal Goat Serum) for 30 min and washed again with PBS for 5 min.

9.3.2. Immunofluorescence analysis of paraffin-embedded tissue samples

Primary antibodies in a 1/50 to 1/25 dilution in blocking solution were incubated at 4ºC o/n in a humidified chamber (see table below). The following day, slides were washed with 0.01% Tween-PBS for 5 min, washed with PBS for 5 min and incubated with the secondary antibodies (see table below) at a 1/200 dilution in blocking solution) for, at least, 1 h at RT in a dark humidified slide box. After washing the slides with PBS for 5 min, they were stained with DAPI (dilution 1/1000, Panreac A4099) for 10 min, washed with PBS for 5 min and then, with distilled water. Finally, slides were mounted with mounting media (Ibidi 5001) or Mowiol (Aldrich 32,459-0) and analyzed by immunofluorescence microscopy (Nikon Eclipse TE300).

Primary antibodies (IF)	Isotype	Laboratory	Reference
Cleaved Caspase 3	Rabbit	Cell Signaling Technology	9661
Ki67	Rabbit	Cell Signaling Technology	9129
Vimentin	Mouse	Dako	M0725
Pan-Cytokeratin	Rabbit	Santa Cruz Biotechnology	sc-8018

Secondary antibodies (IF)	Reactivity	Laboratory	Reference
FITC	Anti-mouse	Sigma	F0257
Alexa-Fluor 488	Anti-rabbit	Invitrogen	A32731
Alexa-Fluor 594	Anti-rabbit	Invitrogen	A32740
Alexa-Fluor 488	Anti-mouse	Invitrogen	A32723
Alexa-Fluor 594	Anti-mouse	Invitrogen	A32744

9.3.3. Immunohistochemistry analysis of paraffin-embedded tissue samples

Sections were incubated with primary antibody (1/25-1/50) diluted in blocking solution o/n in a humidified chamber at 4ºC (α-SMA, Dako M0851; C3G H300, Santa Cruz Biotechnologies sc-15359). Preparations were washed with PBS for 5 min and incubated with the appropriate secondary biothynilated antibody (1/200 diluted in blocking buffer) anti-rabbit (Vector BA-1100) or anti-mouse (Vector BA-2000) for 1h at RT. Then, tissues were washed 5 min with PBS and incubated with Avidin/Biotin reagent (1:1) (Vector PK-6100) for 30 min at RT in the dark. Then, slides were washed 5 min with PBS and covered with DAB reagent for less than one minute (prepared following manufacturer instructions, Vector SK-41000.) Next, slides were washed 5 min with H_2O and incubated for 10 sec with Hematoxylin (Panreac 255298.1610). After the slides were washed with tap running water, slide dehydration was performed as follows: 70% EtOH 3 min; 80% EtOH 3 min; 90% EtOH 3 min; 100% EtOH 3 min (2 times) and Xylene 2 min (2 times).
Finally, slides were mounted with DPX (VWR 1.00579.0500P) avoiding air bubbles and left to dry for a few hours before taking photographs in a phase-contrast microscope (Nikon Eclipse TE300).

9.3.4. Hematoxylin/Eosin staining of paraffin-embedded lung metastasis sections

Paraffin-embedded lung metastasis sections were stained with hematoxylin/eosin by successive incubations in the following way: xylene 10 min (2 times); EtOH 100% 5min (2 times), 95% EtOH 2 min, 70% EtOH 2 min, H_2Od 2 min, Hematoxylin 8 min (Panreac 255298.1610), 10 min running water, 2 min H_2Od, 0.5% Eosin (Sigma HT110116) 3 min, EtOH 95% 2min (2 times), EtOH 100% 2min (2 times), xylene 5min (2 times). Finally, slides were mounted with DPX (VWR 1.00579.0500), and metastatic areas were photographed under a phase-contrast microscope (Nikon Eclipse TE300) and analyzed using ImageJ version 1.47v (http://imagej.nih.gov/ij) or Fiji (Just Image J that includes all macros) (Schindelin et al. 2012).

10. Analysis of information from public genomic databases

For the analysis of mRNA C3G levels in a hepatocarcinoma cohort of 365 patients, TCGA (The Cancer Genome Atlas) was used as displayed in the browser The Protein Atlas available at proteinatlas.org (query for *RapGEF1* and liver cancer: https://www.proteinatlas.org/ENSG00000107263-RAPGEF1/pathology/liver+cancer), expressed in fragments per kilobase of exon model per million reads mapped (FPKM). Samples were classified in groups according to their stage of progression: stages I (176 patients), II (84 patients), III (63 patients in stage IIIA, 8 patients in stage IIIB and 9 patients in stage IIIC out of 83 patients) and IV (1 patient in stage IVA, 2 patients in stage IVB and 1 patient not classified out of 4 patients). These data from stage IV were not used for our studies due to their low number. Three additional samples were removed from the dataset as they corresponded to fibrolamellar carcinoma, which was off-limits of our study, 3 samples were removed for incomplete information in TCGA, and another 12 were not taken into account as they did not report *RapGEF1* mRNA levels or information about stages, keeping in total 343 patient samples for our analysis. The AJCC (American Joint Committee on Cancer) TNM staging system (effective January 2018) was used (see table below modified from: https://www.cancer.org/cancer/liver-cancer/detection-diagnosis-staging/staging.html), which takes into account the size of the tumor (T), the spread to lymph nodes (N) and the dissemination to distant organs (M):

AJCC Stage	Stage grouping	Stage description
IA	T1a N0 M0	A single tumor 2 cm or smaller that hasn't grown into blood vessels (T1a). It has not spread to nearby lymph nodes (N0) or to distant sites (M0).
IB	T1b N0 M0	A single tumor larger than 2 cm that hasn't grown into blood vessels (T1b). The cancer has not spread to nearby lymph nodes (N0) or to distant sites (M0).
II	T2 N0 M0	Either a single tumor larger than 2 cm that has grown into blood vessels, OR more than one tumor but none larger than 5 cm across (T2). It has not spread to nearby lymph nodes (N0) or to distant sites (M0).
IIIA	T3 N0 M0	More than one tumor, with at least one tumor larger than 5 cm across (T3). It has not spread to nearby lymph nodes (N0) or to distant sites (M0).
IIIB	T4 N0 M0	At least one tumor (any size) that has grown into a major branch of a large vein of the liver (the portal or hepatic vein) (T4). It has not spread to nearby lymph nodes (N0) or to distant sites (M0).
IVA	Any T N1 M0	A single tumor or multiple tumors of any size (Any T) that has spread to nearby lymph nodes (N1) but not to distant sites (M0).
IVB	Any T Any N M1	A single tumor or multiple tumors of any size (any T). It might or might not have spread to nearby lymph nodes (any N). It has spread to distant organs such as the bones or lungs (M1).

The Kaplan-Meier survival curve, was performed using GraphPad with the same set of patients, divided into two different groups according to their level of expression of C3G mRNA: high expression (patients with an expression higher or equal to the median) and low expression (patients with an expression lower to the median).

The HCMDB (Human Cancer Metastasis Data Base, Zheng et al.2018; https://hcmdb.i-sanger.com/) with data collected from NCBI Gene Expression Omnibus and TCGA datasets, expresses their data in the same relative units (log2 MAS 5.0 signal), allowing the comparison between the different experiments and datasets provided by their platform. The human samples were separated in six groups depending on the site of secondary tumor formation: HCC liver primary tumor with lung metastasis and their corresponding lung metastasis secondary to HCC liver tumor from 3 and 12 patients, respectively; HCC liver primary tumor with adrenal gland metastasis and their corresponding adrenal gland metastasis secondary to HCC liver tumor from 3 patients; HCC liver primary tumor with lymph node metastasis and their corresponding lymph node metastasis secondary to HCC liver tumor from 4 patients.

Due to the relatively novelty of this data base, unique in its characteristics, sometimes, it lacks more detailed information about metastasis in the clinical history of each patient. There are very few HCC metastasis samples.

The Gene Investigator Software (Hruz et al. 2008; https://genevestigator.com/gv/), contains gene expression from several samples of datasets from Affymetrix Human Genome U133 Plus 2.0 Array analyses. We used this platform to compare 535 control liver samples with 232 HCC samples from patients, 30 patient-derived xenografts (HCC-PDX; Patient-derived xenograft) and 15 HCC-metastatic samples, expressed in log2 of RNA-Seq by Expectation Maximization (RSEM) units (Sequera et al. 2018).

For the study of somatic mutations and other genetic alterations (amplifications, deep deletions, etc), we used the cBioportal database (https://www.cbioportal.org/), which is comprised by three datasets: the TCGA (PanCancer Altlas) set with 366 cases, AMC (Asian Medical Centre, Seoul, South Korea; Hepatology, 2014) set with 231 cases and the Inserm (Nat. Genet., 2015). Additionally, a Kaplan-Meier survival curve was generated from cBioportal with only TCGA dataset corresponding to the overall survival of the group of patients with alterations in RapGEF1 and the group of patients without any alteration. For copy number analysis, searches were performed in OASIS Analytics platform (http://www.oasis-genomics.org/), which hosted different datasets. The first dataset is Pfizer, ACRG (Asian Cancer Research Group; Singapore) with 217 donors; the second one is TCGA (MD, USA) with 212 donors; and thirdly the Pfizer, Samsumg (Seoul, North Korea) with 272 donors.

11. Statistical analysis

Data has been represented as the mean value of, at least, 3 independent experiments ± S.E.M. Comparisons between two experimental groups were statistically analyzed using unpaired Student's t-test. To compare more than two groups with one variable, one-way ANOVA was used, or two-way ANOVA for two variables, followed by a multiple comparison, either Tukey or Bonferroni test, taking into account GraphPad Prism recommendation for each case. Results were considered significant when p value was ≤0.05. Specifically, we used the following notation: $p>0.05$ (n.s); $p\leq0.05$ (*); $p\leq0.01$ (**); $p\leq0.001$ (***) and $p\leq0.0001$ (****). For performing the statistical analysis both GraphPad Prism version 6.01 and Excel 2013 were used.

8. RESULTS

1. INCREASED C3G EXPRESSION AND GENETIC ALTERATIONS IN HEPATOCARCINOMA. C3G AS A NEW POTENTIAL PROGNOSTIC BIOMARKER FOR HUMAN HEPATOCARCINOMA PROGRESSION.

Hepatocarcinoma is a very heterogeneous cancer with no clear subgroups that can help clinicians in prognostic or treatment purposes, being sorafenib the main used drug when high RTKs levels, including Met, are detected. On the other hand, data from the literature reported that other RapGEFs, different from C3G (RapGEF1), such as Epac, are important for liver physiopathology. However, there was no literature regarding the role of C3G in liver function or HCC. Therefore, we wanted to determine if human HCC development and progression was accompanied by C3G expression changes that could play a role in HCC development, so that they could be used as a biomarker tool for HCC patient prognosis and/or treatment classification.

1.1. C3G expression increases in human hepatocarcinoma versus healthy adult liver

Using data provided from GTEXportal, GTEX Analysis Release V8 (dbGaP Accession phs000424.v8.p2) we had access to RapGEF1 mRNA expression in different healthy human tissues (Sequera et al., 2018; data updated in 2019). Surprisingly, the liver was the organ that expressed the lowest levels of C3G mRNA with 12.77 TPM (Transcript per Millions) (n=226; n= number of samples). In contrast, other organs expressed higher levels

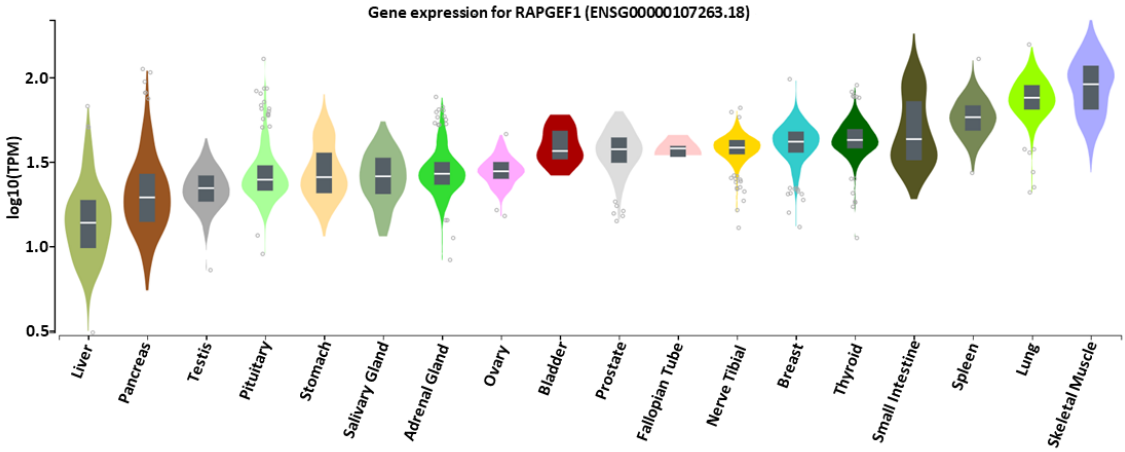

Figure 1. Comparison of C3G mRNA levels in different organs. *Violin box plot representing log10 (TPM (Transcript per Million)) of C3G mRNA expression in different human healthy organs for better visualization than linear TPM. RapGEF1 gene expression was calculated from a gene model where isoforms are quantified together. Median, 25th and 75th percentiles are shown. Points are displayed as outliers if they are above or below 1.5 times the interquartile range (modified from: gtexportal.org/home/gene/ENSG00000107263).*

of C3G mRNA. Some examples are the pancreas expressing 18.48 TPM (n=328), adrenal gland expressing 25.99 TPM (n=258), breast-mammary tissue expressing 40.97 TPM (n=459), and the two tissues expressing more are the lungs with 74.66 TPM (n=578) and skeletal muscle with 90.68 (n=803) (Figure 1). Although, this database allows a sex filter, the slight decrease in C3G mRNA in male samples was not significant, being in female 14.07 TPM (n=65) and in male samples 12.27 TPM (n=161).

Next, using the Firebrowse platform which uses different datasets, we compared normal healthy liver samples versus tumor liver samples from HCC patients. In a first dataset from The Cancer Genome Altlas (TCGA), we found a significant 2.42-fold increase in C3G mRNA levels, expressed in log2 Reads Per Kilobase Per Million (RPKM), in tumor samples (n= 17) as compared to control liver samples (n= 9) (Figure 2, left panel). In a second dataset from the same platform, and consistent with the previous one, there was also a significant, but less striking, 1.18-fold increase in tumor samples (n=373) as compared to control liver samples (n=50). In this case, it was expressed as log2 RSEM (accurate transcript quantification for RNA-Seq data) (data not shown). Searching in another database, Gene Investigator Software, which compiles the gene expression of different datasets derived from Affymetrix Human Genome U133 Plus 2.0 Array and expressed in log2 RSEM, we found that both HCC patient tumor samples (n=232) and patient-derived xenografts (HCC-PDX; n=30) showed higher C3G mRNA levels than control liver samples (n=535). In contrast, we found that samples classified as metastatic (n=15) expressed lower levels of C3G mRNA as compared to both control and HCC samples (Figure 2, right panel). When comparing data from different databases, we found different outcomes due to the reduced number of samples, or the different methods used for normalization by each

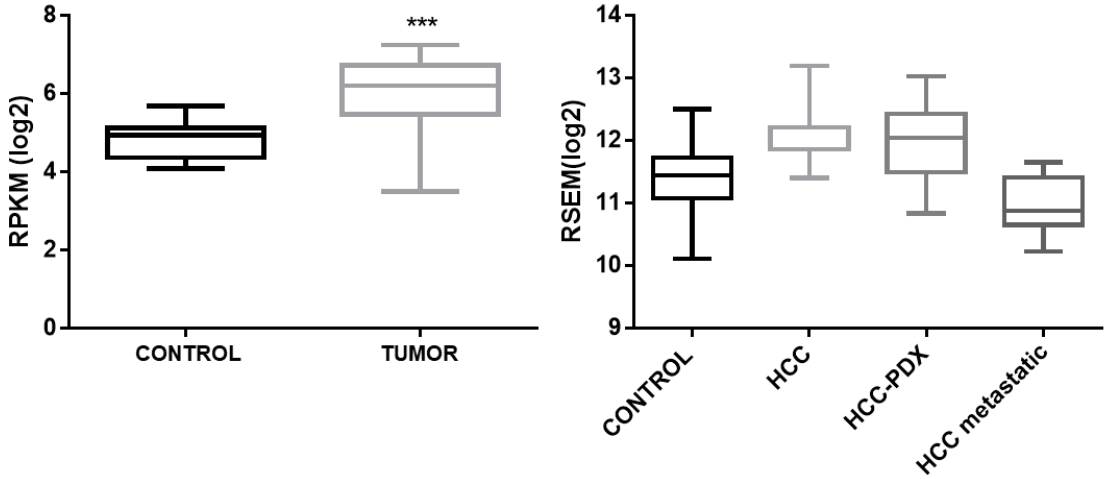

Figure 2. Comparison of C3G mRNA levels in control liver versus HCC tumor samples. Left panel**: Boxplot showing C3G mRNA levels in control (n=9) and tumor liver (n=17) tissues from Firebrowse platform. TCGA set expressed in log2 RPKM (Reads Per Kilobase Per Million). Statistical analysis using Student's t-test revealed significant difference (p≤0.001). **Right panel**: Boxplot shows C3G mRNA levels in control liver (n=535), HCC (n=232), HCC-PDX (Patient-Derived Xenograft, n=30) and HCC metastatic (n=15) samples, in log2RSEM (Accurate transcript quantification from RNA-Seq data) from Gene Investigator Software with Affymetrix Human Genome U133 Plus 2.0 Array analysis. Statistical analysis was performed using one-way ANOVA followed by Bonferroni multiple comparison and revealed not significant differences.*

platform. However, in all of them there was a consensus: an increase of C3G mRNA in HCC patients versus control samples.

Based on all this, we analyzed C3G protein levels by western-blot in different human HCC cell lines as compared to mouse immature neonatal, adult hepatocytes and liver progenitor cells (oval cells). We found that C3G protein is highly expressed in human HCC Hep3B and HLE cell lines, as compared to adult hepatocytes, with C3G levels comparable to those found in neonatal hepatocytes and oval cells (Figure 3).

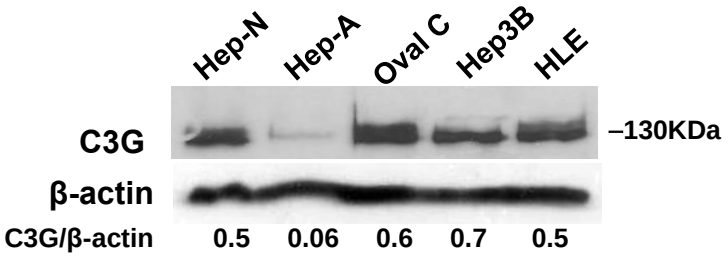

Figure 3. C3G protein levels increases in hepatocarcinoma. *Western-blot analysis of C3G levels in different mouse and human liver cells normalized with β-actin. Neonatal hepatocytes (Hep-N), Adult hepatocytes (Hep-A), Oval cells (Oval C), Hep3B and HLE cells.*

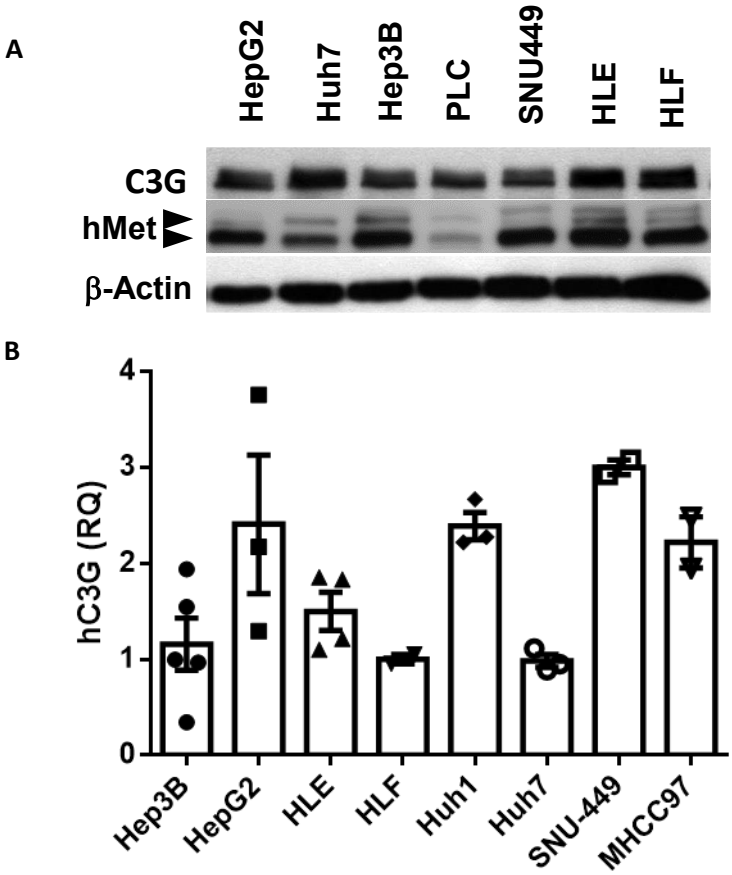

Figure 4. C3G protein and mRNA expression levels in different human HCC cell lines. (A) *Analysis of C3G and human Met protein levels by western-blot in several human HCC cell lines, normalized with β-actin.* ***(B)*** *Analysis of C3G mRNA levels by RT-qPCR in human HCC cell lines. RQ values are relative to Hep3B cells.*

To corroborate these findings, we evaluated C3G protein levels in several human HCC cell lines: HepG2, Huh7, Hep3B, PLC, SNU449, HLE and HLF and we found high C3G levels in all of them (Figure 4A), similar to those previously found in Hep3B and HLE cell lines (Figure 3). In most HCC cell lines, Met had also a high expression. To support protein data, we additionally analyzed, using databases, C3G mRNA levels measured by RT-qPCR in several human HCC cell lines, which revealed similar or even higher expression levels than those found in Hep3B and HLE cells (Figure 4B).

Additionally, in paraffin-embedded liver sections of mouse treated for 9-month with DEN (Diethylnitrosamine) to induce HCC we detected higher C3G expression levels by immunohistochemistry analysis as compared with non-treated animals (control). However, the difference was not statistically significant (p=0.0866), probably due to the few samples available (Figure 5).

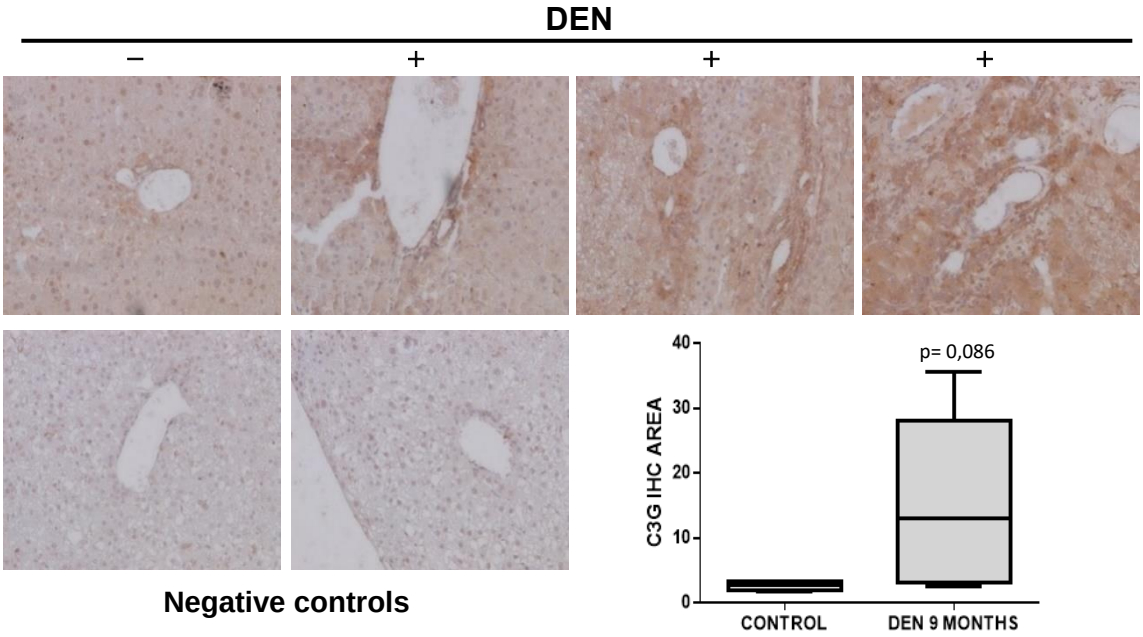

Figure 5. C3G protein levels increases in DEN-induced mouse HCC-model. *Immunohistochemical (IHC) analysis of C3G levels in paraffin-embedded liver samples from mice treated with (+) DEN for 9-months or untreated.* ***Upper panel****, representative images of C3G IHC.* ***Lower panel****, left, negative controls incubated only with secondary antibody; right, positive C3G area measured using ImageJ software and represented as a boxplot of the mean ± S.E.M. Statistical analysis with Student's t-test (p=0.0866).*

In view of the increase in C3G observed in all the tested HCC models, we also analyzed C3G expression in samples from liver tumors and HCC cell lines derived from a mouse model induced by the overexpression of Met in hepatocytes, which recapitulates human HCC, specifically the proliferative subtype progenitor-like subclass (Fan et al., 2017; Arechederra et al., 2018). C3G protein levels were higher in all liver tumors as compared to normal liver tissue, where C3G protein expression was very low or not detected, as shown in Figure 6A. In a similar way, in several mHCC cell lines derived from the mouse model mentioned above, C3G protein levels were upregulated as compared with adult hepatocytes or normal liver tissue, where C3G was undetected (Figure 6B). Taken

together, these data indicate that C3G is highly expressed both at mRNA and protein levels, in liver progenitor cells and neonatal hepatocytes (immature hepatocytes), but it decreases in mature adult hepatocytes, being re-expressed in HCC. Therefore, the next step would be to determine its potential relevance for HCC diagnostic/prognostic of human patients.

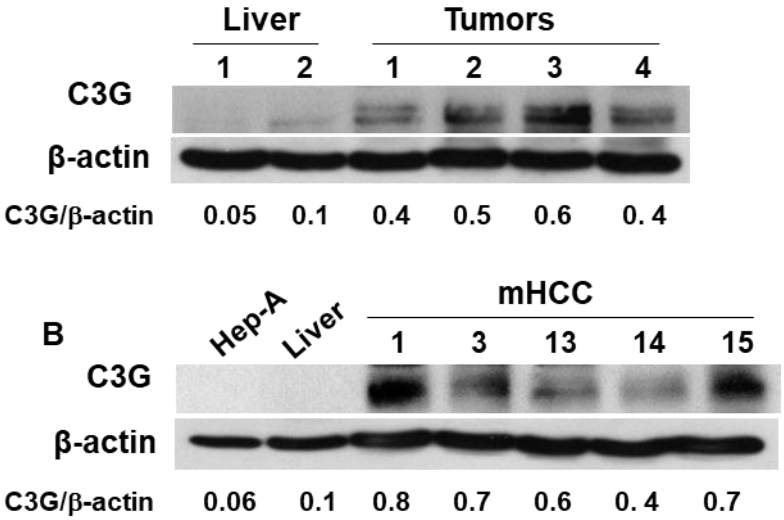

***Figure 6. C3G protein expression is upregulated in mouse liver tumors induced by Met overexpression in hepatocytes. (A** and **B)** C3G protein expression analysis by western-blot normalized with β-actin. **(A)** Control healthy liver (1 and 2) and HCC tumors (1 to 4) from mice overexpressing Met in hepatocytes (mouse Alb-R26^{Met}). **(B)** Adult hepatocytes (Hep-A), control healthy liver and mHCC cells established from liver tumors from the mentioned mouse model (mHCC1, 3, 13, 14 and 15).*

1.2. High C3G mRNA expression positively correlates with human hepatocarcinoma progression and poor prognosis.

In order to investigate whether C3G levels could correlate with HCC progression, TCGA dataset from The Protein Atlas platform was used. HCC patients were divided into different groups according to their progression stage following AJCC guidelines, from stage I to III. We found that C3G mRNA levels exhibited a growing trend during HCC progression, reaching a significant increase at stage III (Figure 7, left panel). These results corroborate the positive correlation between increasing levels of C3G and HCC development, and suggest a potential role for C3G in promoting HCC progression.

In fact, in the same set of patients, a Kaplan-Meier Survival Curve was done comparing two separate groups based on their C3G mRNA levels. We found that the survival was significantly lower in the group of HCC patients with high levels of C3G mRNA versus the group with lower levels of C3G mRNA (Figure 7, right panel), showing an inverse correlation between C3G expression and survival and a direct correlation between high C3G levels and HCC progression.

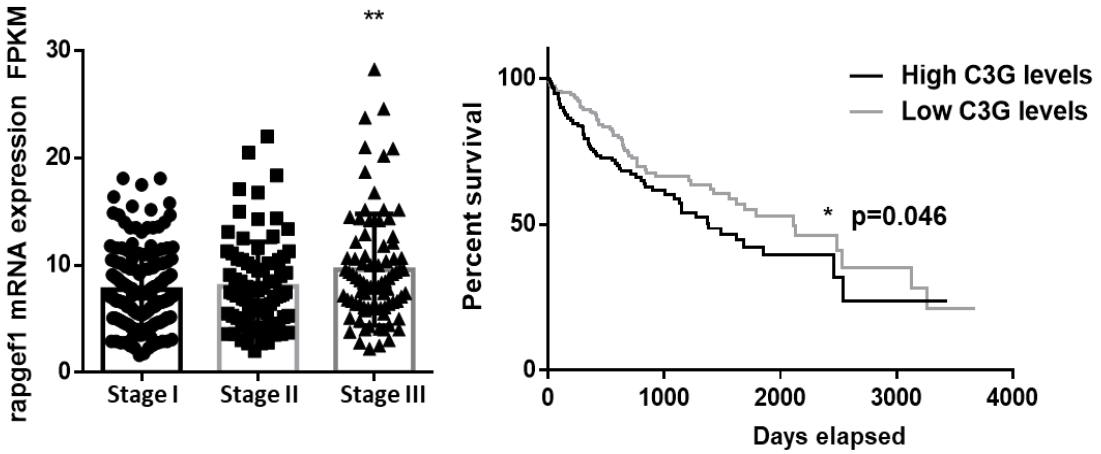

Figure 7. C3G mRNA levels are positively correlated with HCC progression and poor prognosis. Left panel, *Scatter plot with bars represents the mean ± S.E.M. of C3G mRNA levels in HCC patients expressed in FPKM units (fragments per kilobase of exon model per million reads mapped) in different stages of human HCC progression, following AJCC (American Joint Committee on Cancer) guidelines corresponding to 176 patients in stage I, 84 patients in stage II, 83 patients in stage III. Statistical analysis was performed using Graphpad: **p≤0.01, versus stage I, applying one-way ANOVA, followed by multiple comparison.* ***Right panel,*** *Kaplan-Meier survival curve represents patient survival, expressed as percentage, in relation to the days elapsed in two groups of patients: patients with high levels and patients with low levels of C3G mRNA. Statistical analysis between the two groups was performed with Student's t-test (*p≤0.05).* ***Left panel*** *and* ***right panel****, patient data corresponds to TCGA dataset as provided by The Protein Atlas platform.*

1.3. C3G genetic alterations in hepatocarcinoma patients. Association with reduced hepatocarcinoma patient survival.

In order to study whether genetic alterations in *RapGEF1* were also present in HCC patient samples, we extended our database search to include this parameter. For this purpose, we used cBioportal platform were three different datasets are available. The first one is the TCGA, where 3% of the 366 patients presented genetic alterations in *RapGEF1* (11 patients) comprising deep deletion, amplification, and mutations, either missense or nonsense (truncating). The second set, the AMC (Asian Medical Centre, Seoul, South Korea) comprises 231 patients, from which 2.6% (6 cases) presented missense mutations in *RapGEF1*. Finally, the Inserm set, where 2.1% of its 243 patients presented either nonsense or missense mutations in *RapGEF1* (5 patients) (Figure 8, upper panel). Moreover, the localization of mutations of specific amino acids in the structure of C3G protein, revealed a high concentration of the described missense mutations in the N-terminal negative regulatory GEF catalytic domain. A loss of function in this domain could lead to an aberrant sustained GEF catalytic activity, resulting in the hyperactivation of Rap1, and potentially, other Ras GTPases that can be activated by C3G. Nonetheless, the higher number of missense mutations was found at the C-terminal region, within the REM-Cdc25H domains, which conform the GEF catalytic domain, and might be a potential source of dysregulation of the activity of Rap1 and other GTPases. Furthermore, there were two truncating mutations in relevant positions. The first one, directly affected the

tyrosine residue in position 504 (Y504), whose phosphorylation is implicated in C3G activation and localization; hence, the importance of its loss. The second truncating mutation took place in a residue some amino acids upstream from the REM domain, which could lead to the loss of the catalytic region of C3G protein and its associated activity (Figure 8, lower panel).

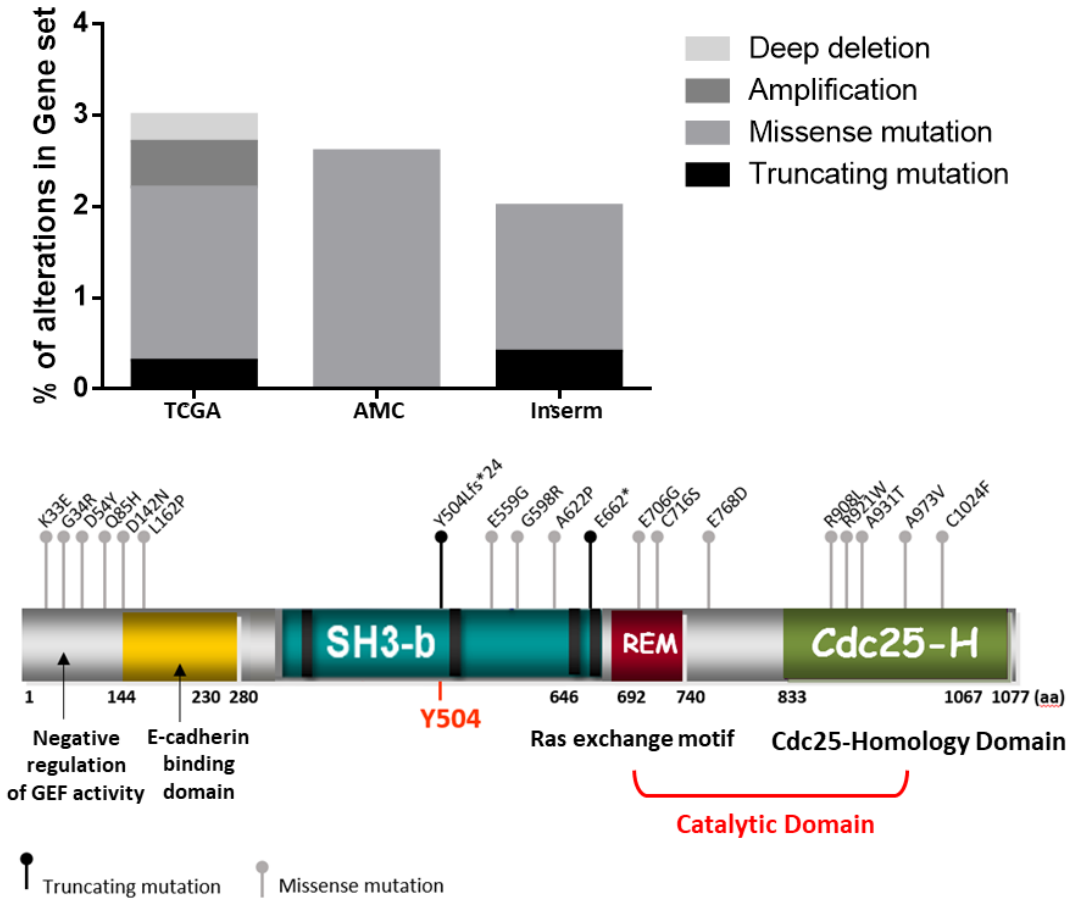

Figure 8. Mutations and other genetic alterations in RapGEF1 gene in HCC patients. *Data correspond to cBioportal dataset, containing TCGA (366 cases), AMC (Asian Medical Center; Hepatology, 2014; 321 cases) and Inserm (Nat. Gent., 2015; 243 cases) sets.* ***Upper panel,*** *piled histogram represents RapGEF1 deep deletions, amplifications, missense mutations and truncating mutations, as percentage of alterations in the gene set.* ***Lower panel,*** *Schematic representation shows C3G domains, from N-terminal to C-terminal: negative regulatory domain of GEF activity, E-cadherin binding domain, SH3-binding domain rich in prolines, Y504 (tyrosine residue, site of phosphorylation), REM and Cdc25-homology domain. The two later forming the GEF catalytic domain. Above the scheme, black pins represent truncating mutations and grey pins represent missense mutations. Above pins, it is annotated the amino acid residue and position of the residue touched by the mutation. Amino acids limiting each domain are displayed below the scheme.*

On the other hand, alterations of the phenotype are not only due to gene mutations, but also to copy number variations. Hence, we resorted to use OASIS Analytics platform, which comprises several liver cancer datasets. On the first one, the Pfizer ACRG (Asian Cancer Research Group, Singapore), there was one patient out of 217 with copy number gain (0.5%), and two patients out of those 217 affected by copy number loss (0.9%). In a second dataset from TCGA (MD, USA) there were no patients, among the 212, with copy number gain and only one patient from a total of 165 had copy number loss (0.6%). Finally,

the Pfizer Samsung (Seoul, South Korea) with 272 patients, did not present any change in copy number. Therefore, with these data we can conclude that the effect of copy number variations in the case of RapGEF1 is non-significant on HCC.

Finally, using cBioportal platform and its TCGA datasets we analyzed the correlation between the presence of mutations in *RapGEF1* and HCC patient survival. The overall survival of the group of HCC patients with genetic alterations in C3G gene was significantly lower, almost 5-fold (4.83), than that of the group of HCC patients without any genetic alteration. In particular, in the group of 11 patients bearing mutations or other genetic alterations in *RapGEF1*, 8 died, presenting a median survival of 14.39 months. In contrast, in the group of 354 patients with no mutations or genetic alterations in RapGEF, 119 died, having a median survival of 69.51 months (Figure 9). Based on these data, we can conclude that the previously mentioned mutations or other genetic alterations in *RapGEF1* do have a high impact on mortality and survival and can be considered as negative prognosis markers in HCC. On the other hand, we still have much to learn about these genetic alterations, such as the moment or context of their occurrence in order to understand their impact in HCC tumorigenesis, progression and metastasis.

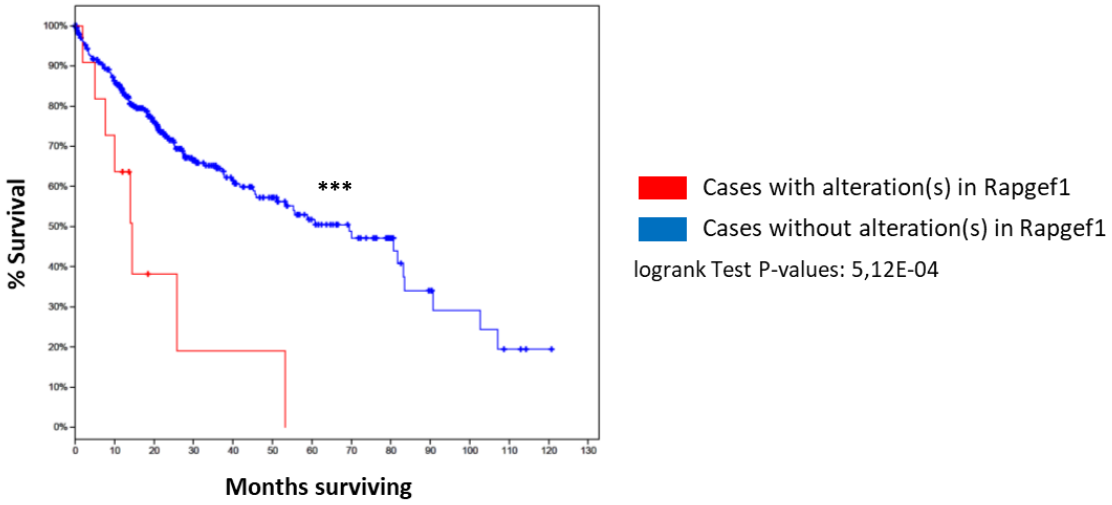

Figure 9. Poor survival of HCC patients with genetic alterations in RapGEF1 gene. *Kaplan-Meier survival curves for two groups of patients expressed as the percentage (%) of alive patients in relation to the time (in months) using data from cBioportal platform containing TCGA database. Blue curve, represent HCC patients without genetic alterations in RapGEF1 gene (354 cases) and the red curve, represents HCC patients with alterations in RapGEF1 (11 cases). Graphic modified from cBioportal. Statistical analysis showed logrank test p-value = 5,12E-04.*

Therefore, we have shown that C3G levels positively correlate with HCC tumorigenesis and progression, where high levels of C3G represent an indicator of bad prognosis. Moreover, mutations or other genetic alterations in *RapGEF1* are also negative prognostic markers for HCC patients. All these data show the relevance to study the function of C3G in the pathogenesis of HCC at a molecular level, as a potential tool for clinicians in order to improve prognosis and treatment of HCC patients. Hence, the next step was to analyze by *in vitro* and *in vivo* functional assays the role played by C3G in HCC tumorigenesis and progression.

2. C3G DOWN-REGULATION REDUCES *IN VITRO* AND *IN VIVO* TUMORIGENESIS, WHILE ENHANCES CELL MIGRATION AND INVASION IN HUMAN HEPATOCARCINOMA CELLS THROUGH INDUCTION OF AN EPITHELIAL-MESENCHYMAL-LIKE TRANSITION.

Taking into account the previously described findings pointing out to an increase in C3G levels in different models of HCC and in samples from human patients, the next step was to analyze the potential tumorigenic role of C3G. To do it, we permanently silenced C3G in Hep3B and HLE, human HCC cells, which have different phenotypic, epithelial- or mesenchymal-like, respectively, and genetic characteristics (Cascione et al., 2019; Zucman-Rossi et al., 2019). C3G was also knocked-down in cells established from mouse liver tumors generated by Met overexpression in hepatocytes (mHCC1 cell line) (Figure 10B). Permanent C3G knock-down was achieved with a mixture of shRNAs and efficiency was verified by western-blot, where C3G levels decreased approximately 50% and 75% in Hep3B and HLE cells C3G silenced cells, respectively (Figure 10A). Similarly, in mHCC1 permanent C3G silencing, a decrease in C3G protein levels ranging 30 to 60 % was achieved, depending on the clone (2.17, 1.2 and 1.3) (Figure 10B). Only mHCC1 2.17 and 1.3 were selected for later functional assays as C3G knock-down was higher.

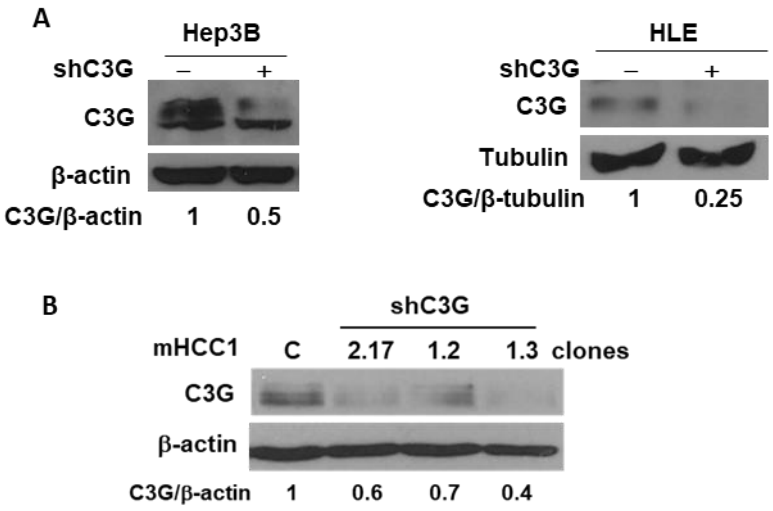

Figure 10. C3G silencing in human and mouse HCC cells. *Western-blot analysis of C3G protein levels normalized with either β-actin or tubulin in* ***(A)*** *human HCC cells (Hep3B and HLE) with (shC3G) or without C3G knock-down (-) and in* ***(B)*** *mouse HCC cells (mHCC1) with (2.17, 1.2 and 1.3 clones) and without (C) C3G knock-down.*

2.1. C3G downregulation reduces foci formation in mouse and human hepatocarcinoma cells.

In order to determine the role of C3G in the tumorigenic capacity of human HCC cells, we first performed anchorage dependent growth assays, using Hep3B and HLE cells, with and without C3G silencing. As shown in Figure 11, we observed a significant decrease in the number of foci in both Hep3B (left panel) and HLE (right panel) cell lines upon C3G knock-down. Moreover, we also found a decrease in the number of cells per focus in C3G silenced cells, which showed (see representative images from the top panel) a lower density of cells, with a more scattered phenotype and with less cell-cell interactions.

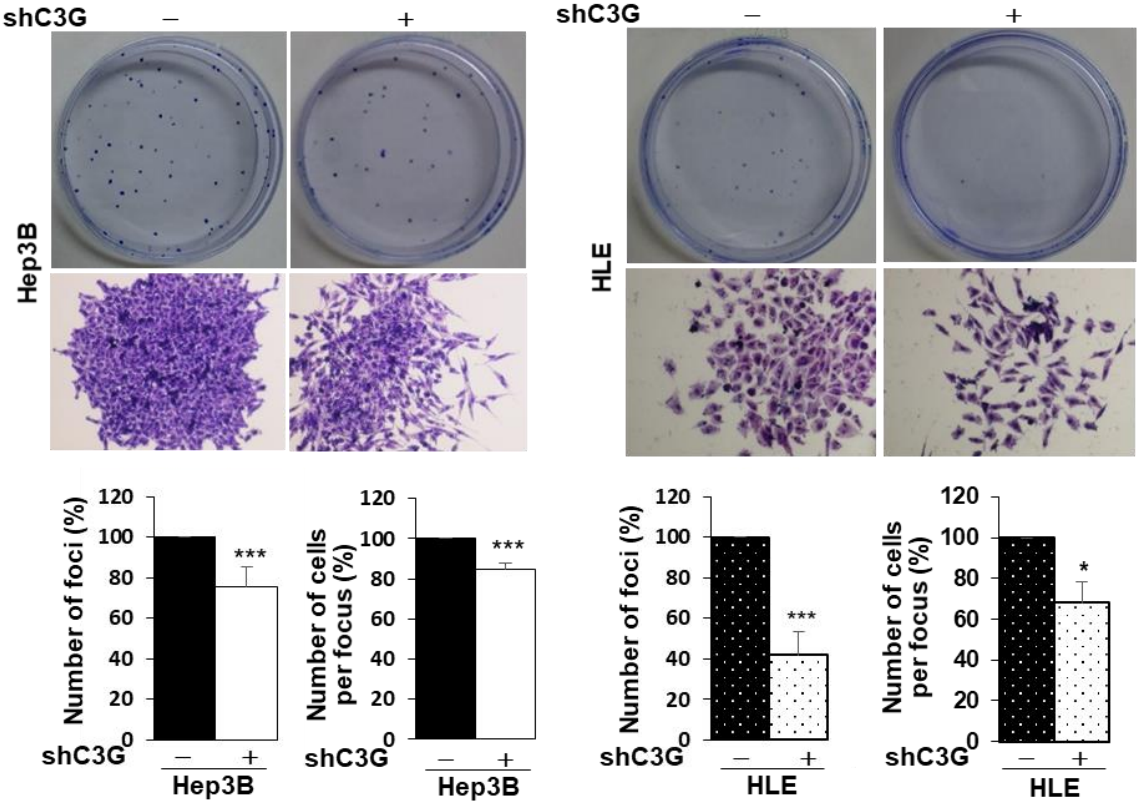

Figure 11. C3G knock-down reduces foci formation in Hep3B and HLE human HCC cell lines. *Hep3B and HLE (non-silenced (-) and C3G knock-down (shC3G)) cells, were maintained in complete medium.* ***Top panel****, representative macroscopic (whole dish) and microscopic (individual focus) images from anchorage-dependent growth assay, with cells stained with crystal violet.* ***Bottom panel****, histograms show the mean ± S.E.M. of the number of foci (%) and the number of cells per focus (%). Individual cells were counted using ImageJ. *p≤0.05, **p≤0.01, ***p≤0.001, versus non-silenced cells (-), Student's t-test, n ≥ 3.*

Moreover, we permanently silenced C3G in Huh7 cells, another human HCC cell line with epithelial-like phenotype, obtaining a 50% of C3G protein levels reduction (Figure 12A). As observed in Figure 12B, in Huh7 cells C3G down-regulation also decreased the number of foci in anchorage-dependent growth assay, and the cells within the foci presented a more scattered phenotype. Additionally, we performed anchorage-dependent assays in mouse HCC mHCC1 cell line, obtaining similar results to those previously described for

human HCC cell lines, a decrease in the number of foci in the two C3G knock-down clones used (Figure 13).

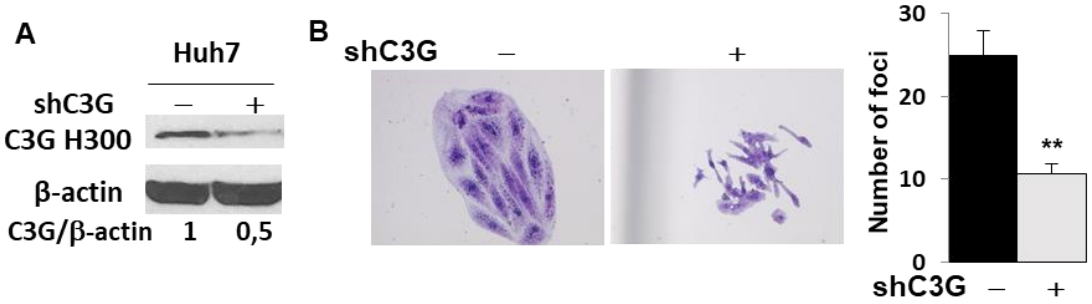

Figure 12. C3G knock-down reduces foci formation in human HCC Huh7 cells. *Non-silenced (-) and C3G knock-down (shC3G) Huh7cells were maintained in complete medium.* ***(A)*** *Western-blot analysis of C3G expression in HCC cells, normalized with β-actin.* ***(B)*** *Representative microscopic (individual foci) images from anchorage-dependent growth assay, with cells stained with crystal violet. Histogram shows the mean ± S.E.M. of the number of foci. **p≤0.01, versus non-silenced cells (-), Student's t-test, n ≥ 3.*

In order to further determine the role of C3G in tumorigenesis, we performed anchorage-independent assays. Hence, we evaluated the ability of Hep3B and HLE cells with and without C3G silencing to form foci in soft-agar. We found more foci in C3G silenced cells, and we confirmed the acquisition of a cell scattered capacity following C3G down-regulation in Hep3B cells, already detected in anchorage-dependent assays. This is illustrated by a significant reduction in the number of cells per colony (about 50%) and the

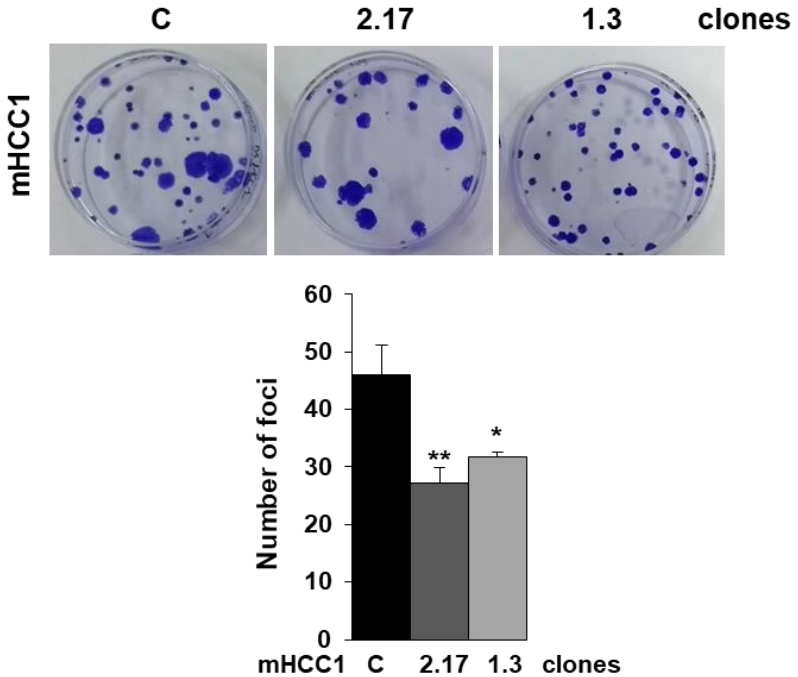

Figure 13. C3G knock-down reduces foci formation in mouse mHCC1 cell line overexpressing Met. *mHCC1 cells with (2.17 and 1.3 clones) and without (C) C3G knock-down, were maintained in complete medium.* ***Top panel,*** *representative macroscopic (whole dish) images from anchorage-dependent growth assay, with cells stained with crystal violet.* ***Lower panel****, histogram shows the mean ± S.E.M. of the number of foci. *p≤0.05; **p≤0.01, versus non-silenced cells (C), One-way ANOVA followed by multiple comparison, n ≥ 3.*

subsequent increased number of colonies (Figure 14). In fact, a closer look to these foci morphology clearly showed that upon C3G downregulation, the cells were scattered with a tendency to escape from the original focus and potentially form another secondary focus. In the case of HLE cells, no foci were formed in either non-silenced or C3G knock-down cells, reason why this cell line was discarded for *in vivo* xenograft experiments. Taking together the results from the anchorage-dependent and –independent growth assays, we can conclude that C3G confers *in vitro* tumorigenic properties to human HCC cells.

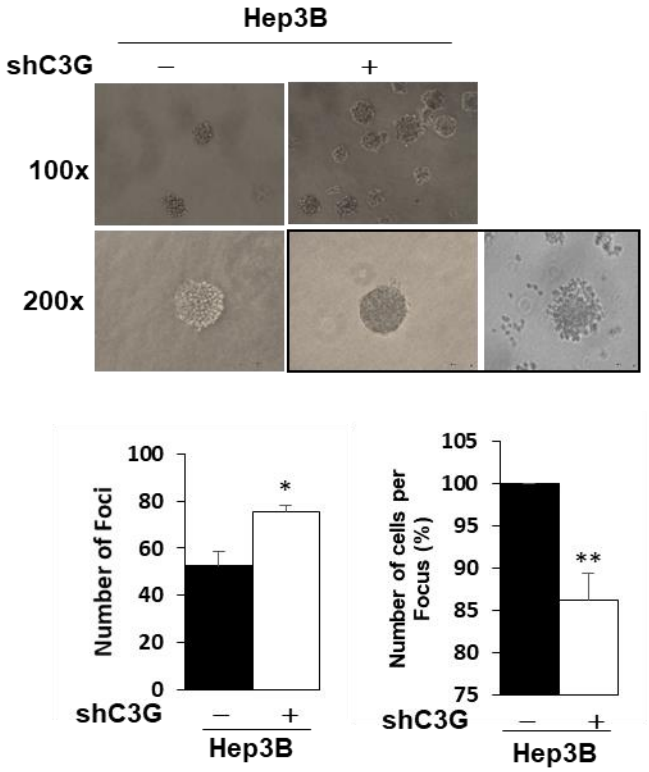

Figure 14. C3G knock-down reduces anchorage-independent growth of Hep3B cells. *Non-silenced (-) and C3G knock-down (shC3G) Hep3B cells were maintained in complete medium.* **Top panel***, representative phase-contrast- microscopy images from foci in anchorage-independent growth of Hep3B cells.* ***Lower panel****, histograms represent the mean ± S.E.M. of number of foci and cells per focus (%). *p≤0.05, **p≤0.01, versus non-silenced cells (-), Student's t-test, n ≥ 3.*

To elucidate the potential mechanisms by which C3G exerts its pro-tumorigenic function, we analyzed the effect of C3G downregulation on apoptosis and cell adhesion. To this end, we first measured apoptotic cell death of Hep3B cells with and without C3G knock-down under different culture conditions. We found no differences in apoptosis in Hep3B cells maintained under adherent cell culture conditions, either in the presence (Figure 15A) or absence of 10% serum (data not shown). Hence, we next explored whether C3G down-regulation could influence the capacity of cells to survive in the absence of adhesion to a substrate and without cell-cell contacts. To do it, cells were maintained in suspension in the presence of serum for 6h in a tube, gently shaken every 15 min. Under these conditions, a significant increase in apoptotic cells was observed in C3G knock-down Hep3B cells (Figure 15A). This could be a potential explanation for the decreased number of cells per focus in the anchorage-independent assay in C3G knock-down cells.

On the other hand, the analysis of the adhesion capacity at different time points, 15 and 30 min, showed that C3G down-regulation, as expected, significantly decreased adhesion (Figure 15B). This is in agreement with smaller foci with dispersed cells observed in anchorage-dependent growth assays (Figure 11). Collectively, these findings indicate that C3G is not only relevant for adhesion of HCC cells, but it also allows their survival in the absence of attachment, which might contribute to promote tumorigenesis, at least, *in vitro.*

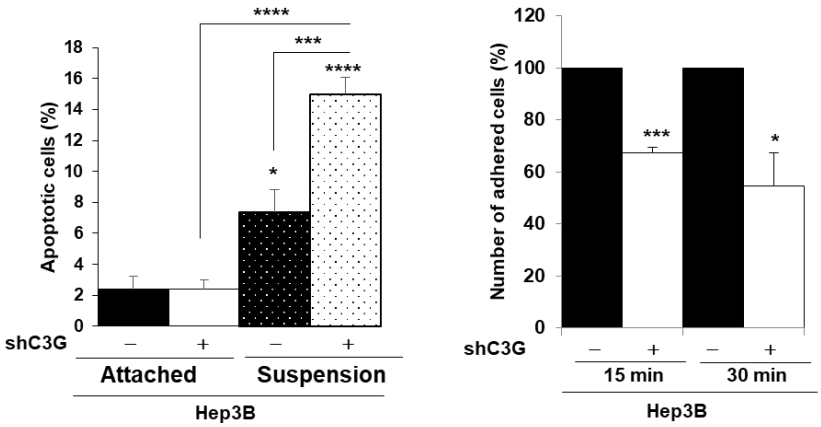

Figure 15. C3G promotes in vitro survival under non-adherent conditions and cell adhesion. *Non-silenced (-) and C3G knock-down (shC3G) Hep3B cells were maintained in complete medium.* ***Left panel****, histogram shows the mean ± S.E.M. of the percentage (%) of Hep3B cells with a lower DNA content than 2C (apoptotic) analyzed by cytometry, in cells maintained in culture under adherent or suspension conditions for 6h.* ***Right panel****, histogram represents the mean ± S.E.M. of the number of adhered cells (%) as compared with non-silenced cells (100%) after 15 and 30 min of their seeding. Individual cells, stained with crystal violet, were counted using ImageJ. *p≤0.05, ***p≤0.001, ****p≤0.0001, versus non-silenced cells (-), One-way ANOVA followed by multiple comparison (left panel) and Student's t-test (right panel), n ≥ 3.*

2.2. C3G down-regulation promotes migration and invasion of human hepatocarcinoma cells, through induction of an epithelial-mesenchymal-transition-like process.

Previous data from our group showed that C3G downregulation promoted migration and invasion in CRC HCT116 cells (Priego et al., 2016). Furthermore, as we have mentioned in the previous section, C3G knock-down HCC cells presented a more scattered phenotype with a tendency of cells to disperse in both, anchorage dependent- and independent-growth assays. This might indicate a higher motile capacity of these cells. In favor of this hypothesis, C3G silenced Hep3B cells did present lower adhesion. Hence, we decided to assess the role played by C3G in migration and invasion of HCC cells using in *vitro* functional assays.

In order to evaluate migration, we performed wound healing assays, measuring wound closure at 8 and 24h, in Hep3B and HLE cells. We found that C3G knock-down promoted

cell migration (Figure 16). We also performed invasion assays through matrigel, which showed an increased invasion in C3G silenced Hep3B and HLE cells (Figure 17).

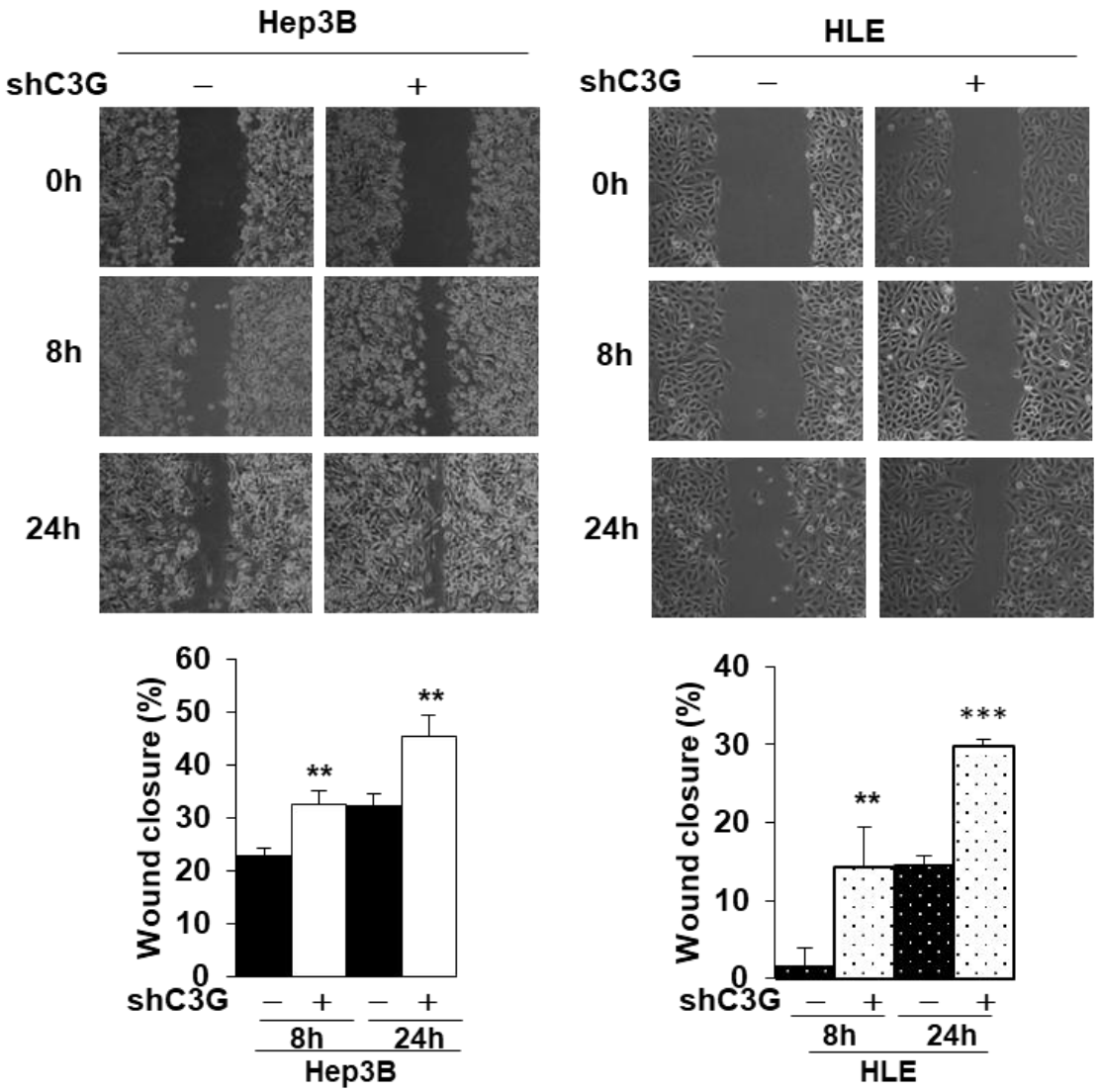

Figure 16. C3G knock-down increases Hep3B and HLE migratory capacity. *Wound healing assay in non-silenced (-) and C3G knock-down (+) Hep3B (left) and HLE (right) cells.* ***Top panel****, representative images from phase-contrast microscopy after 0, 8 and 24h of migration in the absence of serum with a previous pre-treatment with Mitomycin C.* ***Bottom panel****, histograms show the mean ± S.E.M. of the percentage of wound closure (%) analyzed using TScratch software. **p≤0.01, ***p≤0.001, versus non-silenced cells (-), Student's t-test, n ≥ 3.*

In an attempt to evaluate the mechanisms mediating these pro-migratory and –invasive properties, we decided to investigate whether human HCC cells were undergoing an epithelial to mesenchymal transition-like process induced by C3G down-regulation. We found that upon C3G silencing in Hep3B cells (epithelial-like phenotype), Vimentin and N-cadherin expression was up-regulated (Figure 18A, left panel), reaching levels comparable to those found in non-silenced cells submitted to a short-term treatment (48h) with TGF-β1, a well-documented inducer of EMT in HCC cells (Nieto et al., 2011; O'Connor and Gomez, 2014; Brown et al., 2004), used as a positive control. Additionally, Occludin, a

protein present in the tight junctions, was down-regulated upon both C3G knock-down and TGF-β1 treatment in Hep3B cells (Figure 18A, left panel). Moreover, β-catenin, a known EMT inducer, was internalized upon C3G knock-down in Hep3B cells (Figure 19). In contrast, in non-silenced Hep3B cells, β-catenin was localized in the membrane, in cell-cell junctions (Figure 19).

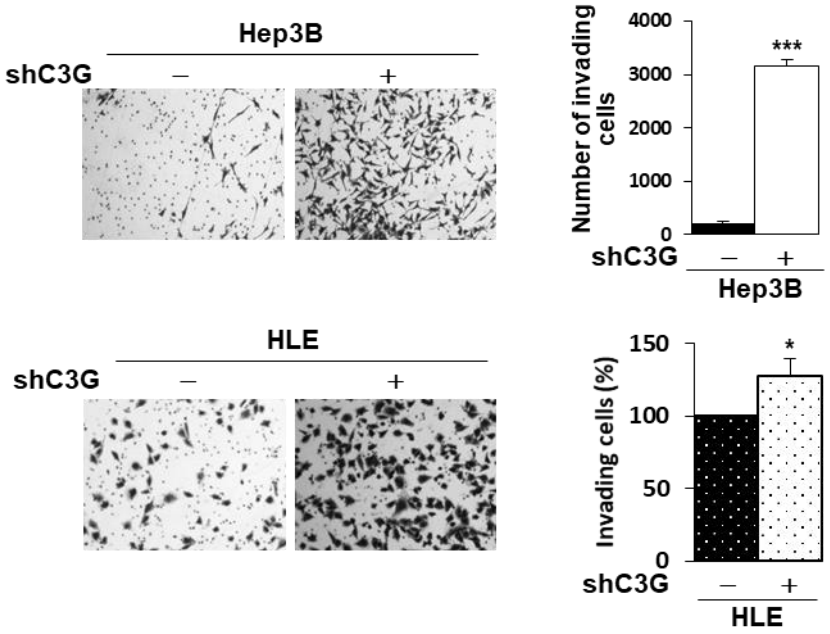

Figure 17. C3G knock-down increases Hep3B and HLE invasive capacity. *Non-silenced (-) and C3G knock-down (shC3G) Hep3B and HLE cells were used for invasion assays through matrigel using 10% FBS as chemoattractant.* ***Top panels****, representative images from phase-contrast microscopy of invading cells after 24h, stained with crystal violet.* ***Bottom panels****, histograms show the mean ± S.E.M. of the number of invading cells (Hep3B) or its percentage (%) (HLE) referred to non-silenced cells (100%). *p≤0.05, ***p≤0.001, versus non-silenced cells (-), Student's t-test, n ≥ 3****.*

In HLE cells (mesenchymal-like phenotype), Vimentin expression increased upon C3G down-regulation, reaching comparable levels to those induced by a short-term TGF-β1-treatment (Figure 18A, right panel). Taken together these data indicate that C3G knock-down mimics in a certain way the effects of TGF-β1, leading to an EMT-like process in HCC cells (Bertran et al., 2013). Therefore, we analyzed the expression of relevant transcription factors involved in EMT induction. We found that *Twist1* mRNA levels were up-regulated in a significant way in non-TGF-β1-treated C3G-silenced Hep3B cells, reaching levels comparable to those found in TGF-β1-treated (6h) non-silenced cells (Figure 18B, left). TGF-β1 had no additional effect on *Twist1* expression in C3G knock-down cells. Similarly, *Zeb2* mRNA levels exhibited analogous changes, although they did not reach statistical significance (Figure 18B, right). Taken together all these data indicate that C3G down-regulation promotes migration and invasion in human HCC cell lines by inducing an EMT-like process, mimicking TGF-β1 effect.

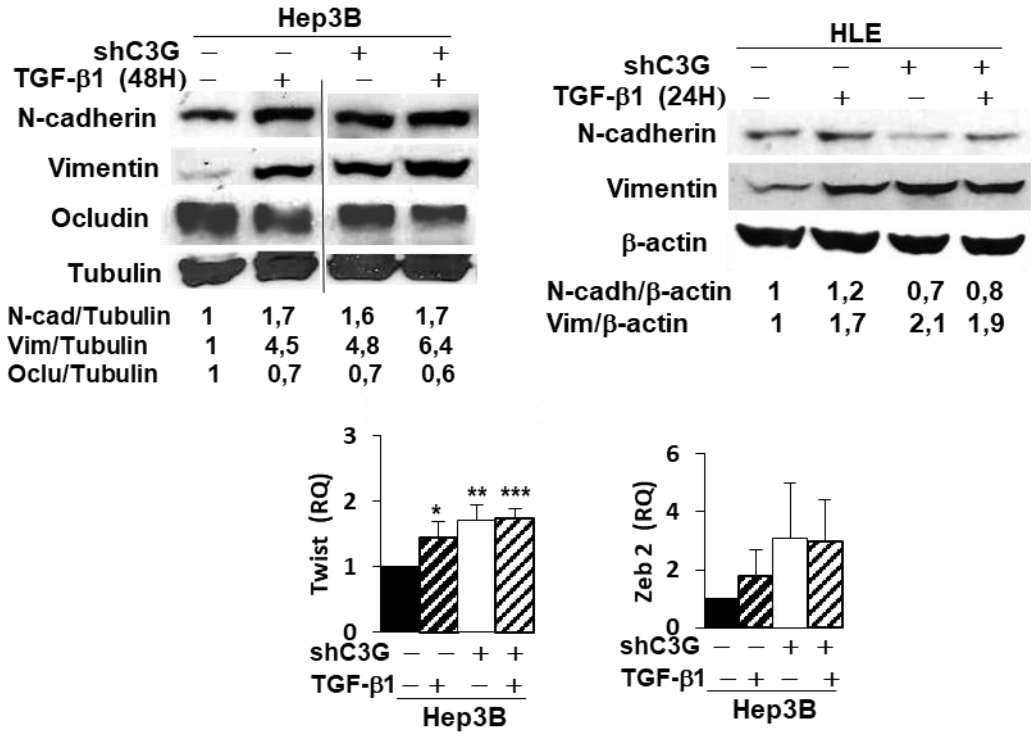

Figure 18. C3G knock-down induces an EMT-like process mimicking TGF-β1 effect in HCC cells. *Non-silenced (-) and C3G knock-down (+) Hep3B or HLE cells with (+) or without (-) were maintained untreated or treated with TGF-β1 (5ng/ml) for the indicated time to induce EMT.* ***(A)*** *Western-blot analysis of N-cadherin, Vimentin and Occludin, normalized with Tubulin or β-actin.* ***(B)*** *RT-qPCR analysis of Twist1 and Zeb2 mRNA levels. Histograms show the mean ± S.E.M. of RQ values referred to the control (untreated non-silenced cells). *p≤0.05, **p≤0.01, ***p≤0.001, versus untreated non-silenced cells, One-way ANOVA followed by multiple comparison, n ≥ 3.*

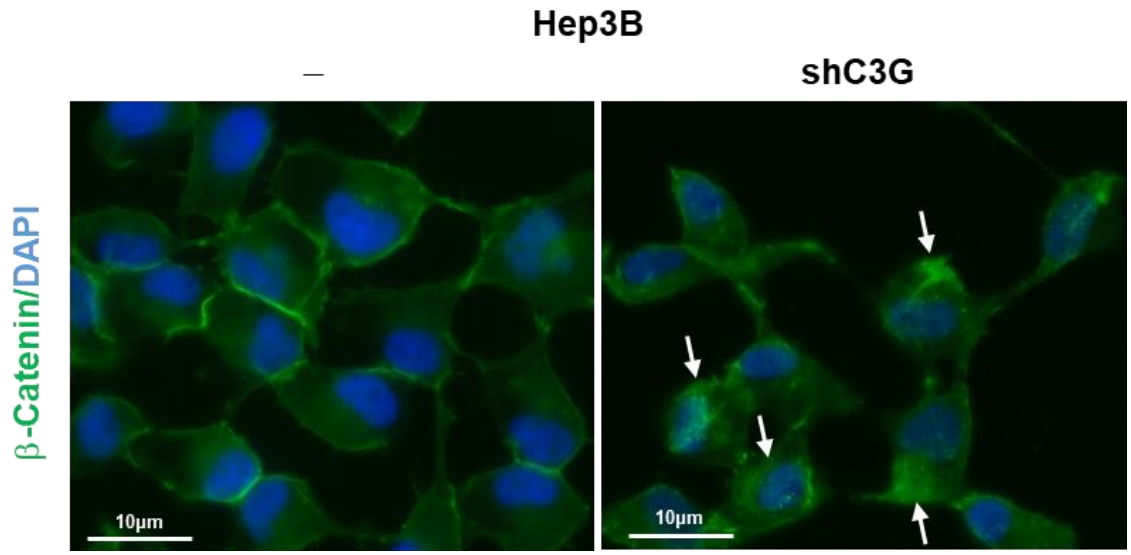

Figure 19. β-catenin is internalized upon C3G knock-down in Hep3B cells. *Immunofluorescence staining of β-catenin (green) in Hep3B cells with (shC3G) or without (-) C3G knock-down, under serum-starved conditions. Nuclei were stained with DAPI (blue). Representative images from immunofluorescence microscopy. White arrows point at internalized β-catenin.*

As an additional approach, to further confirm that C3G down-regulation induces an EMT-like process responsible for the enhanced HCC cells migration and invasion, we compared the effect of a long-term treatment with TGF-β1, known to induce a stable EMT process in these cells (Bertran et al., 2013), with the effect of C3G knock-down. As expected, TGF-β1-induced stable EMT, highly increased migration of non-silenced Hep3B and HLE cells up to the levels of C3G silenced cells in a wound healing assay (Figure 20). TGF-β1-treatment additionally increased migration in C3G knock-down HLE cells, but differences were not statically significant. Similarly, the long-term treatment with TGF-β1 highly enhanced invasion in non-silenced Hep3B cells up to the level found in C3G knock-down

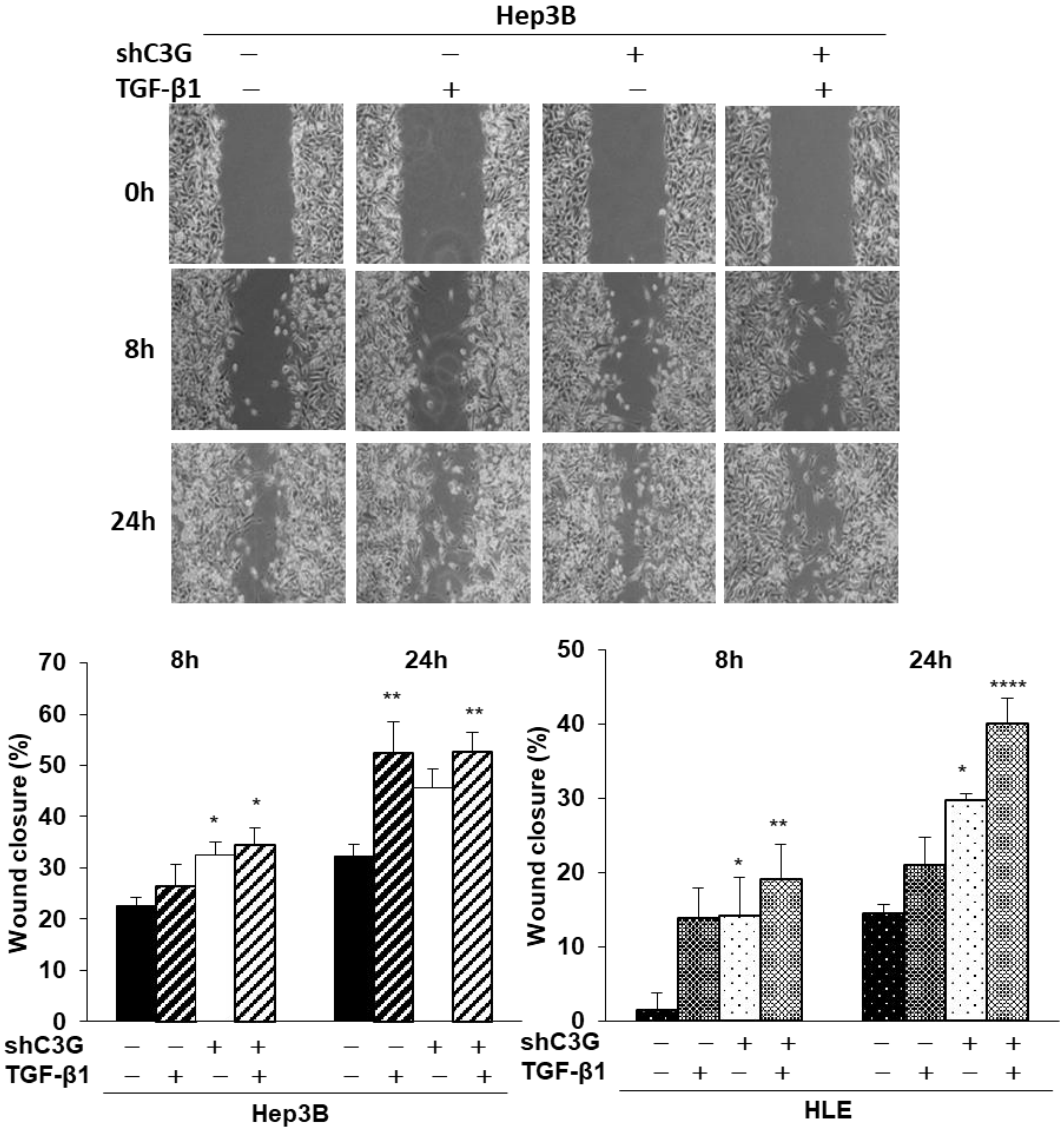

Figure 20. C3G knock-down enhances migration through the induction of an EMT-like process in HCC cells. *Non-silenced (-) and C3G knock-down (+) Hep3B cells were maintained untreated (–) or were treated chronically with TGF-β1 (2.5ng/ml) to maintain mesenchymal phenotype.* ***Top panel****, representative images from phase-contrast microscopy after 0, 8 and 24h of migration in the absence of serum with a previous pre-treatment with Mitomycin C.* ***Bottom panel****, histograms show the mean ± S.E.M. of the wound closure percentage (%) analyzed using TScratch software. *p≤0.05, **p≤0.01, ****p≤0.0001, versus non-silenced cells (-), One-way ANOVA followed by multiple comparison, n ≥ 3.*

Hep3B cells, where TGF-β1 treatment additionally increased invasion without reaching significance (Figure 21A).

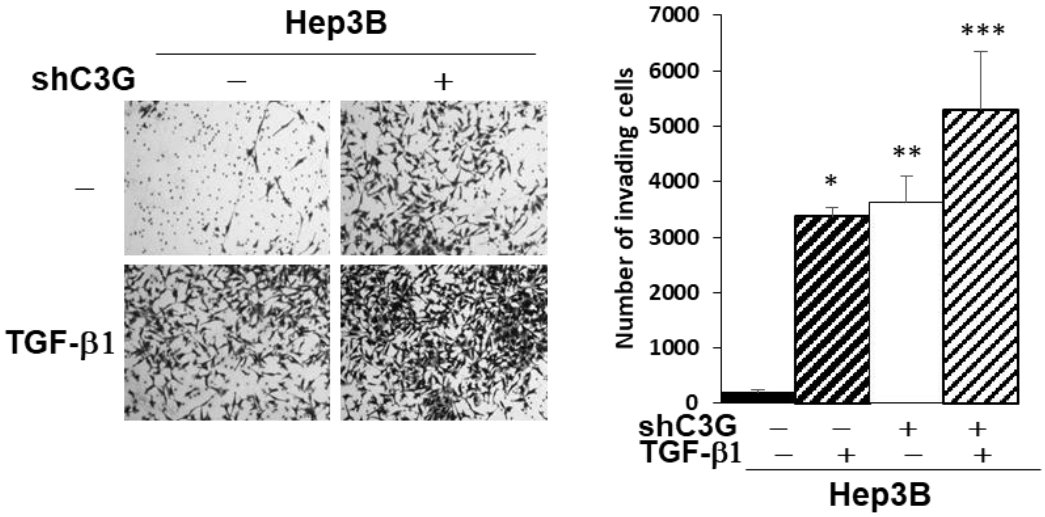

Figure 21. C3G knock-down increases invasion through the induction of an EMT-like process in HCC cells. *Non-silenced (-) and C3G knock-down (+) Hep3B cells with (+) or without (-) were maintained untreated (–) or were treated chronically with TGF-β1 (2.5ng/ml) to maintain mesenchymal phenotype. Invasion assay through matrigel using 10% FBS as chemoattractant.* ***Left panels****, representative images from phase-contrast microscopy of invading cells after 24h, stained with crystal violet.* ***Right panels****, histogram shows the mean ± S.E.M. of the number of invading cells. *p≤0.05, **p≤0.01, ***p≤0.001, versus non-silenced cells (-), One-way ANOVA followed by multiple comparison, n ≥ 3.*

Altogether, the previously described data indicate that C3G down-regulation in HCC cells leads to changes in the expression of genes associated with EMT and the acquisition of pro-migratory/invasive phenotype reminiscent to the TGF-β1-induced EMT. However, the fact that TGF-β1 has a tendency to exert an additional effect over that elicited by C3G

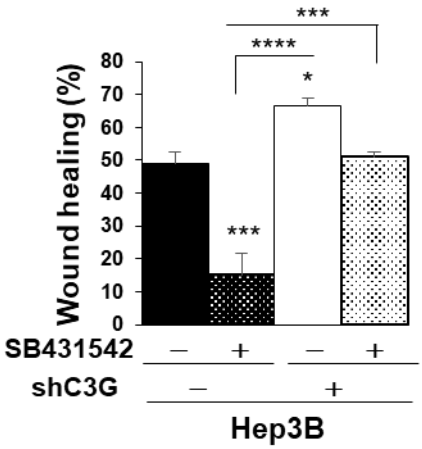

Figure 22. C3G knock-down induces migration through an EMT-like process partially independent of TGF-β1 in HCC cells. *Non-silenced (-) and C3G knock-down (+) Hep3B cells with (+) or without (-) were maintained untreated (–) or were treated chronically with TGF-β1 (2.5ng/ml) to maintain mesenchymal phenotype. Histogram represents the mean ± S.E.M. of wound closure (%) after 6 hours with (+) or without (-) SB431542 TGF-β1 inhibitor treatment. *p≤0.05, ***p≤0.001, **** p≤0.0001 versus non-silenced cells (-), Two-way ANOVA, followed by multiple comparison, n ≥ 3.*

down-regulation in Hep3B cells in terms of Vimentin expression and both, cell migration and invasion, suggests that C3G silencing could be acting through TGF-β1 dependent and independent mechanisms. To test this hypothesis, we analyzed the effect of a TGF-β1-receptor inhibitor (SB431542) on cell migration. Treatment with this inhibitor decreased cell migration, but its effect was only significant in non-silenced cells, but not in C3G-silenced cells (Figure 22). These data suggest that C3G down-regulation promotes an EMT-like process through a mechanism that is, at least, partially independent of TGF-β1.

On the other hand, previous data from our laboratory, showed that in CRC HCT116 cells, C3G down-regulation enhanced pro-migratory and –invasive capacities through the increase of p38α MAPK activity (Priego et al., 2016). As shown in Figure 23A, we observed that under basal conditions, phospho-p38 MAPK levels were higher in C3G silenced than in non-silenced HCC cells. Moreover, the increased migration and invasion induced by C3G down-regulation in Hep3B cells was significantly decreased upon p38α/β MAPK inhibition with SB203580, reaching the same level than non-silenced cells (Figure 23B). Therefore, in agreement with the CRC model, in human HCC cells, p38 MAPK activation would contribute to the enhanced migration and invasion induced by C3G silencing.

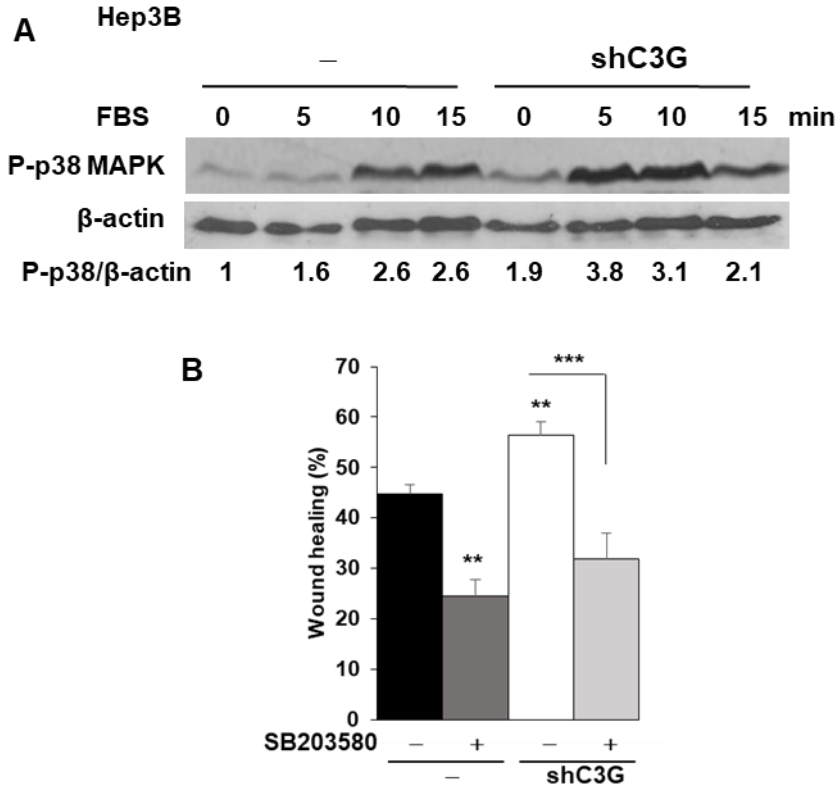

Figure 23. C3G knock-down increases p38 MAPK activation, which contributes to C3G knock-down induced migration in Hep3B cells. *Hep3B (non-silenced and C3G knock-down (shC3G)) cells were used.* ***(A)*** *Cells were serum-starved and stimulated with 10% FBS for 5-15min. Activation of p38 MAPK was determined by western-blot analysis of P-p38 MAPK levels and normalized with β-actin.* ***(B)*** *Wound healing assay. Cells were maintained in the absence of serum, untreated (–) or treated with the p38 MAPK inhibitor, SB203580 (5μM) and were allowed to migrate after doing the wound. Histogram represents the mean ± S.E.M. of wound closure percentage (%). **p≤0.01, ***p≤0.001, versus non-silenced cells (-), Two-way ANOVA, followed by multiple comparison, n ≥ 3.*

2.3. C3G induces *in vivo* hepatocarcinoma tumor growth.

In the previous sections, we demonstrated by *in* vitro functional assays that C3G confers tumorigenic properties to HCC cell lines, while its down-regulation enhances their migratory and invasive capacities. Therefore, to further characterize the role of C3G in the tumorigenic properties of HCC cells, we next explored whether C3G down-regulation affects *in vivo* tumor growth of HCC cells by performing xenograft assays in nude mice. C3G knock-down and non-silenced Hep3B cells were injected into the flanks of nude mice and tumor size was monitored along the time. We found that the volume of tumors generated by C3G-silenced Hep3B cells at the end point was significantly reduced as compared with that of tumors originated by non-silenced cells (Figure 24).

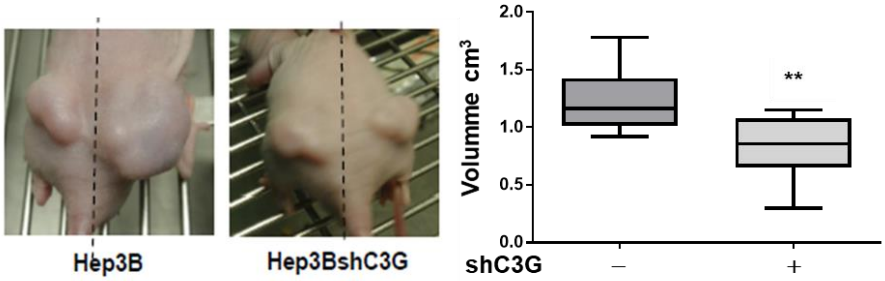

Figure 24. C3G promotes in vivo tumor growth. *Xenograft assay was performed by subcutaneous injection of non-silenced (-) and C3G knock-down (shC3G) Hep3B cells into nude mice flanks.* ***Left panel****, representative images of mice flanks showing tumors at end point.* ***Right panel****, box plot shows the mean ± S.E.M. of tumor volume in cm^3 at end point, calculated by the formula V= π/6*1.69*(L*W)^(3/2), where L is length and W is width. **p≤0.01, versus non-silenced cells (-), Student's t-test, n=2 (each independent experiment with a group of 8 nude mice to comply with the institutions guidelines that recommend the use of the minimum necessary number of animals for experimental purposes).*

In order to explore the potential mechanisms mediating the decreased *in vivo* tumor growth upon C3G knock-down in Hep3B cells, we measured apoptosis and proliferation in tumor sections through the quantification by immunofluorescence of active caspase 3 and Ki67, respectively. We found that, the active caspase 3-stained area was significantly higher in tumors originated by Hep3B cells with C3G down-regulation than those originated by non-silenced cells, while Ki67-positive (proliferating) cells were significantly decreased (Figure 25). These results indicate that C3G down-regulation reduced *in vivo* tumor growth of human HCC cells through a mechanism that involves both an up-regulation of apoptosis and a decrease in cell proliferation.

Additionally, in tumors generated by C3G knock-down Hep3B cells, we found an upregulation of the mesenchymal marker, Vimentin, coherent with its upregulation in cultured cells (Figure 25).

We have demonstrated that C3G promotes tumor growth in xenograft assays, as shown by a bigger size of tumors generated by non-silenced HCC cells, which exhibited higher proliferation and lower apoptosis as compared to those originated by C3G silenced cells. To further elucidate the mechanisms involved in the described tumor growth, we

considered the potential implication of tumor microenvironment. Hence, we analyzed the presence of fibroblasts in the stroma of the tumors generated in xenograft experiments. To this end, an immunostaining of α-SMA (α-smooth muscle actin), a marker of active fibroblasts (myofibroblasts), was performed that revealed significant higher levels of α-SMA in the tumors generated by non-silenced Hep3B cells (Figure 26A). This suggests that high levels of C3G in HCC cells would promote the activation of fibroblasts and might induce a bilateral communication between tumor stromal and tumor cells, creating a more favorable niche for tumor growth.

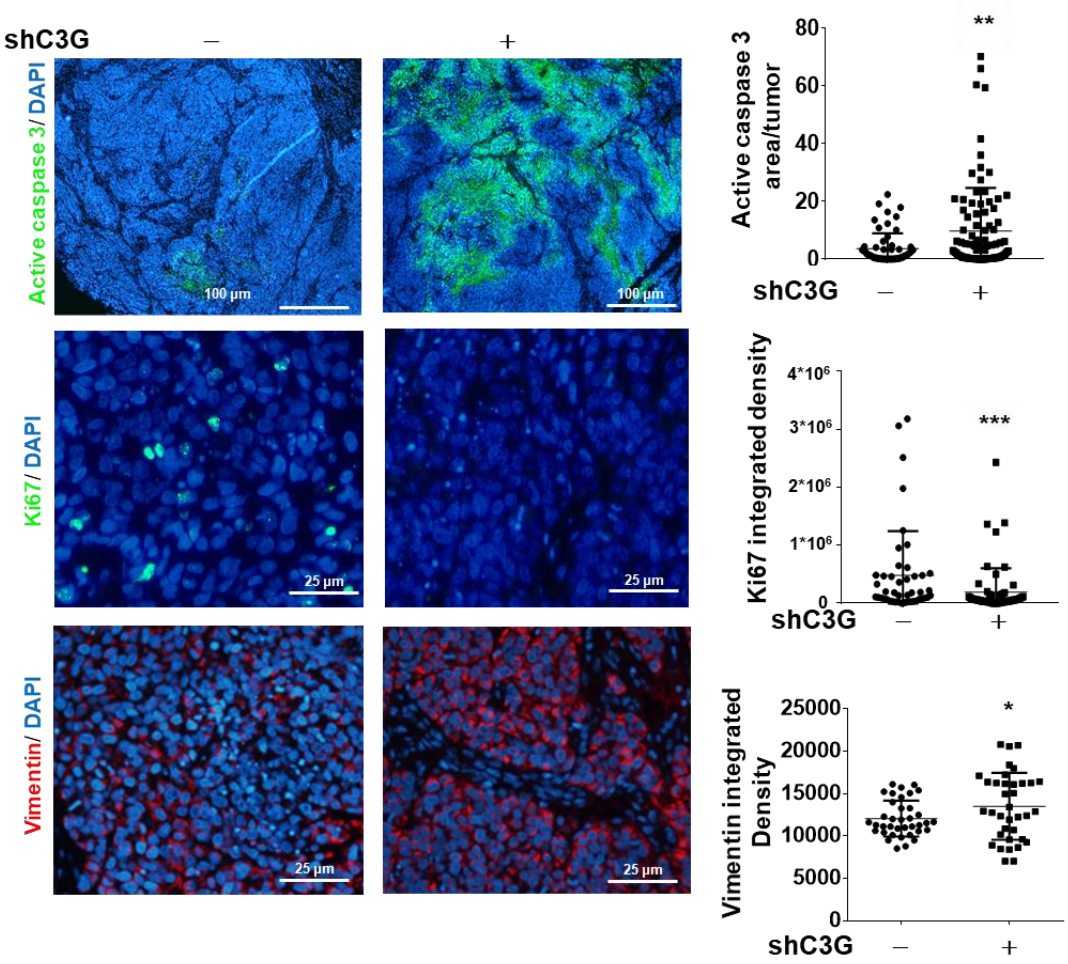

Figure 25. C3G promotes in vivo tumor growth by increasing proliferation while impairing apoptosis. *Xenograft assay was performed by subcutaneous injection of non-silenced (-) and C3G knock-down (+) Hep3B cells into nude mice flanks.* ***Left panels****, representative microscope images showing immunofluorescence of active caspase 3 (green); ki67 (green); and Vimentin (red), from paraffin-embedded tumor sections. Dapi (blue) was used for nuclei staining.* ***Right panels****, scatter plots showing the mean ± S.E.M. of active caspase 3 positive area/tumor; Ki67 and Vimentin integrated density/Dapi area. Images were analyzed using ImageJ. *p≤0.05, **p≤0.01, ***p≤0.001 versus non-silenced cells (-) Student's t-test, n=2.*

In order to test this hypothesis, we analyzed mRNA expression of some growth factors and cytokines, HGF, TGF-β1 and IL-6, in both mouse (tumor stroma) and human (tumor) cells. Although the results were not statistically significant, we found a higher expression of HGF, TGF-β1 and IL-6 mRNAs from mouse origin, likely coming from the stroma of

tumors generated by non-silenced Hep3B cells as compared to those originated by cells with C3G down-regulation (Figure 26B). Hence, the stroma generated by non-silenced cells, with higher HGF, TGF-β1 and IL-6 expression would support the hypothesis of its potential contribution to increase tumor growth, progression and immune tolerance. The pattern of expression of HGF, TGF-β1 and IL-6 mRNAs by HCC cells was different. TGF-β1 mRNA expression was similar in both C3G silenced and non-silenced cells, while HGF and IL-6 mRNA levels had a tendency to be higher in tumors derived from non-silenced cells (Figure 26B). The higher HGF expression might be an attempt to overcome a defective Met signaling (later described in section 3), while the increase in human IL-6 levels might act as a pro-metastatic signal (Wang et al., 2016).

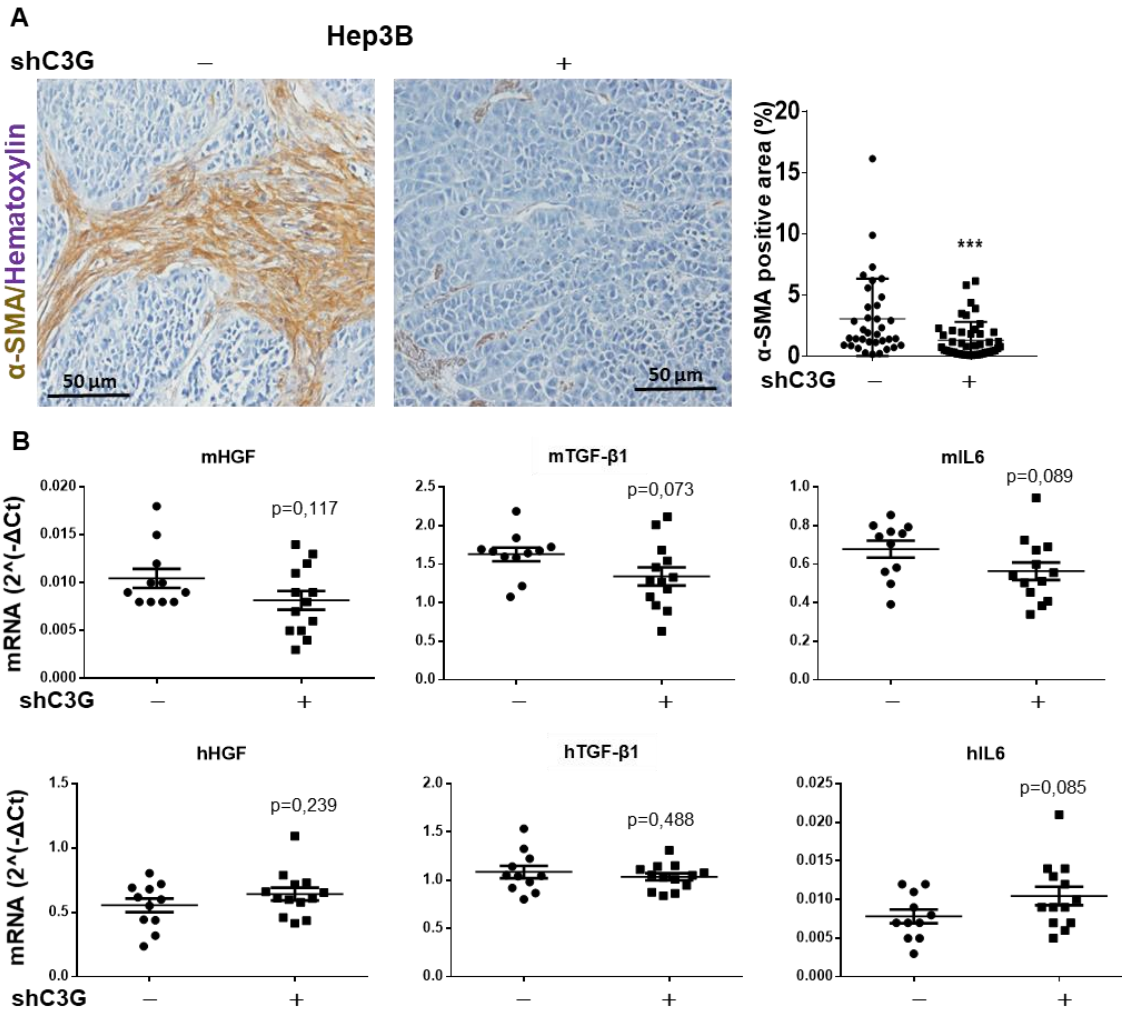

Figure 26. Xenograft tumors generated by non-silenced Hep3B cells are highly infiltrated by fibroblasts. *Xenograft assay generated by subcutaneous injection of (non-silenced (-) and C3G knock-down (+) Hep3B cells into nude mice flanks.* ***(A)*** *Left panel, representative images from phase-contrast microscopy of α-SMA immunohistochemical staining of paraffin-embedded xenograft tumor sections. Right panel, scatter-plot represents α-SMA positive area expressed as percentage (%). Images were analyzed using ImageJ software. ***p≤0.001, versus non-silenced cells (-), Student's t-test, n ≥ 2.* ***(B)*** *RT-qPCR analysis of HGF, TGF-β1 and IL-6 mRNAs from mouse (m) or human (h) origin. Histograms show the mean ± S.E.M. of 2^(-ΔCt) values. No statistical significance was obtained by Student's t-test.*

Based on the increased migration and invasion found in HCC cells with C3G down-regulation, accompanied by higher levels of mesenchymal markers like Vimentin, found by *in vitro* and *in vivo* assays, we hypothesized that C3G down-regulation might facilitate HCC cells dissemination. Therefore, we analyzed the presence of disseminated tumor cells (DTCs) in the bone marrow of mice used for the xenograft assays. We found that in nude mice injected with C3G knock-down Hep3B cells, the number of DTCs was higher as compared to non-silenced, even though the differences did not reach significance (Figure 27). This might support the idea of a potential increased metastatic potential of HCC cells with low levels of C3G.

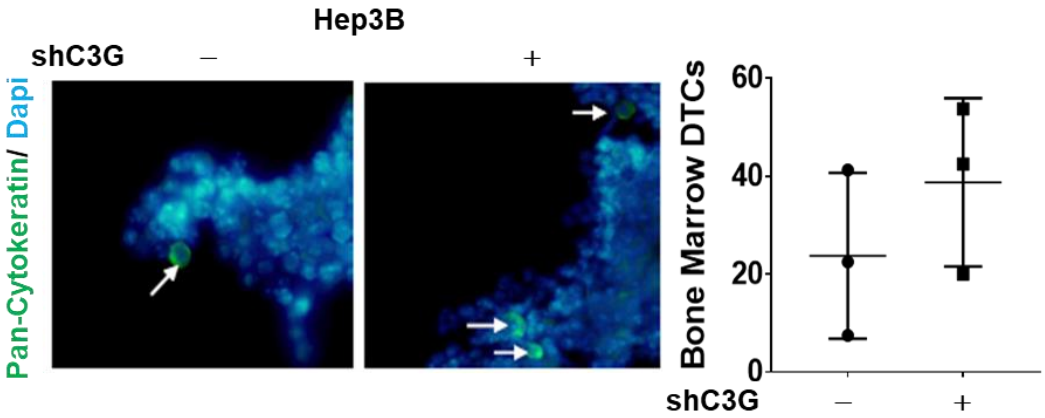

Figure 27. C3G promotes in vivo dissemination of Distant Tumor Cells in Bone Marrow. *Bone marrow cytospins obtained from nude mice used in xenograft assays performed with non-silenced (-) and C3G knock-down (+) Hep3B cells. Immunofluorescence staining with Pan-cytokeratin (green) and nuclear Dapi (blue) was performed to detect disseminated tumor cells (DTCs).* ***Left panel****, representative images from immunofluorescence microscopy. White arrows mark positive cells.* ***Right panel****, scatter plot of the mean ± S.E.M of the number of Bone Marrow DTCs, after quantification of pan-cytokerakin positive cells using ImageJ.*

3. FUNCTION OF C3G IN THE GENERATION OF METASTASIS BY MOUSE HEPATOCARCINOMA CELLS OVEREXPRESSING MET. KEY ROLE OF C3G IN HGF/MET PATHWAY.

3.1. Function of C3G in the generation of lung metastasis by mouse hepatocarcinoma cells overexpressing Met.

Taking into account the above data, C3G knock-down exacerbates the pro-migratory and invasive capacities of HCC cells. Moreover, there is a tendency to disseminate to bone marrow for those Hep3B cells with C3G down-regulation. Thus, we analyzed whether low levels of C3G confers to HCC cells any advantage to generate lung metastases. To do it, we performed heterotopic xenograft assays using various mHCC (Mouse Alb-R26^{Met}) cells

lines that express different C3G levels (mHCC1<mHCC13<mHCC14), as shown in Figure 6B. Once the tumors grew, they were removed and mice were kept alive for a period of approximately 4 months to allow lung metastasis development. Lungs were then removed and analyzed. We found that the percentage of mice that developed lung metastasis inversely correlated with C3G protein levels initially present in the HCC cells (Figure 6B), being 50% for mHCC1 cells, 66.7% for mHCC13 and 80% for mHCC14, as shown in Figure 28A. The volume of lung macro-metastasis was also inversely correlated with C3G levels in these HCC cells, being progressively higher in lung tumors derived from mHCC1<mHCC13 <mHCC14 (Figure 28B).

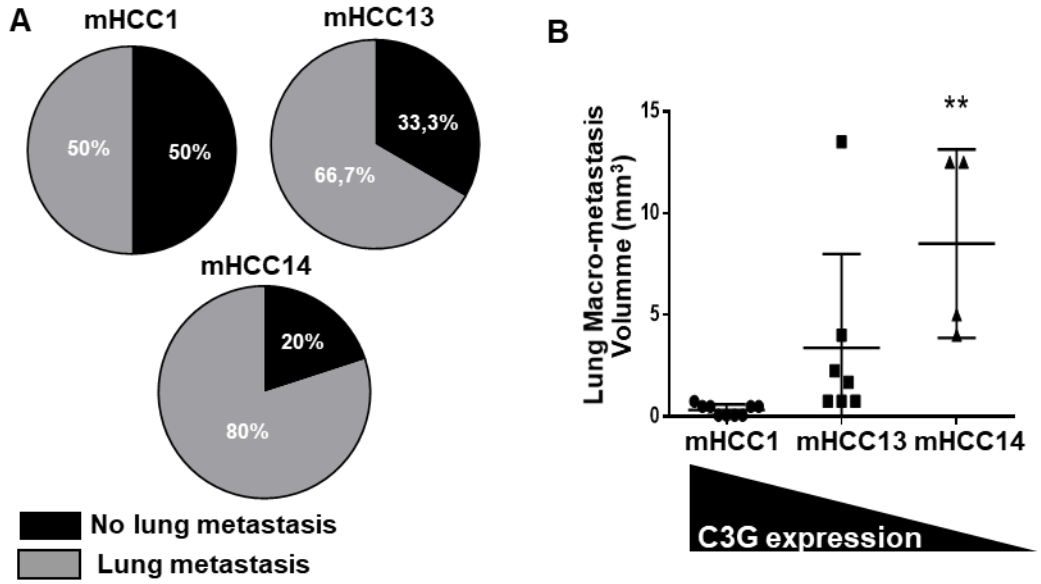

Figure 28. C3G expression inversely correlates with lung metastatic potential in mouse HCC cell lines. *Mouse Alb-R26^{Met} HCC cell lines (mHCC1, mHCC13, and mHCC14) were injected subcutaneously into the flank of wild type mice (from the same genetic background of mice used to obtain mHCC cells) to generate heterotopic tumors and lung metastasis. (A) Pie charts indicate the percentage of mice with or without lung metastasis for each mHCC cell line. (B) Scatter plot shows the mean ± S.E.M of the volume in mm^3 of lung macro-metastasis for each mHCC cell line. Black triangle shows the corresponding decreasing levels of C3G in mHCC cell lines. **p≤0.01, versus mHCC1, one-way ANOVA followed by multiple comparison, n=2.*

Moreover, a closer examination of the lung sections revealed that the area of micro-metastases was also higher in lung tumors generated from mHCC13 and mHCC14 (Figure 29). To our surprise, C3G protein levels increased in all lung metastases as compared to their corresponding primary xenograft tumors (Figure 30). This suggests that C3G could be necessary for the growth of these secondary tumors (metastases), at least, in lung. Therefore, even though the migratory and invasive capacity increases in HCC upon C3G down-regulation, C3G re-expression might be required for the proliferation and survival of the HCC cells generating the metastases as it occurs in primary tumors. However, our previous analyses using the information from public databases showed that metastatic samples from HCC patients expressed lower levels of C3G mRNA as compared to HCC samples (Sequera et al., 2018). Therefore, we performed further analyses taking into

account the metastasis location. To do it, we used HCMDB classifying HCC primary tumors according to their site of metastasis, lung, adrenal gland or lymph node, and compared them with their respective metastasis. We found that in agreement with the increased

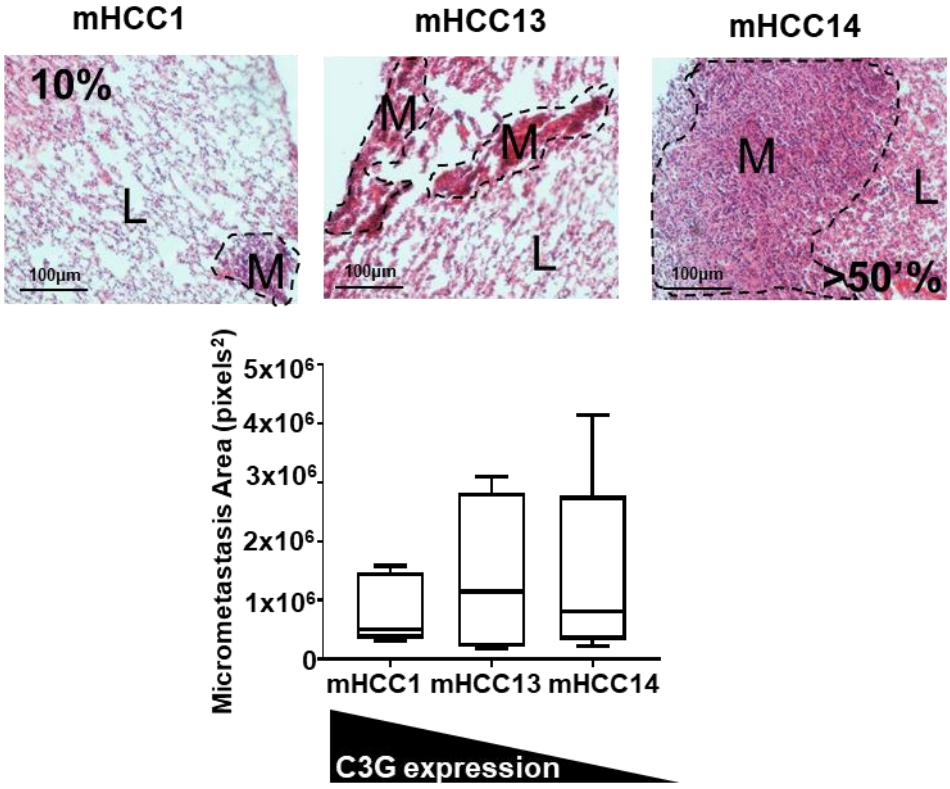

Figure 29. Area of lung micro-metastasis is inversely correlated to C3G expression in mHCC cell lines. *Mouse Alb-R26^{Met} HCC cell lines (mHCC1, mHCC13, and mHCC14) were injected subcutaneously into the flank of wild type mice (from the same genetic background of mice used to obtain mHCC cells) to generate heterotopic tumors and lung metastasis.* ***Top panel****, representative images of the Hematoxylin/Eosin stained lungs. Lung (L), Metastasis (M). Dotted lines delimit metastasis area.* ***Bottom panel,*** *box plot represents the mean ± S.E.M of lung micro-metastasis area (pixels^2) for each mHCC cell line, analyzed in Hematoxylin/Eosin-stained paraffin-embedded lung sections using ImageJ. Black triangle shows the corresponding decreasing levels of C3G in mHCC cell lines p=0.4, versus mHCC1, one-way ANOVA followed by multiple comparison, n=2.*

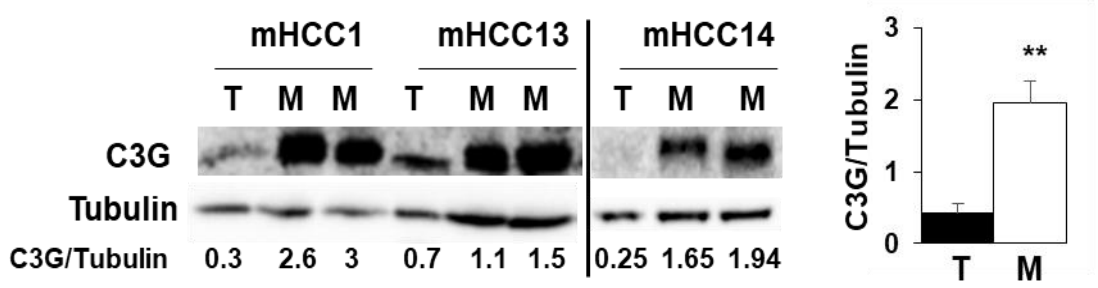

Figure 30. C3G protein levels increase in lung metastasis samples generated by Met overexpressing mouse HCC cells. *Western-blot analysis of C3G protein levels in liver tumor (T) and lung metastasis (M) samples from xenograft assays for each mHCC cell line, normalized with tubulin. Right panel, histogram represents the quantification of C3G/tubulin levels of tumor (T) and metastasis (M) samples from western-blot. **p≤0.01, versus tumor samples, Student's t-test, n ≥ 3.*

C3G protein levels in lung metastasis, C3G mRNA levels have a tendency to be higher in patient samples from lung metastasis (the most prevalent type) as compared to primary tumor samples (Figure 31). In contrast, a significant decrease in C3G mRNA levels was observed in patient samples from adrenal gland metastasis and no differences were detected in lymph node metastasis as compared to the primary tumor (Figure 31). Therefore, it is possible that depending on the organ where the metastasis is generated, the requirements of C3G might be different.

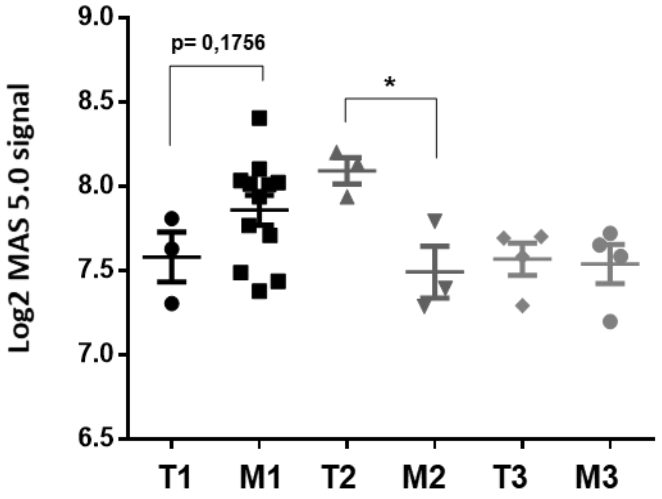

***Figure 31**. **C3G mRNA expression increases in lung metastasis of HCC patients.** Scatter plot represent mean ± S.E.M. of RapGEF1 mRNA levels expressed as log2 MAS 5.0 signal of HCC primary tumors and metastasis, separated by anatomic location: HCC liver primary tumor with lung metastasis (T1; 3 patients) and their corresponding lung metastasis (M1; 12 patients); HCC liver primary tumor with adrenal gland metastasis (T2; 3 patients) and their corresponding adrenal gland metastasis (M2; 3 patients); HCC liver primary tumor with lymph node metastasis (T3; 4 patients) and their corresponding lymph node metastasis (M3; 4 patients). *p≤0.05, versus corresponding primary tumor, Student's t-test. Data was collected from HCMDB (Human Cancer Metastasis Data Base).*

3.2. C3G ensures a full activation of HGF/Met signaling pathway in human hepatocarcinoma cells.

The effect of C3G knock-down decreasing anchorage-dependent growth in HCC cells derived from mouse liver tumors generated by Met overexpression and the high C3G protein expression in these tumors indicates that C3G might play a key role in HGF/Met pathway in HCC cells. Thus, we analyzed the effect of C3G knock-down on Met signaling activation in response to HGF stimulation in Hep3B cells. First, we evaluated the activation of Met and Gab1, an important adaptor for Met signaling, upon HGF stimulation. We found that tyrosine phosphorylation of Met (in Tyr1234/1235) and Gab1 was highly reduced in C3G silenced Hep3B cells (Figure 32). Moreover, the levels of phosphorylated Abl, p38 MAPK and ERKs were also reduced in C3G knock-down cells. These results indicate that HGF/Met signaling is defective in C3G silenced HCC cells. In agreement with this, we found that HGF was not able to promote cell migration in C3G knock-down Hep3B

cells (Figure 33) and inhibition of Met with SU11274 has a very limited effect decreasing migration as compared to non-silenced cells.

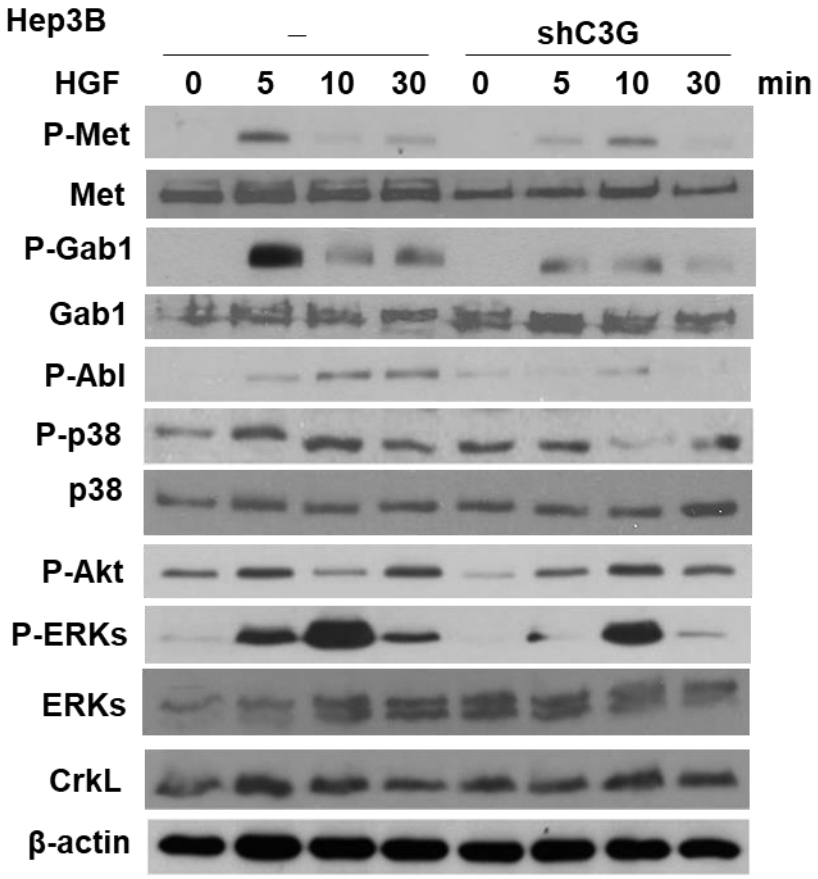

Figure 32. HGF/Met signaling is defective in C3G knock-down HCC cells. *Non-silenced (-) and C3G knock-down (shC3G) Hep3B cells were serum starved for 24h and then, stimulated with HGF (40ng/ml) for the indicated time. Western-blot analysis of P-Met (Y1234-1235), Met, P-Gab1 (Y627), Gab1, P-Abl (Y412), P-p38 (Thr180/Tyr182), p38, P-Akt (Ser473), P-ERKs (Thr202/Tyr204), ERKs, CrkL and normalization with β-actin.*

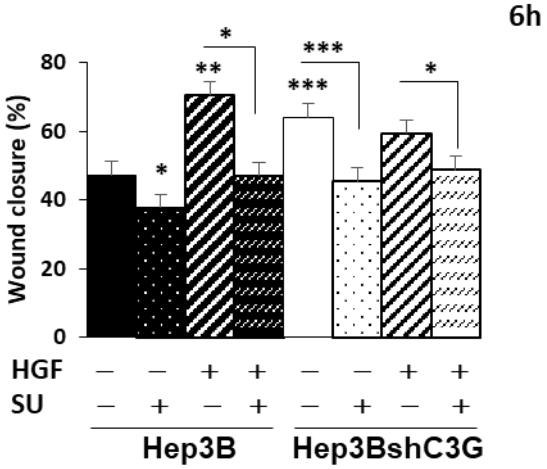

Figure 33. HGF was unable to promote migration in C3G knock-down Hep3B cells. *Wound healing assay in non-silenced (-) and C3G knock-down (shC3G) Hep3B cells. Cells were maintained in the absence of serum, untreated or treated with HGF (40ng/ml) and/or SU11274 (5μM) and were allowed to migrate after doing the wound. Histogram shows the mean ± S.E.M. of wound closure percentage (%), analyzed by using TScratch software. Two-way ANOVA followed by multiple comparison, *p≤0.05, **p≤0.01, ***p≤0.001, n ≥ 3.*

Data from the literature showed that in HEK293 cells, HGF induced the interaction between Gab1 and CrkL upon exogenous Gab1 overexpression, being C3G also present in this complex, as it is associated to CrkL already in unstimulated cells (Sakkab et al., 2000). Therefore, we evaluated the potential association between endogenous C3G and Gab1 in Hep3B cells and the effect of C3G knock-down. We found that in response to HGF, only in Hep3B non-silenced cells, C3G co-immunoprecipitated with Gab1, while in both non-silenced and C3G silenced cells, the interaction with CrkL remained unaltered, independently of the presence or absence of HGF (Figure 34). These results indicate that HGF induces Gab1 binding to C3G in Hep3B cells, which supports the defective HGF/Met signaling found in C3G knock-down cells. However, CrkL would not be the necessary mediator. Indeed, CrkL might be associated to Gab1 in unstimulated cells and C3G would bind to Gab1 only in response to HGF. Surprisingly, pull-down assays with GST protein fused to Crk SH3 domains revealed an interaction of Crk SH3 domain with P-Gab1 and P-Met in non-silenced Hep3B cells in response to HGF, probably mediated by an adaptor protein (Figure 35).

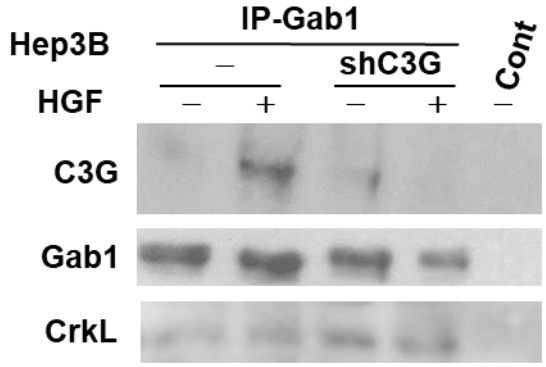

Figure 34. HGF-induced C3G interaction with Gab1 in HCC cells. *Non-silenced (-) and C3G knock-down (shC3G) Hep3B cells were serum starved for 24h and stimulated with HGF (40ng/ml) for 5min. Immunoprecipitation of Gab1 (IP-Gab1) in lysates and western-blot analysis of C3G, Gab1 and CrkL. As a negative control, sepharose beads were incubated with lysates.*

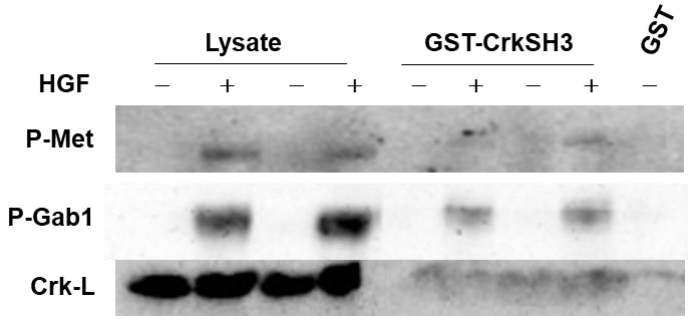

Figure 35. Crk SH3 domains interact with P-Gab1 and P-Met in Hep3B cells. *Hep3B cells were serum starved for 24h and stimulated with HGF (40ng/ml) for 5min. Western-blot analysis of P-Met, P-Gab1 and CrkL in total lysates and in samples from pull down assays performed with GST fused to Crk SH3 domains (GST-CrkSH3). As a negative control, lysates were incubated with GST-beads.*

On the other hand, HGF treatment of Hep3B cells induced the binding of P-Gab1, but not CrkL, to C3G proline-rich domain (C3GSH3b) in pull down assays (Figure 36). Therefore, C3G might use an alternative adaptor containing SH3 domains to mediate its association with P-Gab1.

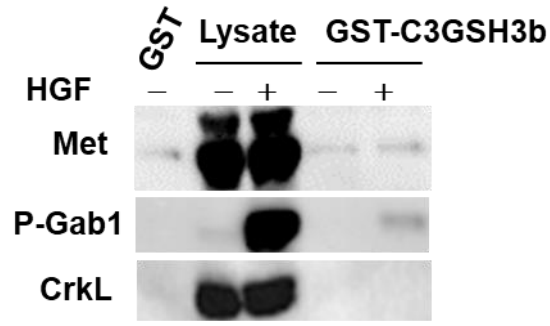

Figure 36. C3G SH3 binding domain interacts with P-Gab1 independently of CrkL in Hep3B cells. *Hep3B cells were serum starved for 24h and stimulated with HGF (40ng/ml) for 5min. Western-blot analysis of Met, P-Gab1 and CrkL in lysates and in samples from pull down assays performed with GST fused to C3G SH3-binding domain (GST-C3GSH3b). As a negative control, lysates were incubated with GST-beads.*

To further characterize the mechanisms implicated in the defective HGF/Met signaling in HCC cells with C3G down-regulation, we performed additional assays in mouse HCC cell lines overexpressing Met (mHCC1). C3G was clearly detected in both Met and Gab1 immunoprecipitates (Figure 37A). Additionally, phosphorylated Met was detected in both Gab1 and Met immunoprecipitates (Figure 37A), which indicates that active Met forms complexes, either directly or indirectly, with C3G and Gab1. Neither C3G nor P-Met could be detected in Abl immunoprecipitates. Furthermore, the interaction between C3G and Met was highly reduced in C3G silenced mHCC1 cells, as predicted (Figure 37B).

On the other hand, taking into account that Abl can contribute to HGF/Met signaling (Furlan et al., 2012) and that C3G and Met form complexes, we determined the effect of Abl inhibition by Imatinib on Met activation. We found that HGF-induced Met phosphorylation decreases upon Abl inhibition, although it was not abolished. In contrast,

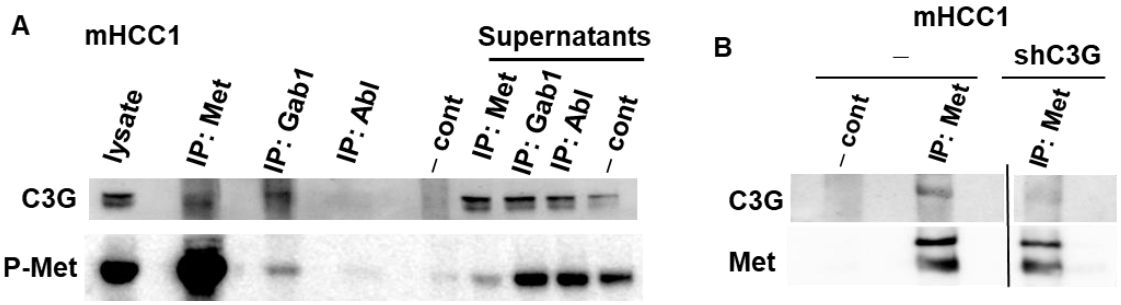

Figure 37. C3G interacts with P-Met and Gab1 in a mouse HCC cell line overexpressing Met. *Mouse Alb-R26^{Met} mHCC1 cells were maintained in the absence of serum for 24h.* ***(A)*** *Western-blot analysis of P-Met, C3G, Gab1 and Abl proteins in immunoprecipitates performed with Met (IP-Met), Gab1 (IP-Gab1) and Abl (IP-Abl) antibodies, in their supernatants and total lysates.* ***(B)*** *Western-blot analysis of Met and C3G in Met immunoprecipitates (IP-Met) of non-silenced (-) and C3G silenced (shC3G) mHCC1 lysates.* ***(A** and **B)*** *As a negative control, lysates were incubated with sepharose beads.*

Met inhibition with SU11274 totally abolished Met phosphorylation. Hence, it is possible that Abl might contribute to facilitate Met activation through its association with C3G (Figure 38), although we have been unable to detect this interaction. Therefore, all these data, support an interaction between active Met with C3G and Gab1 that might facilitate the full activation of Met and the downstream pathways. In addition, a potential contribution of Abl to Met activation is observed.

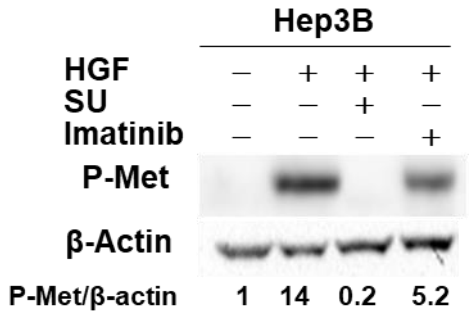

Figure 38. Abl inhibition decreases Met phosphorylation. *Hep3B cells were serum starved for 24h and stimulated with HGF (40ng/ml) for 5 min. When indicated, cells were pre-treated with SU11274 or Imatinib. Western-blot analysis of P-Met (Y1234-1235), normalized with β-actin.*

Data from the literature indicate that E-cadherin associates with Met and this interaction increased after HGF treatment leading to an amplification of HGF-Met signaling in MCF-7 breast cancer cells (Matteucci et al., 2006). E-cadherin also interacts with Met in other cell types (Kamei et al., 1999; Zhao et al., 2007). Therefore, E-cadherin might be a potential candidate to facilitate the interaction between Met and C3G at the membrane level, as well as HGF/Met signaling. In agreement with this, in a pull-down assay using GST protein fused to the E-cadherin domain known to interact with C3G, we found that C3G only interacted with E-cadherin in response to HGF in Hep3B cells (Figure 39). This supports the hypothesis that E-cadherin might facilitate the association of Met with C3G at the membrane level in Hep3B cells, favoring HGF/Met signaling.

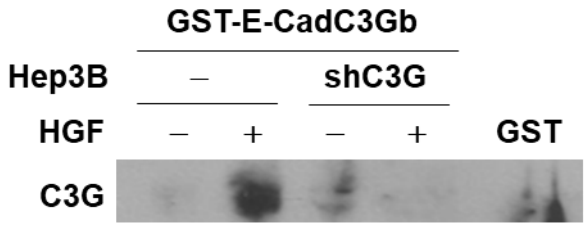

Figure 39. C3G binds to the E-cadherin domain, known to interact with C3G, in response to HGF. *Non-silenced (-) and C3G knock-down (shC3G) Hep3B cells were serum starved for 24h and treated with HGF (40ng/ml) for 5min. Western-blot analysis of C3G in lysates and in samples from pull down assays performed with GST fused to E-cadherin domain known to bind C3G (GST-E-CadC3Gb). As a negative control, lysates were incubated with GST-beads.*

9. DISCUSSION

1. INCREASED C3G EXPRESSION AND GENETIC ALTERATIONS IN HEPATOCARCINOMA. C3G AS A NEW POTENTIAL PROGNOSTIC BIOMARKER IN HUMAN HCC PROGRESSION.

So far there was no mention in the scientific literature about the role of C3G (RapGEF1) in healthy liver or in HCC before the initiation of this work, although some functions of other Rap GEFs such as Epac1 (RapGEF3) or Epac2 (RapGEF4) had been described in liver pathologies. Different from C3G, Epac1 and Epac2 mediate Rap1 activation through their C-terminal GEF-catalytic domain, once cAMP binds to the cAMP docking site, located in the N-terminal cyclic nucleotide-binding domain (Guo et al., 2016). Like C3G, Epac members play also relevant roles in integrin-mediated adhesion (Rangarajan et al., 2003) or endothelial cell-cell junction formation (Fukuhara et al., 2005; Cullere et al., 2004; Kooistra et al., 2005). In liver, Epac was described to have antifibrotic properties, owing to its effects on HSCs (Windmeier and Gressner, 1997; Yokoyama et al., 2008). However, in a rat model of alcoholic liver disease, Epac2/Rap1 favored fibrotic responses, while Epac1/Rap1 had a protective role by preventing HSCs activation and proliferation (Hernández-Gea and Friedman, 2011; Yan et al., 2016).

In this work, we uncover a previously unknown function of C3G in human HCC development and progression. Initially, we observed that C3G levels were increased in human HCC cells lines (Hep3B, HLE and others) as compared to mouse adult hepatocytes, reaching levels comparable to those found in mouse immature neonatal hepatocytes and mouse liver progenitor cells (oval cells) (Fig. 3-4). In agreement with this, in an *in vivo* mouse model of DEN-induced HCC, higher C3G levels were found by IHC staining in these livers as compared with non-treated livers (Fig.5). High C3G protein levels were also observed in a mouse HCC model, where Met is overexpressed in hepatocytes (mouse *Alb-R26*^{Met}), as well as in mouse HCC (mHCC) cell lines generated from these liver tumors (Fig. 6). Taking into account that in HCC, fetal genes are re-expressed (Dhanasekaran et al., 2018; Zucman-Rossi et al., 2015), we can explain that immature neonatal hepatocytes and liver progenitor cells present similarities with HCC cells, such as a high C3G expression. Therefore, C3G might be relevant not only in HCC, but also during liver development, a task that our group is now conducting to elucidate the expression pattern and the role played by C3G in the different stages of liver development, from fetal to neonatal and adult stage.

Our analyses of C3G mRNA levels in human HCC patient samples using public genomic databases supports the results derived from *in vitro* and mouse HCC studies and indicate they may have a potential clinical relevance (Fig. 2). Thus, the increased RapGEF1 expression in human HCC samples and patient-derived xenografts as compared to normal control livers suggests that C3G expression analysis might be important for diagnosis and/or prognosis (Sequera et al. 2018). In fact, the increase in C3G mRNA levels positively correlates with HCC progression (from stage I to stage III, following AJCC guideline), being

statically significant at stage III (Fig. 7). Moreover, Kaplan-Meier survival analysis using the same set of patient showed a lower survival for those HCC patients with higher levels of C3G mRNA (Fig. 7). Therefore, this positive correlation between C3G levels, HCC progression and patients survival, points out to C3G expression as a prognostic factor. On the other hand, mutations and other genetic alterations of C3G (amplifications, deletions, etc) (Fig. 8), not previously linked to HCC or other cancers, were found to be relevant for HCC patient survival (Fig. 9). Hence, genetic databases revealed that some HCC patients did have mutations in *RapGEF1* gene and this was associated with lower survival. The location of the mutations (e.g. affecting GEF-catalytic domain, E-cadherin docking site, tyrosine residues that can be phosphorylated or the negative regulatory domain) give us an idea of their potential high impact on C3G functionality. However, it would be necessary to determine the effect of each mutation or other genetic alterations in *in vitro* functional assays to establish their relevance on C3G function.

Taking into account all these data we can propose the quantification of C3G levels in liver biopsies as a potential prognostic biomarker for HCC patients. However, a clinical study should be performed in HCC patients to assess its feasibility and its precise prognostic value. In addition, the continuous increase in tumor and metastasis sample number in the databases along with more complete patient clinical histories will help to further improve our current knowledge on C3G clinical relevance for HCC prognosis.

2. C3G PROMOTES *IN VITRO* AND *IN VIVO* TUMOR GROWTH, WHILE REDUCES CELL MIGRATION AND INVASION IN HEPATOCARCINOMA CELLS.

C3G role in cancer appears to be dependent on the cellular context, stage or genetic alterations, among other factors. Hence, there are controversial data about its function, as it can act as either a tumor suppressor or promoter. In fibroblasts, C3G acts as a tumor suppressor by inhibiting oncogenic malignant transformation (Guerrero et al., 1998; Martín-Encabo et al., 2007), in agreement with the decrease in C3G levels observed in cervical squamous carcinoma (Okino et al., 2006). In contrast, C3G also acts as an oncogene in non-small cell lung cancer, where its levels are increased (Hirata et al., 2004). In agreement with this, high levels of p87C3G isoform are associated with chronic myeloid leukemia development (Gutiérrez-Berzal et al., 2006). However, our group previously found that in colon carcinoma (CRC) HCT116 cells, C3G plays a dual role, as it inhibits migration and invasion by decreasing p38α activity, while promotes tumor growth through a p38α-independent mechanism (Priego et al., 2016). C3G also inhibits migration in highly invasive breast cancer (Dayma and Radha, 2011).

In HCC, the *in vitro* tumorigenic assays (Fig. 11-14), as well as the *in vivo* data derived from the xenografts assays using C3G silenced human HCC cells (Fig. 24-25) support a pro-tumorigenic role for C3G, owing to its effect increasing cell proliferation and survival (Fig. 15, 25). This is in agreement with previous data from our group concerning CRC HCT116 cells (Priego et al., 2016). Our data derived from the *in vitro* analysis of migration and

invasion showed that C3G silenced cells presented a higher migratory and invasive capacity (Fig. 16-17), which is also in agreement with previous results from our group in CRC HCT116 cells (Priego et al., 2016). This pro-migratory effect of C3G downregulation is also supported by *in vivo* data derived from the quantification of bone marrow disseminated cells (BMDCs) in xenograft assays performed with Hep3B cells, as cells with low levels of C3G have a higher tendency to spread and reach the bone marrow than non-silenced cells (Fig. 27). Therefore, altogether, these data indicate that C3G down-regulation enhances migration and invasion, facilitating the dissemination of tumor cells to secondary locations. Moreover, we demonstrate that the enhanced motility resulting from C3G silencing might be a consequence of the induction of an EMT-like process, similar to that induced by TGFβ treatment, used as a positive control (Fig. 18-21). However, the mechanisms used by C3G to regulate this process would be, at least, partially independent of TGF-β, as the inhibition of the receptor has only a very limited and non-significant effect reducing migration in C3G knock-down HCC cells (Fig. 22). Therefore, it is likely that TGF-β-independent pathways might be implicated, although both TGF-β and C3G down-regulation converge on some downstream targets, such as the transcription factor Twist.

In MCF-7 breast cancer cells, β-catenin down-regulation mediates inhibition of migration by C3G (Dayma et al., 2012), but no changes in β-catenin levels were observed in C3G silenced HCC cells (data not shown) that could account for the enhanced migration. However, the internalization of β-catenin observed in C3G silenced Hep3B cells by immunofluorescence microscopy might play a role, favoring an EMT-like process (Fig. 19). Hence, in non-silenced Hep3B cells, β-catenin is mainly present in the membrane, in cell-cell junctions, while it is predominantly localized in the cytoplasm in C3G knock-down cells, which supports its potential contribution to the regulation of the expression of genes involved in EMT. This would be in agreement with data from intestinal cancer, where an increase in cytoplasmic free β-catenin is produced, although in this case it is mediated by β-catenin phosphorylation in Y654 by RTKs, which reduces its affinity to bind membrane E-cadherin (Van Veelen et al., 2011; Piedra et al., 2001). β-catenin can also be phosphorylated by kinases, such as PKA in Ser675, promoting β-catenin translocation to the nucleus, where it induces the activation of the transcription factors TCF4, TBP and CBP, promoting tumorigenesis (Van Veelen et al., 2011; Piedra et al., 2001). In the case of HCC, HIFα, Foxo, TCF or LEF can be activated by β-catenin, inducing EMT, dissemination, stemness and proliferation of tumor cells (Perugorria et al., 2019). Other proteins can phosphorylate β-catenin in Y654, such as FAK in HCC (Na et al., 2019), or in other models, Src (Huber and Weis, 2001) or Abl (Coluccia et al., 2007; Roura et al., 1999) in Y489 with similar results (Rhee et al., 2007). Src, Abl and FAK can form complexes with C3G protein (Radha et al., 2004; Maia et al., 2013). Thus, in cells with low levels of C3G, the lack of interaction between these tyrosine kinases and C3G might facilitate its accessibility to β-catenin and the subsequent phosphorylation. In addition, in C3G silenced Hep3B cells, β-catenin could be accumulated in the cytoplasm, as a consequence of PTP1B downregulation, avoiding its degradation (Xu et al., 2014). This is a marker of poor

prognosis in HCC (Zhen et al., 2012), as the accumulation of free β-catenin enhances the invasive capacity of HCC cells and HCC progression.

The high activation of p38 MAPK in C3G silenced HCC cells could also play a role promoting migration, as its inhibition decreases migration (Fig. 23). This agrees with CRC data, where C3G down-regulation enhanced migration and invasion by increasing p38α MAPK activation (Priego et al., 2016). In addition, several reports on HCC also support a function for p38 promoting invasion (Hsieh et al., 2007; Chen et al., 2018; Luk et al., 2019). Hence, p38α MAPK activation was described as necessary for invasion of human HCC cells (Hsieh et al., 2007), inducing an increase in MMP9 expression (Park et al., 2011; Min et al., 2018). In hypoxic microenvironments, p38α MAPK activation also leads to enhanced migration, invasion and metastasis (Chen et al., 2018). Moreover, very recent data indicate that the enhanced p38 activation induced by REX1 deficiency contributes to the metastatic potential of HCC cells (Luk et al., 2019). On the other hand, in advanced HCC, p38α MAPK activation was shown to inhibit tumorigenesis and proliferation (Min et al., 2011). In agreement with this, lower levels of phospho-p38α MAPK were found in human HCC tumor samples as compared to normal tissue, which was associated to a lower apoptosis and enhanced survival (Iyoda et al., 2003). This might explain the increased survival observed in tumors generated by non-silenced Hep3B cells in the xenograft assays. This would be also in agreement with previous data from our group demonstrating a pro-apoptotic role for p38α (Porras et al., 2004).

Although some of the actions of C3G are not dependent on its GEF activity (Guerrero et al., 1998; Shivakupa et al., 2003; Guerrero et al., 2004; Martin-Encabo et al., 2007; Gutiérrez-Uzquiza et al., 2010; Priego et al., 2016), C3G performs important functions through its GEF activity on Rap (Maia et al., 2009; Gutiérrez-Herrero et al., 2012; Ortiz-Rivero et al., 2018). Thus, Rap might mediate C3G effects in HCC. However, there is no much information about Rap function in HCC, and that available, is quite controversial (Sequera et al., 2018). Rap1 was shown to suppress tumorigenesis in Hep3B cells by inhibiting Ras pathway and cell proliferation (Lin et al., 2000), while other studies suggest that Rap1B could participate in HCC induction by promoting tumor growth and migration (Su et al., 2009; Sheng et al., 2014). More recent studies found an upregulation of either Rap2B (Zhang et al., 2017) or Rap1B expression (Tang et al. 2018) in some human HCC samples and cell lines, which promotes proliferation and migration. Although we have not determined whether Rap mediates C3G actions in the HCC cell lines used for our studies, Rap1 protein levels were quite low in Hep3B cells (data not shown). This suggests that it would not be a relevant mediator. Moreover, based on previous published data, Rap1 plays an opposite function in Hep3B cells to that uncovered here for C3G (Lin et al., 2000). Therefore, we would not expect Rap1 to be a mediator of C3G, at least in Hep3B cells.

In HCC, as in other types of cancer, the tumor microenvironment is of great relevance for tumor growth, progression and metastasis (Birgani and Carloni, 2017; Novikova et al., 2017). Hence, the higher levels of α-SMA found in xenograft tumors generated by non-silenced Hep3B as compared to tumors derived from C3G knock-down cells indicate the presence of more infiltrated fibroblasts (Fig. 26). This correlates with an increased size of

tumors (Fig. 24) and might be associated to a more developed and active stroma (with CAFs, TAMs, etc) and the establishment of a bilateral communication between tumor and stromal cells (Novikova et al., 2017; Kalluri et al., 2006; Jia et al., 2013) that would promote proliferation and survival. According to this, in the tumors generated by non-silenced Hep3B cells, although not statistically significant, higher levels of mouse HGF, TGFβ1 and IL-6 mRNAs were detected (Fig. 26), likely produced by mouse cells infiltrated into the tumors, which might contribute to promote proliferation and survival of non-silenced HCC cells.

Other stroma components are also relevant for HCC development and progression. Therefore, a deep understanding of the role played by C3G in HCC requires a detailed analysis of the relationship between HCC cancer cells and its microenvironment using additional HCC models, alternative to heterotopic xenografts, where the specific contribution of liver stroma to HCC development could be determined.

3. FUNCTION OF C3G IN THE GENERATION AND ESTABLISHMENT OF METASTASIS.

During the second phase of tumor metastasis promotion, the BMDTCs are involved in the preparation of the pre-metastatic niche that will welcome tumor cells, indicating that BMDTCs can promote metastasis (Liu et al., 2016). Therefore, taking into account the higher number of BMDTCs in xenograft assays generated by C3G silenced cells and their increased pro-migratory and –invasive capacity, we expect these cells could have enhanced pro-metastatic properties. In addition, based on lung metastasis assays performed with mouse HCC cells, an inverse correlation between C3G levels and lung metastasis frequency was found. Thus, HCC cell lines with lower C3G protein levels generated lung metastasis with a higher frequency, being also higher in number and size (Fig. 28-29). It is important to mention that the mouse HCC cell lines used for the lung metastasis assay display very similar Met expression levels and pro-tumorigenic capacity (Fan et al., 2017; Arechederra et al., 2018). Therefore, the differences in their pro-metastatic potential are not likely due to distinct Met expression levels, but there are rather associated to C3G levels. However, even though the mouse HCC cell lines with higher metastatic potential expressed initially lower levels of C3G, their corresponding lung metastases presented very high levels of C3G (Fig. 30). This might suggest that C3G re-expression would be necessary for metastasis to grow, at least, in the lung microenvironment. Patient data support this idea. Hence, a tendency to have higher C3G mRNA levels in lung metastasis than their corresponding liver primary tumors is observed in HCC patients (Fig. 31), which could also explain why HCC patients with higher C3G mRNA levels do have a lower survival (Fig. 7). On the other hand, C3G mRNA levels in secondary tumors located in other tissues and organs, such as those in adrenal gland or lymph nodes, do decrease or do not change, respectively, as compared to the primary tumor. All these differences in the expression of C3G in the metastases can be explained by circumstances, such as the pre-metastatic niche preparation (Peinado et al., 2017;

Doglioni et al., 2019; Liu et al., 2016), different gradient of oxygen, distinct dissemination pathways or C3G levels in the secondary niche. Therefore, according to our model of HCC lung metastasis, primary HCC cells express higher levels of C3G than normal healthy liver cells. In fact, although C3G is highly ubiquitous, the adult liver expresses less C3G levels than other organs, such as adrenal gland or lung (Tanaka et al., 1994; Fig. 1). These increased levels of C3G in HCC cells would promote tumor growth through enhancing proliferation and survival. A plausible development of events would be the following. When the lung pre-metastatic niche is ready to host the liver tumor cells, diverse signals are send by the niche and collected by the primary tumor, which undergoes a change in the phenotype to a more mesenchymal one through an EMT-like process facilitated by a decrease in C3G levels. This allows the acquisition of a higher migratory and invasive capacity, enabling liver tumor cells to actively disseminate through blood vessels to reach and metastasize the lung favorable niche. Once in the lung, liver tumor cells will adapt and start a bilateral communication with the new niche, where they will regain their epithelial characteristics through the reverse process, MET, facilitated by the re-expression of high levels of C3G, even higher than in the primary location. This would promote the growth of a new tumor, which will give rise, first, to a micro-metastasis and then, to a macro-metastasis (Figure 40). In fact, lung is the most prevalent site of metastasis for HCC (Chua et al., 2011; Becker et al., 2014), where liver tumor cells, residing in a hypoxic ambient, find a more oxygenated and favorable place to grow (Clever et al., 2016; Lewis et al., 2016; Nobre et al., 2018).

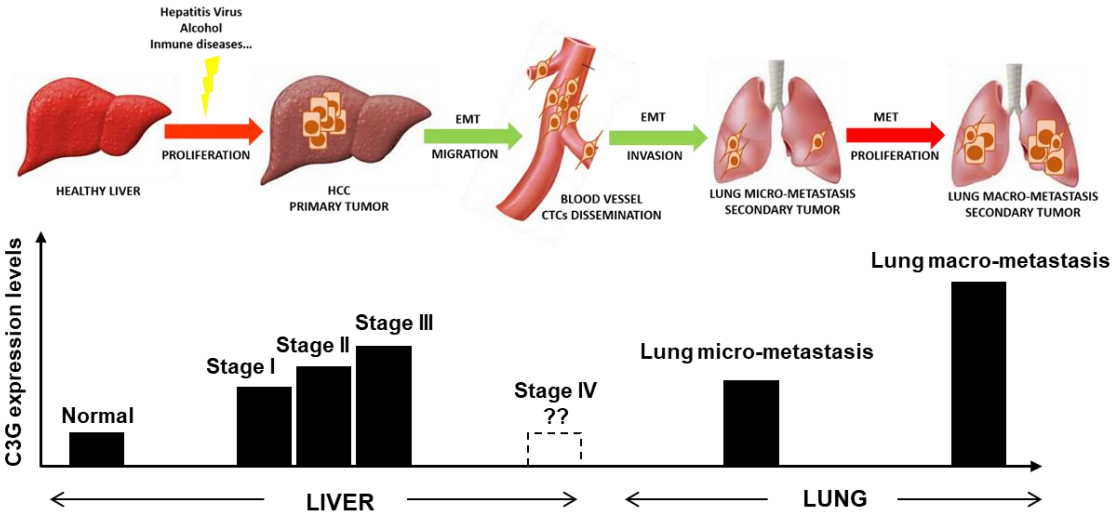

Figure 40. From healthy adult liver to HCC tumor growth and progression. *Schematic representation of the potential changes in the pattern of C3G expression levels, leading to HCC tumor growth and progression to lung metastasis. Red arrows represent increase and green arrows decrease of C3G levels.*

In the case of lymph node HCC metastasis there is no change in C3G mRNA expression levels (Fig. 31), which could be explained by the dissemination of the tumor cells through lymph vessels, most commonly to regional nodes (Kummar et al., 2003). This spread would be passive, as the pressure exerted by tumor growth will create spaces between lymph pericytes, enabling the drainage of the lymph contained in the liver to the lymphatic vessels dragging tumor cells through a non-return system (Shayan et al., 2006; Scallan et al., 2010; Pepper et al., 2001; Swartz and Skobe, 2001). This will force cells

spreading to regional nodes where they metastasize and grow. Therefore, this passive dissemination might not require changes in C3G expression by tumor cells to become more migratory or invasive. The low C3G levels in adrenal gland metastasis could be a consequence of a less favorable niche with fewer proliferative and survival signals. This would explain why adrenal gland is only the fifth prevalent site for HCC metastasis (Terence et al., 2011; Becker et al., 2014).

4. FUNCTION OF C3G IN HGF/MET SIGNALING IN HEPATOCARCINOMA.

Our data also support an interaction between active Met with C3G, which is required to ensure a full activation of Met (in terms of phosphorylation of Y1234/1235) and downstream pathways (Figure 32). Met is frequently overexpressed in HCC patients (You et al., 2011; Kaposi-Novak et al., 2006; Goyal et al., 2013) and correlates with higher recurrence and poor prognosis (Kim et al., 2017). Therefore, the defective HGF/Met signaling that we observed in human C3G silenced HCC cells, might, at least, partially explain the reduced proliferation and survival of cells from HCC tumors bearing low levels of C3G. In fact, both Hep3B and HLE human HCC cells lines overexpress Met receptor (Fig. 4). Additionally, in mouse HCC cells overexpressing Met, anchorage-dependent growth was also decreased in C3G knock-down cells (Fig. 13), which further supports the potential relevance of C3G role as a mediator of Met induced tumor growth.

Abl might also facilitate Met activation when C3G is present. Hence, although we have not been able to find Abl in the Met or Gab1 immunoprecipitates (Fig. 37), where C3G was present, C3G is known to interact with Abl (Radha et al., 2007; Huang et al., 2008; Nolz et al., 2008; Maia et al., 2013). Therefore, it is likely that Abl might associate with Met through C3G, facilitating Met activation. This interaction would be supported by the decrease in HGF-induced Met activation in Hep3B cells upon Abl inhibition with Imatinib.

On the other hand, previous published data indicate that in HEK293 cells overexpressing Gab1, once Gab1 is phosphorylated in response to HGF, CrkL-C3G complex binds to P-Gab1, leading to Rap1 activation (Sakkab et al. 2000). However, our data does not fit with this proposed model, as we found an interaction between Gab1 and CrkL in untreated cells (Fig. 34-35). This agrees with previous studies where Crk was found to interact with Gab1 in unstimulated cells through its N-terminal SH3 domain (Wanatable et al., 2009). Furthermore, our data indicate that C3G proline rich domain associates with phosphorylated Gab1 in Hep3B cells treated with HGF, but not with CrkL (Fig. 36). Therefore, in this context, CrkL would not be the necessary mediator for C3G binding to Gab1. In fact, CrkL might be bound to Gab1 in unstimulated cells and C3G would interact with Gab1 only in response to HGF, most probably through alternative mediators. Thus, it is possible that other adaptors containing SH3 domains such as Grb2 (Buday et al., 1999; Tanaka et al., 1994; Smit et al., 1996) or p130Cas (Kirsch et al., 1998; Birge et al., 2009; Maia et al., 2013; Lamorte et al., 2002; Bos, 2005) could be mediating the interaction between P-Gab1 and C3G proline rich domain (Lamorte et al., 2002). It is also conceivable

that other proteins can contribute to mediate the association between C3G and P-Gab1 such as Abl, through its SH3 domain (Radha et al., 2007). E-cadherin is another potential candidate, as both C3G and Met can interact with it (Asuri et al., 2008; Radha et al., 2011; Sciarratta et al., 2006; Matteucci et al., 2006). For example, in MCF-7 breast cancer cells, E-cadherin associates with Met and this interaction increased after HGF treatment leading to an amplification of HGF-Met signaling (Matteucci et al., 2006). This Met-E-cadherin interaction has also been described in other cell types (Kamei et al., 1999; Zhao et al., 2007). Therefore, it is likely that E-cadherin might facilitate the interaction between Met and C3G at the membrane level, as well as HGF/Met signaling. In agreement with this, in the pull-down assay using GST fused to the E-cadherin domain known to interact with C3G, we found its interaction with C3G only upon HGF stimulation in Hep3B cells (Fig. 39).

5. GENERAL DISCUSSION

In the first part of this study, we have reported the existence of a high expression of C3G protein in several human and mouse HCC cell lines and in two mouse HCC tumor models (induced by either DEN treatment or Met overexpression in hepatocytes) as compared to adult hepatocytes or normal liver tissue samples. Moreover, genomic databases indicate that C3G mRNA levels are higher in human HCC patient samples than in control livers, increasing significantly in advanced stages of the disease, which is associated with a lower survival. C3G genetic alterations (mutations, deletions, amplifications, etc) are also correlated to a poor survival in HCC patients. Therefore, C3G might be considered as a new potential biomarker of prognosis for HCC. We have also demonstrated by *in vitro* and *in vivo* experiments using human and mouse HCC cells, as well as mice models that C3G has pro-tumorigenic function in HCC by increasing proliferative and survival capacities, as shown in xenograft assays. On the other hand, a reduction in C3G levels in human HCC cell lines enhances their pro-migratory and pro-invasive abilities, likely through the induction of an EMT like process that would facilitate tumor cells dissemination, as demonstrated by the higher number of BMDTCs. Moreover, mouse HCC cells overexpressing Met with lower levels of C3G generate lung metastases, with a higher frequency and size, confirming that HCC cells with C3G down-regulation have a higher dissemination competence. However, the growth of lung metastasis might require an increase in the expression of C3G, as C3G protein levels are higher in the metastasis than in the primary tumor. C3G mRNA levels data from HCC patients are in agreement with these results. All these data support the hypothesis that once HCC cells with low levels of C3G reach the lung niche, they need to revert their phenotype, potentially through a MET process, to re-acquire a high proliferative and survival capacity in order to promote tumor growth in the lung.

Moreover, we show that C3G is necessary for a full activation of Met in response to HGF, which might, at least, partially explain its pro-tumorigenic function. C3G interacts with Met and Gab1 through a mechanism not dependent on CrkL. Thus, other proteins with

SH3 domains such as Abl or p130Cas might facilitate the interaction between Met and C3G and/or with Gab1 at the membrane level. E-cadherin is also a good candidate for it, as both Met and C3G can interact with E-cadherin. Moreover, C3G plays a relevant role to localize E-cadherin in the membrane (Hogan et al., 2004; Rufanova et al., 2009; Kooistra et al., 2007; Asuri et al., 2008; Sciarratta et al., 2006).

In conclusion, we have demonstrated for the first time that C3G has a pro-tumorigenic function in human HCC, promoting tumor growth by facilitating cell proliferation and survival of the primary tumor. In addition, down-regulation of C3G levels confers HCC cells pro-migratory and pro-invasive properties, enhancing their competence to disseminate, which might favor their ability to metastasize into the lung. Moreover, according to the inverse correlation between high C3G levels, progression and survival in HCC patients, based on databases, C3G could be considered as a new biomarker of prognosis, with a potential clinical relevance. Finally, we demonstrate that in human HCC cells, C3G is required for a full activation of HGF/Met signaling, which might also have high relevance for HCC patients, taking into account that Met is frequently overexpressed in HCC.

10. CONCLUSIONS

1. C3G protein levels are increased in human and mouse HCC cell lines and in mouse liver tumors as compared to normal liver and adult hepatocytes, reaching similar levels to those expressed by liver progenitor cells and immature hepatocytes.

2. *C3G (RapGEF1)* mRNA levels are directly correlated with HCC progression, while inversely associated to patient survival according to public databases. Therefore, C3G can be proposed as a new potential prognostic biomarker for HCC patients.

3. *RapGEF1* mutations and other genetic alterations, such as deletions or amplifications are correlated with poor HCC patient survival, according to public genomic databases.

4. C3G enhances *in vitro* and *in vivo* tumor growth of HCC cells, through increasing proliferation, survival and cell adhesion.

5. C3G down-regulation enhances migration and invasion of HCC cells by promoting an EMT-like process, mimicking TGF-β-induced EMT. p38 MAPK contributes to the increased migration induced by C3G down-regulation.

6. C3G expression in HCC cells promotes the presence of active fibroblasts in HCC tumor stroma, favoring the expression of pro-tumorigenic and survival signals.

7. The expression of low levels of C3G in HCC cells favors their dissemination to bone marrow and the generation of lung metastasis.

8. C3G protein levels increases in lung metastatic samples generated by HCC xenograft tumors.

9. C3G is required for a full activation of Met receptor by HGF, as well as its downstream signaling pathways in HCC cells.

10. In response to HGF, C3G interacts with P-Met and Gab1 in HCC cells, independently of CrkL adaptor. Moreover, C3G proline rich domain binds to P-Gab1 and P-Met through a mechanism not mediated by CrkL.

CONCLUDING REMARKS

C3G expression increases in human HCC during disease progression, being correlated with a poor prognosis of these patients. Moreover, C3G promotes HCC tumor growth *in vitro* and *in vivo*, in both human and mouse HCC cells, while low levels of C3G enhances pro-migratory and invasive properties of HCC cells by inducing an EMT-like process that facilitates tumor cell dissemination and generation of lung metastasis. Furthermore, C3G is necessary for a full activation of Met receptor by HGF, which might facilitate the pro-tumorigenic function of HGF/Met pathway in HCC. Therefore, C3G is a new key player in HCC that promotes tumor growth and progression, and thus has a potential to be used as a poor prognosis biomarker for HCC patients.

11. CONCLUSIONES

1. Los niveles proteicos de C3G están aumentados en líneas celulares de HCC humanas y murinas, y en tumores hepáticos de ratón en comparación con el hígado normal y los hepatocitos adultos, alcanzando niveles similares a los que presentan las células progenitoras hepáticas y los hepatocitos inmaduros.

2. Los niveles de RNAm de C3G (*RapGEF1*) se correlacionan directamente con la progresión del HCC e inversamente con la supervivencia de los pacientes, de acuerdo con las bases de datos públicas. Por tanto, C3G puede proponerse como un nuevo potencial biomarcador de pronóstico para pacientes de HCC.

3. Las mutaciones y otras alteraciones genéticas de *RapGEF1,* como deleciones o amplificaciones, se correlacionan con una menor supervivencia en los pacientes con HCC, de acuerdo con las bases de datos genómicas públicas.

4. C3G aumenta el crecimiento tumoral de las células de HCC *in vitro* e *in vivo* a través del incremento de la proliferación, supervivencia y adhesión celular.

5. La disminución de los niveles de C3G incrementa la migración e invasión de las células de HCC promoviendo un proceso de tipo EMT, semejante a la EMT inducida por TGF-β. p38 MAPK contribuye al aumento de la migración inducida por la disminución de los niveles de C3G.

6. La expresión de C3G en las células de HCC promueve la presencia de fibroblastos activados en el estroma tumoral del HCC, favoreciendo la expresión de señales pro-tumorigénicas y de supervivencia.

7. La expresión de bajos niveles de C3G en células de HCC favorece su diseminación a médula ósea y la generación de metástasis en pulmón.

8. Los niveles proteicos de C3G aumentan en las muestras de metástasis de pulmón generadas por los tumores de HCC de los xenotransplantes.

9. C3G se requiere para una completa activación del receptor Met por HGF, así como de las rutas de señalización que éste activa en HCC.

10. En respuesta al HGF, C3G interacciona con P-Met y Gab1 en células de HCC, independientemente del adaptador CrkL. Además, el dominio rico en prolinas de C3G se une a P-Gab1 y P-Met a través de un mecanismo no mediado por CrkL.

CONCLUSIONES FINALES

La expresión de C3G aumenta en el HCC humano durante la progresión de la enfermedad, correlacionándose con un mal pronóstico de estos pacientes. Además, C3G promueve el crecimiento tumoral del HCC *in vitro* e *in vivo*, tanto en células de HCC humanas como de ratón, mientras que los niveles bajos de C3G dan lugar a un aumento de las propiedades pro-migratorias e invasivas de las células de HCC mediante la inducción de un proceso similar a la EMT que facilita la diseminación de las células tumorales y la generación de metástasis en pulmón. Además, C3G es necesario para una activación completa del

receptor Met por HGF, lo que podría facilitar la función pro-tumorigénica de la vía del HGF/Met en HCC. Por tanto, C3G es una nueva pieza clave en el HCC que promueve el crecimiento y progresión tumoral, y, por tanto, podría usarse potencialmente como un biomarcador de mal pronóstico para pacientes de HCC.

12. REFERENCES

Aasrum M, Ødegård J, Thoresen GH, Brusevold IJ, Sandnes DL, Christoffersen T. Gab1 amplifies signaling in response to low-intensity stimulation by HGF. Cell Biol Int. 2015 Oct;39(10):1177-84.

Affo S, Yu LX, Schwabe RF. The Role of Cancer-Associated Fibroblasts and Fibrosis in Liver Cancer. Annu Rev Pathol. 2017 Jan 24;12:153-186.

Afify SM, Hassan G, Osman A, Calle AS, Nawara HM, Zahra MH, et al. Metastasis of Cancer Stem Cells Developed in the Microenvironment of Hepatocellular Carcinoma. Bioengineering (Basel). 2019 Aug 23;6(3).

Alsayed Y, Modi S, Uddin S, Mahmud N, Druker BJ, Fish EN, et al. All-trans-retinoic acid induces tyrosine phosphorylation of the CrkL adapter in acute promyelocytic leukemia cells. Exp Hematol. 2000 Jul;28(7):826-32.

Anstee QM, Reeves HL, Kotsiliti E, Govaere O, Heikenwalder M. From NASH to HCC: current concepts and future challenges. Nat Rev Gastroenterol Hepatol. 2019 Jul;16(7):411-428.

Arai A, Nosaka Y, Kanda E, Yamamoto K, Miyasaka N, Miura O. Rap1 is activated by erythropoietin or interleukin-3 and is involved in regulation of beta1 integrin-mediated hematopoietic cell adhesion. J Biol Chem. 2001 Mar 30;276(13):10453-62.

Arechederra M, Daian F, Yim A, Bazai SK, Richelme S, Dono et al. Hypermethylation of gene body CpG islands predicts high dosage of functional oncogenes in liver cancer. Nat Commun. 2018 Aug 8;9(1):3164.

Arechederra M, Carmona R, González-Nuñez M, Gutiérrez-Uzquiza A, Bragado P, Cruz-González I, et al. Met signaling in cardiomyocytes is required for normal cardiac function in adult mice. Biochim Biophys Acta. 2013 Dec;1832(12):2204-15.

Arnold L, Enders J, Thomas SM. Activated HGF-c-Met Axis in Head and Neck Cancer. Cancers (Basel). 2017 Dec 12;9(12).

Arriazu E, Ruiz de Galarreta M, Cubero FJ, Varela-Rey M, Pérez de Obanos MP, et al. Extracellular matrix and liver disease. Antioxid Redox Signal. 2014 Sep 1;21(7):1078-97.

Asuri S, Yan J, Paranavitana NC, Quilliam LA. E-cadherin dis-engagement activates the Rap1 GTPase. J Cell Biochem. 2008 Nov 1;105(4):1027-37.

Baglieri J, Brenner DA, Kisseleva T. The Role of Fibrosis and Liver-Associated Fibroblasts in the Pathogenesis of Hepatocellular Carcinoma. Int J Mol Sci. 2019 Apr 7;20(7).

Bazzoni G, Martinez-Estrada OM, Orsenigo F, Cordenonsi M, Citi S, Dejana E. Interaction of junctional adhesion molecule with the tight junction components ZO-1, cingulin, and occludin. J Biol Chem. 2000 Jul 7;275(27):20520-6.

Becker AK, Tso DK, Harris AC, Malfair D, Chang SD. Extrahepatic metastases of hepatocellular carcinoma: A spectrum of imaging findings. Can Assoc Radiol J. 2014 Feb;65(1):60-6.

Benvenuti S and Comoglio PM. The MET receptor tyrosine kinase in invasion and metastasis. J Cell Physiol. 2007 Nov;213(2):316-25.

Berasain C, Castillo J, Perugorria MJ, Latasa MU, Prieto J, Avila MA. Inflammation and liver cancer: new molecular links. Ann N Y Acad Sci. 2009 Feb;1155:206-21.

Bergers G and Coussens LM. Extrinsic regulators of epithelial tumor progression: metalloproteinases. Curr Opin Genet Dev. 2000 Feb;10(1):120-7.

Bertran E, Crosas-Molist E, Sancho P, Caja L, Lopez-Luque J, Navarro E, et al. Overactivation of the TGF-β pathway confers a mesenchymal-like phenotype and CXCR4-dependent migratory properties to liver tumor cells. Hepatology. 2013 Dec;58(6):2032-44

Birchmeier C, Birchmeier W, Gherardi E, Vande Woude GF. Met, metastasis, motility and more. Nat Rev Mol Cell Biol. 2003 Dec;4(12):915-25.

Birgani Tahmasebi M, and Carloni V. Tumor Microenvironment, a Paradigm in Hepatocellular Carcinoma Progression and Therapy. Int J Mol Sci. 2017 Feb 14;18(2).

Birge RB, Kalodimos C, Inagaki F, Tanaka S. Crk and CrkL adaptor proteins: networks for physiological and pathological signaling. Cell Commun Signal. 2009 May 10;7:13.

Bladt F, Riethmacher D, Isenmann S, Aguzzi A, Birchmeier C. Essential role for the c-met receptor in the migration of myogenic precursor cells into the limb bud. Nature. 1995 Aug 31;376(6543):768-71.

Boix L, Rosa JL, Ventura F, Castells A, Bruix J, Rodés, et al. c-met mRNA overexpression in human hepatocellular carcinoma. Hepatology. 1994 Jan;19(1):88-91.

Bolanos-Garcia VM. MET meet adaptors: functional and structural implications in downstream signalling mediated by the Met receptor. Mol Cell Biochem. 2005 Aug;276(1-2):149-57.

Borowiak M, Garratt AN, Wüstefeld T, Strehle M, Trautwein C, Birchmeier C. Met provides essential signals for liver regeneration. Proc Natl Acad Sci U S A. 2004 Jul 20;101(29):10608-13.

Bos JL. Linking Rap to cell adhesion. Curr Opin Cell Biol. 2005 Apr;17(2):123-8.

Bottaro DP, Rubin JS, Faletto DL, Chan AM, Kmiecik TE, Vande Woude GF, et al. Identification of the hepatocyte growth factor receptor as the c-met proto-oncogene product. Science. 1991 Feb 15;251(4995):802-4.

Bouattour M, Raymond E, Qin S, Cheng AL, Stammberger U, Locatelli G, et al. Recent developments of c-Met as a therapeutic target in hepatocellular carcinoma. Hepatology. 2018 Mar;67(3):1132-1149.

Bradford MM. A rapid and sensitive method for the quantitation of microgram quantities of protein utilizing the principle of protein-dye binding. Anal Biochem. 1976 May 7;72:248-54.

Bragado P, Estrada Y, Parikh F, Krause S, Capobianco C, Farina HG, et al. "TGF-beta2 dictates disseminated tumour cell fate in target organs through TGFbeta-RIII and p38alpha/beta signalling." Nat Cell Biol 2013 ; 15(11): 1351-1361.

Brown KA, Aakre ME, Gorska AE, Price JO, Eltom SE, Pietenpol JA, et al. Induction by transforming growth factor-beta1 of epithelial to mesenchymal transition is a rare event in vitro. Breast Cancer Res. 2004;6(3):R215-31.

Buday L. Membrane-targeting of signalling molecules by SH2/SH3 domain-containing adaptor proteins. Biochim Biophys Acta. 1999 Jul 6;1422(2):187-204.

Buensuceso CS and O'Toole TE. The association of CRKII with C3G can be regulated by integrins and defines a novel means to regulate the mitogen-activated protein kinases. J Biol Chem. 2000 Apr 28;275(17):13118-25.

Campbell HK, Maiers JL, DeMali KA. Interplay between tight junctions & adherens junctions. Exp Cell Res. 2017 Sep 1;358(1):39-44.

Castelli G, Pelosi E, Testa U. Liver Cancer: Molecular Characterization, Clonal Evolution and Cancer Stem Cells. Cancers (Basel). 2017 Sep 20;9(9).

Che YL, Luo SJ, Li G, Cheng M, Gao YM, Li XM, et al. The C3G/Rap1 pathway promotes secretion of MMP-2 and MMP-9 and is involved in serous ovarian cancer metastasis. Cancer Lett. 2015 Apr 10;359(2):241-9.

Che YL, Luo SJ, Li G, Cheng M, Gao YM, Li XM, et al. The C3G/Rap1 pathway promotes secretion of MMP-2 and MMP-9 and is involved in serous ovarian cancer metastasis. Cancer Lett. 2015 Apr 10;359(2):241-9.

Cheerathodi M, Vincent JJ, Ballif BA. Quantitative comparison of CrkL-SH3 binding proteins from embryonic murine brain and liver: Implications for developmental signaling and the quantification of protein species variants in bottom-up proteomics. J Proteomics. 2015 Jul 1;125:104-11.

Chen J, Chen L, Zern MA, Theise ND, Diehl AM, Liu P, et al. The diversity and plasticity of adult hepatic progenitor cells and their niche. Liver Int. 2017 Sep;37(9):1260-1271.

Chen X, Zhang S, Wang Z, Wang F, Cao X, Wu Q, et al. Supervillin promotes epithelial-mesenchymal transition and metastasis of hepatocellular carcinoma in hypoxia via activation of the RhoA/ROCK-ERK/p38 pathway. J Exp Clin Cancer Res. 2018 Jun 28;37(1):128.

Cheng Z, Li X, Ding J. Characteristics of liver cancer stem cells and clinical correlations. Cancer Lett. 2016 Sep 1;379(2):230-8.

Chiang SH, Baumann CA, Kanzaki M, Thurmond DC, Watson RT, Neudauer CL, et al. Insulin-stimulated GLUT4 translocation requires the CAP-dependent activation of TC10. Nature. 2001 Apr 19;410(6831):944-8.

Chua TC, Al-Alem I, Zhao J, Glenn D, Liauw W, Morris DL. Radiofrequency ablation of concomitant and recurrent pulmonary metastases after surgery for colorectal liver metastases. Ann Surg Oncol. 2012 Jan;19(1):75-81.

Chua TC, Morris DL. Exploring the role of resection of extrahepatic metastases from hepatocellular carcinoma. Surg Oncol. 2012 Jun;21(2):95-101.

Clever D, Roychoudhuri R, Constantinides MG, Askenase MH, Sukumar M, Klebanoff CA, et al. Oxygen Sensing by T Cells Establishes an Immunologically Tolerant Metastatic Niche. Cell. 2016 Aug 25;166(5):1117-1131.e14.

Coluccia AM1, Vacca A, Duñach M, Mologni L, Redaelli S, Bustos VH, et al. Bcr-Abl stabilizes beta-catenin in chronic myeloid leukemia through its tyrosine phosphorylation. EMBO J. 2007 Mar 7;26(5):1456-66.

Comoglio PM and Trusolino L. Invasive growth: from development to metastasis. J Clin Invest. 2002 Apr;109(7):857-62.

Cooper CS, Park M, Blair DG, Tainsky MA, Huebner K, Croce CM, et al. Molecular cloning of a new transforming gene from a chemically transformed human cell line.

Coulouarn C, Corlu A, Glaise D, Guénon I, Thorgeirsson SS, Clément B. Hepatocyte-stellate cell cross-talk in the liver engenders a permissive inflammatory microenvironment that drives progression in hepatocellular carcinoma. Cancer Res. 2012 May 15;72(10):2533-42.

Cullere X, Shaw SK, Andersson L, Hirahashi J, Luscinskas FW, Mayadas TN. Regulation of vascular endothelial barrier function by Epac, a cAMP-activated exchange factor for Rap GTPase. Blood. 2005 Mar 1;105(5):1950-5.

Cummins PM. Occludin: one protein, many forms. Mol Cell Biol. 2012 Jan;32(2):242-50.

Daveau M, Scotte M, François A, Coulouarn C, Ros G, Tallet Y, et al. Hepatocyte growth factor, transforming growth factor alpha, and their receptors as combined markers of prognosis in hepatocellular carcinoma. Mol Carcinog. 2003 Mar;36(3):130-41.

Dayma K, and Radha V. Cytoskeletal remodeling by C3G to induce neurite-like extensions and inhibit motility in highly invasive breast carcinoma cells. Biochim Biophys Acta. 2011 Mar;1813(3):456-65.

Dayma K, Ramadhas A, Sasikumar K, Radha V. Reciprocal Negative Regulation between the Guanine Nucleotide Exchange Factor C3G and β-Catenin. Genes Cancer. 2012 Sep;3(9-10):564-77.

De Falco V, Castellone MD, De Vita G, Cirafici AM, Hershman JM, Guerrero C, et al. RET/papillary thyroid carcinoma oncogenic signaling through the Rap1 small GTPase. Cancer Res. 2007 Jan 1;67(1):381-90.

de Herreros AG, Peiró S, Nassour M, Savagner P. Snail family regulation and epithelial mesenchymal transitions in breast cancer progression. J Mammary Gland Biol Neoplasia. 2010 Jun;15(2):135-47

Del Castillo G, Murillo MM, Alvarez-Barrientos A, Bertran E, Fernández M, Sánchez A, et al. Autocrine production of TGF-beta confers resistance to apoptosis after an epithelial-mesenchymal transition process in hepatocytes: Role of EGF receptor ligands. Exp Cell Res. 2006 Sep 10;312(15):2860-71.

Derynck R, Muthusamy BP, Saeteurn KY. Signaling pathway cooperation in TGF-β-induced epithelial-mesenchymal transition. Curr Opin Cell Biol. 2014 Dec;31:56-66.

Dhanasekaran R, Nault JC, Roberts LR, Zucman-Rossi J. Genomic Medicine and Implications for Hepatocellular Carcinoma Prevention and Therapy. Gastroenterology. 2019 Jan;156(2):492-509.

Díaz LA and Barrera F. Clasificación Barcelona Clinic Liver Cancer (BCLC) de carcinoma hepatocelular. Gastroenterol. Latinoam 2015; Vol 26, Nº1: 63-68.

Díaz-Coránguez M, Liu X, Antonetti DA. Tight Junctions in Cell Proliferation. nt J Mol Sci. 2019 Nov 27;20(23). pii: E5972.

Doglioni G, Parik S, Fendt SM. Interactions in the (Pre)metastatic Niche Support Metastasis Formation. Doglioni G, Parik S, Fendt SM. Front Oncol. 2019 Apr 24;9:219

Dongre A, Weinberg RA. New insights into the mechanisms of epithelial-mesenchymal transition and implications for cancer. Nat Rev Mol Cell Biol. 2019 Feb;20(2):69-84.

Duarte S, Baber J, Fujii T, Coito AJ. Matrix metalloproteinases in liver injury, repair and fibrosis. Matrix Biol. 2015 May-Jul;44-46:147-56.

Ehrhardt A, Ehrhardt GR, Guo X, Schrader JW. Ras and relatives--job sharing and networking keep an old family together. Exp Hematol. 2002 Oct;30(10):1089-106.

Esrefoglu M. Role of stem cells in repair of liver injury: experimental and clinical benefit of transferred stem cells on liver failure. World J Gastroenterol 2013;19(40):6757-6773.

Fabregat I, Moreno-Càceres J, Sánchez A, Dooley S, Dewidar B, Giannelli G, et al. TGF-β signalling and liver disease. FEBS J. 2016 Jun;283(12):2219-32.

Fan Y, Arechederra M, Richelme S, Daian F, Novello C, Calderaro J, et al. A phosphokinome-based screen uncovers new drug synergies for cancer driven by liver-specific gain of nononcogenic receptor tyrosine kinases. Hepatology. 2017 Nov;66(5):1644-1661.

Fan Y, Bazai SK, Daian F, Arechederra M, Richelme S, Temiz NA, et al. Evaluating the landscape of gene cooperativity with receptor tyrosine kinases in liver tumorigenesis using transposon-mediated mutagenesis. J Hepatol. 2019 Mar;70(3):470-482.

Fanning AS, Van Itallie CM, Anderson JM. Zonula occludens-1 and -2 regulate apical cell structure and the zonula adherens cytoskeleton in polarized epithelia. Mol Biol Cell. 2012 Feb;23(4):577-90.

Fanning AS, Anderson JM. Zonula occludens-1 and -2 are cytosolic scaffolds that regulate the assembly of cellular junctions. Ann N Y Acad Sci. 2009 May;1165:113-20.

Farazi PA and DePinho RA. Hepatocellular carcinoma pathogenesis: from genes to environment. Nat Rev Cancer. 2006 Sep;6(9):674-87.

Faria C, Smith C, Rutka J. The role of HGF/c-Met pathway signaling in human medulloblastoma. Molecular Targets of CNS Tumors, Edited by Miklos Garami, chapter 6. DOI: 10.5772/23296.

Fausto N and Campbell JS. The role of hepatocytes and oval cells in liver regeneration and repopulation. Mech Dev. 2003 Jan;120(1):117-30.

Fausto N, Laird AD, Webber EM. Liver regeneration. 2. Role of growth factors and cytokines in hepatic regeneration. FASEB J. 1995 Dec;9(15):1527-36.

Feldman JP, Goldwasser R, Mark S, Schwartz J, Orion I. A mathematical model for tumor volume evaluation using two-dimensions. JAQM 2009; Vol.4 Nº4:455-462.

Forbes SJ and Parola M. Liver fibrogenic cells. Best Pract Res Clin Gastroenterol. 2011 Apr;25(2):207-17.

Frantz C, Stewart KM, Weaver VM. The extracellular matrix at a glance. J Cell Sci. 2010 Dec 15;123(Pt 24):4195-200

Franz CM, Jones GE, Ridley AJ. Cell migration in development and disease. Dev Cell. 2002 Feb;2(2):153-8.

Friedl P, Bröcker EB. T cell migration in three-dimensional extracellular matrix: guidance by polarity and sensations. Dev Immunol. 2000;7(2-4):249-66.

Friedl P, Locker J, Sahai E, Segall JE. Classifying collective cancer cell invasion. Nat Cell Biol. 2012 Aug;14(8):777-83.

Friedl P, Wolf K. Tumour-cell invasion and migration: diversity and escape mechanisms. Nat Rev Cancer. 2003 May;3(5):362-74.

Friedman, A. Y. H. a. S. L. Sinusoidal events during fibrosing liver injury. Expert Reviews in Molecular Medicine 2003.

Fu Y, Liu S, Zeng S, Shen H. From bench to bed: the tumor immune microenvironment and current immunotherapeutic strategies for hepatocellular carcinoma. J Exp Clin Cancer Res. 2019 Sep 9;38(1):396.

Fukuhara S, Sakurai A, Sano H, Yamagishi A, Somekawa S, Takakura N, Saito Y, et al. Cyclic AMP potentiates vascular endothelial cadherin-mediated cell-cell contact to enhance endothelial barrier function through an Epac-Rap1 signaling pathway. Mol Cell Biol. 2005 Jan;25(1):136-46.

Furge KA, Zhang YW, Vande Woude GF. Met receptor tyrosine kinase: enhanced signaling through adapter proteins. Oncogene. 2000 Nov 20;19(49):5582-9.

Furlan A, Lamballe F, Stagni V, Hussain A, Richelme S, Prodosmo, et al. Met acts through Abl to regulate p53 transcriptional outcomes and cell survival in the developing liver. J Hepatol. 2012 Dec;57(6):1292-8.

Furlan A, Stagni V, Hussain A, Richelme S, Conti F, Prodosmo A, et al. Abl interconnects oncogenic Met and p53 core pathways in cancer cells. Cell Death Differ. 2011 Oct;18(10):1608-16.

Garcia-Guzman M, Dolfi F, Russello M, Vuori K. Cell adhesion regulates the interaction between the docking protein p130(Cas) and the 14-3-3 proteins. J Biol Chem. 1999 Feb 26;274(9):5762-8.

Garcia-Guzman M, Dolfi F, Zeh K, Vuori K. Met-induced JNK activation is mediated by the adapter protein Crk and correlates with the Gab1 - Crk signaling complex formation. Oncogene. 1999 Dec 16;18(54):7775-86.

García-Vilas and Medina, 2018

García-Vilas JA and Medina MÁ. Updates on the hepatocyte growth factor/c-Met axis in hepatocellular carcinoma and its therapeutic implications. World J Gastroenterol. 2018 Sep 7;24(33):3695-3708.

García-Vilas JA, Medina MÁ. Updates on the hepatocyte growth factor/c-Met axis in hepatocellular carcinoma and its therapeutic implications. World J Gastroenterol. 2018 Sep 7;24(33):3695-3708.

Gardel ML, Schneider IC, Aratyn-Schaus Y, Waterman CM. Mechanical integration of actin and adhesion dynamics in cell migration. Annu Rev Cell Dev Biol. 2010;26:315-33.

Gaudino G, Follenzi A, Naldini L, Collesi C, Santoro M, Gallo KA, et al. RON is a heterodimeric tyrosine kinase receptor activated by the HGF homologue MSP. EMBO J. 1994 Aug 1;13(15):3524-32.

Gebäck T, Schulz MM, Koumoutsakos P, Detmar M. TScratch: a novel and simple software tool for automated analysis of monolayer wound healing assays. Biotechniques. 2009 Apr;46(4):265-74.

Gerashchenko TS, Novikov NM, Krakhmal NV, Zolotaryova SY, Zavyalova MV, Cherdyntseva NV, et al. Markers of Cancer Cell Invasion: Are They Good Enough? J Clin Med. 2019 Jul 24;8(8). pii: E1092.

Giebeler A, Boekschoten MV, Klein C, Borowiak M, Birchmeier C, Gassler N, et al. c-Met confers protection against chronic liver tissue damage and fibrosis progression after bile duct ligation in mice. Gastroenterology. 2009 Jul;137(1):297-308, 308.e1-4.

Gloushankova NA, Rubtsova SN, Zhitnyak IY. Cadherin-mediated cell-cell interactions in normal and cancer cells. Tissue Barriers. 2017 Jul 3;5(3):e1356900.

González-Mariscal L, Betanzos A, Avila-Flores A. MAGUK proteins: structure and role in the tight junction. Semin Cell Dev Biol. 2000 Aug;11(4):315-24.

Gotoh T, Hattori S, Nakamura S, Kitayama H, Noda M, Takai Y, et al. Identification of Rap1 as a target for the Crk SH3 domain-binding guanine nucleotide-releasing factor C3G. Mol Cell Biol. 1995 Dec;15(12):6746-53.

Gotoh T, Niino Y, Tokuda M, Hatase O, Nakamura S, Matsuda M, et al. Activation of R-Ras by Ras-guanine nucleotide-releasing factor. J Biol Chem. 1997 Jul 25;272(30):18602-7.

Gout S and Huot J. Role of cancer microenvironment in metastasis: focus on colon cancer. Cancer Microenviron. 2008 Dec;1(1):69-83.

Goyal L, Muzumdar MD, Zhu AX. Targeting the HGF/c-MET pathway in hepatocellular carcinoma. Clin Cancer Res. 2013 May 1;19(9):2310-8.

Granito A, Guidetti E, Gramantieri L. c-MET receptor tyrosine kinase as a molecular target in advanced hepatocellular carcinoma. J Hepatocell Carcinoma. 2015 Apr 24;2:29-38.

Granito A, Guidetti E, Gramantieri L. c-MET receptor tyrosine kinase as a molecular target in advanced hepatocellular carcinoma. J Hepatocell Carcinoma. 2015 Apr 24;2:29-38.

Grünert S, Jechlinger M, Beug H. Diverse cellular and molecular mechanisms contribute to epithelial plasticity and metastasis. Nat Rev Mol Cell Biol. 2003 Aug;4(8):657-65.

Guerrero C, Fernandez-Medarde A, Rojas JM, Font de Mora J, Esteban LM, Santos E. Transformation suppressor activity of C3G is independent of its CDC25-homology domain. Oncogene. 1998 Feb 5;16(5):613-24.

Guerrero C, Martín-Encabo S, Fernández-Medarde A, Santos E. C3G-mediated suppression of oncogene-induced focus formation in fibroblasts involves inhibition of ERK activation, cyclin A expression and alterations of anchorage-independent growth. Oncogene. 2004 Jun 17;23(28):4885-93.

Guo X, Li T, Xu Y, Xu X, Zhu Z, Zhang Y, et al. Increased levels of Gab1 and Gab2 adaptor proteins skew interleukin-4 (IL-4) signaling toward M2 macrophage-driven pulmonary fibrosis in mice. J Biol Chem. 2017 Aug 25;292(34):14003-14015.

Gutiérrez-Berzal J, Castellano E, Martín-Encabo S, Gutiérrez-Cianca N, Hernández JM, Santos E, et al. Characterization of p87C3G, a novel, truncated C3G isoform that is overexpressed in chronic myeloid leukemia and interacts with Bcr-Abl. Exp Cell Res. 2006 Apr 1;312(6):938-48.

Gutiérrez-Herrero S, Maia V, Gutiérrez-Berzal J, Calzada N, Sanz M, González-Manchón C, et al. C3G transgenic mouse models with specific expression in platelets reveal a new role for C3G in platelet clotting through its GEF activity. Biochim Biophys Acta. 2012 Aug;1823(8):1366-77.

Gutiérrez-Uzquiza Á, Arechederra M, Bragado P, Aguirre-Ghiso JA, Porras A. p38α mediates cell survival in response to oxidative stress via induction of antioxidant genes: effect on the p70S6K pathway. J Biol Chem. 2012 Jan 20;287(4):2632-42.

Gutiérrez-Uzquiza A, Arechederra M, Molina I, Baños R, Maia V, Benito M, et al. C3G down-regulates p38 MAPK activity in response to stress by Rap-1 independent mechanisms: involvement in cell death. Cell Signal. 2010 Mar;22(3):533-42.

Halper J and Kjaer M. Basic components of connective tissues and extracellular matrix: elastin, fibrillin, fibulins, fibrinogen, fibronectin, laminin, tenascins and thrombospondins. Adv Exp Med Biol. 2014;802:31-47.

Hata S, Namae M, and Nishina H. Liver development and regeneration: from laboratory study to clinical therapy. Dev Growth Differ 2007;49(2): 163-170.

Hernandez-Gea V, Friedman SL. Pathogenesis of liver fibrosis. Annu Rev Pathol. 2011;6:425-56.

Hirata T, Nagai H, Koizumi K, Okino K, Harada A, Onda M, et al. Amplification, up-regulation and over-expression of C3G (CRK SH3 domain-binding guanine nucleotide-releasing factor) in non-small cell lung cancers. J Hum Genet. 2004;49(6):290-5.

Hogan C, Serpente N, Cogram P, Hosking CR, Bialucha CU, Feller SM, et al. Rap1 regulates the formation of E-cadherin-based cell-cell contacts. Mol Cell Biol. 2004 Aug;24(15):6690-700.

Holczbauer Á, Factor VM, Andersen JB, Marquardt JU, Kleiner DE, Raggi C, et al. Modeling pathogenesis of primary liver cancer in lineage-specific mouse cell types. Gastroenterology. 2013 Jul;145(1):221-231.

Hruz T, Laule O, Szabo G, Wessendorp F, Bleuler S, Oertle L, et al. Genevestigator v3: a reference expression database for the meta-analysis of transcriptomes. Adv Bioinformatics 2008; 2008:420747.

Hsieh YH, Wu TT, Huang CY, Hsieh YS, Hwang JM, Liu JY. p38 mitogen-activated protein kinase pathway is involved in protein kinase Calpha-regulated invasion in human hepatocellular carcinoma cells. Cancer Res. 2007 May 1;67(9):4320-7.

Hu H, Gehart H, Artegiani B, LÖpez-Iglesias C, Dekkers F, Basak O, et al. Long-Term Expansion of Functional Mouse and Human Hepatocytes as 3D Organoids. Cell. 2018 Nov 29;175(6):1591-1606.e19.

Huang X, Wu D, Jin H, Stupack D, Wang JY. Induction of cell retraction by the combined actions of Abl-CrkII and Rho-ROCK1 signaling. J Cell Biol. 2008 Nov 17;183(4):711-23.

Huber AH, Weis WI. The structure of the beta-catenin/E-cadherin complex and the molecular basis of diverse ligand recognition by beta-catenin. Cell. 2001 May 4;105(3):391-402.

Huff JL, Jelinek MA, Borgman CA, Lansing TJ, Parsons JT. The protooncogene c-sea encodes a transmembrane protein-tyrosine kinase related to the Met/hepatocyte growth factor/scatter factor receptor. Proc Natl Acad Sci U S A. 1993 Jul 1;90(13):6140-4.

Huh CG, Factor VM, Sánchez A, Uchida K, Conner EA, Thorgeirsson SS. Hepatocyte growth factor/c-met signaling pathway is required for efficient liver regeneration and repair. Proc Natl Acad Sci U S A. 2004 Mar 30;101(13):4477-82.

Ichiba T, Hashimoto Y, Nakaya M, Kuraishi Y, Tanaka S, Kurata T, et al. Activation of C3G guanine nucleotide exchange factor for Rap1 by phosphorylation of tyrosine 504. J Biol Chem. 1999 May 14;274(20):14376-81.

Ichiba T, Kuraishi Y, Sakai O, Nagata S, Groffen J, Kurata T, et al. Enhancement of guanine-nucleotide exchange activity of C3G for Rap1 by the expression of Crk, CrkL, and Grb2. J Biol Chem. 1997 Aug 29;272(35):22215-20.

Inagaki Y, Higashi K, Kushida M, Hong YY, Nakao S, Higashiyama R, et al. Hepatocyte growth factor suppresses profibrogenic signal transduction via nuclear export of Sm ad3 with galectin-7. Gastroenterology. 2008 Apr;134(4):1180-90.

Iyoda K, Sasaki Y, Horimoto M, Toyama T, Yakushijin T, Sakakibara M, et al. Involvement of the p38 mitogen-activated protein kinase cascade in hepatocellular carcinoma. Cancer. 2003 Jun 15;97(12):3017-26.

Ji J, Eggert T, Budhu A, Forgues M, Takai A, Dang H et al. Hepatic stellate cell and monocyte interaction contributes to poor prognosis in hepatocellular carcinoma. Hepatology. 2015 Aug;62(2):481-95.

Jia CC, Wang TT, Liu W, Fu BS, Hua X, Wang GY et al. Cancer-associated fibroblasts from hepatocellular carcinoma promote malignant cell proliferation by HGF secretion. PLoS One. 2013 May 7;8(5):e63243.

Jin S, Zhai B, Qiu Z, Wu J, Lane MD, Liao K. c-Crk, a substrate of the insulin-like growth factor-1 receptor tyrosine kinase, functions as an early signal mediator in the adipocyte differentiation process. J Biol Chem. 2000 Nov 3;275(44):34344-52.

Jindal A, Thadi A, Shailubhai K. Hepatocellular Carcinoma: Etiology and Current and Future Drugs. J Clin Exp Hepatol. 2019 Mar-Apr;9(2):221-232.

Ju MJ, Qiu SJ, Fan J, Xiao YS, Gao Q, Zhou J, et al. Peritumoral activated hepatic stellate cells predict poor clinical outcome in hepatocellular carcinoma after curative resection. Am J Clin Pathol. 2009 Apr;131(4):498-510.

Kalluri R and Zeisberg M. Fibroblasts in cancer. Nat Rev Cancer. 2006 May;6(5):392-401.

Kamei T, Matozaki T, Sakisaka T, Kodama A, Yokoyama S, Peng YF, et al. Coendocytosis of cadherin and c-Met coupled to disruption of cell-cell adhesion in MDCK cells--regulation by Rho, Rac and Rab small G proteins. Oncogene. 1999 Nov 18;18(48):6776-84.

Kanemura H, Iimuro Y, Takeuchi M, Ueki T, Hirano T, Horiguchi K, et al. Hepatocyte growth factor gene transfer with naked plasmid DNA ameliorates dimethylnitrosamine-induced liver fibrosis in rats. Hepatol Res. 2008 Sep;38(9):930-9.

Kang LI, Mars WM, Michalopoulos GK. Signals and cells involved in regulating liver regeneration. Cells. 2012 Dec 13;1(4):1261-92.

Kaposi-Novak P, Lee JS, Gòmez-Quiroz L, Coulouarn C, Factor VM, Thorgeirsson SS. Met-regulated expression signature defines a subset of human hepatocellular carcinomas with poor prognosis and aggressive phenotype. J Clin Invest. 2006 Jun;116(6):1582-95.

Karsdal MA, Manon-Jensen T, Genovese F, Kristensen JH, Nielsen MJ, Sand JM, et al. Novel insights into the function and dynamics of extracellular matrix in liver fibrosis. Am J Physiol Gastrointest Liver Physiol. 2015 May 15;308(10):G807-30.

Karsdal MA, Manon-Jensen T, Genovese F, Kristensen JH, Nielsen MJ, Sand JM, et al. Novel insights into the function and dynamics of extracellular matrix in liver fibrosis. Am J Physiol Gastrointest Liver Physiol. 2015 May 15;308(10):G807-30.

Kim TH, Mars WM, Stolz DB, Petersen BE, Michalopoulos GK. Extracellular matrix remodeling at the early stages of liver regeneration in the rat. Hepatology. 1997 Oct;26(4):896-904.

Kim WH, Matsumoto K, Bessho K, Nakamura T. Growth inhibition and apoptosis in liver myofibroblasts promoted by hepatocyte growth factor leads to resolution from liver cirrhosis. Am J Pathol. 2005 Apr;166(4):1017-28.

Kim W, Khan SK, Liu Y, Xu R, Park O, He Y, et al. Hepatic Hippo signaling inhibits protumoural microenvironment to suppress hepatocellular carcinoma. Gut. 2018 Sep;67(9):1692-1703.

Kinoshita T, Tashiro K, Nakamura T. Marked increase of HGF mRNA in non-parenchymal liver cells of rats treated with hepatotoxins. Biochem Biophys Res Commun. 1989 Dec 29;165(3):1229-34.

Kirsch KH, Georgescu MM, Hanafusa H. Direct binding of p130(Cas) to the guanine nucleotide exchange factor C3G. J Biol Chem. 1998 Oct 2;273(40):25673-9.

Kiss A, Wang NJ, Xie JP, Thorgeirsson SS. Analysis of transforming growth factor (TGF)-alpha/epidermal growth factor receptor, hepatocyte growth Factor/c-met,TGF-
beta receptor type II, and p53 expression in human hepatocellular carcinomas. Clin Cancer Res. 1997 Jul;3(7):1059-66.

Koeppen and Stanton: Berne and Levi Physiology, 6th Edition (2008) by Mosby, an imprint of Elsevier, Inc.

Kooistra MR, Dubé N, Bos JL. Rap1: a key regulator in cell-cell junction formation. J Cell Sci. 2007 Jan 1;120(Pt 1):17-22.

Kooistra MR, Dubé N, Bos JL. Rap1: a key regulator in cell-cell junction formation. J Cell Sci. 2007 Jan 1;120(Pt 1):17-22.

Kourtidis A, Lu R, Pence LJ, Anastasiadis PZ. A central role for cadherin signaling in cancer. Exp Cell Res. 2017 Sep 1;358(1):78-85.

Kummar S, Shafi NQ. Metastatic hepatocellular carcinoma. Clin Oncol (R Coll Radiol). 2003 Aug;15(5):288-94.

Lai Q, Vitale A, Manzia TM, Foschi FG, Levi Sandri GB, Gambato M, et al. Platelets and Hepatocellular Cancer: Bridging the Bench to the Clinics. Cancers (Basel). 2019 Oct 15;11(10).

Lamorte L, Rodrigues S, Naujokas M, Park M. Crk synergizes with epidermal growth factor for epithelial invasion and morphogenesis and is required for the met morphogenic program. J Biol Chem. 2002 Oct 4;277(40):37904-11

Lamorte L, Royal I, Naujokas M, Park M. Crk adapter proteins promote an epithelial-mesenchymal-like transition and are required for HGF-mediated cell spreading and breakdown of epithelial adherens junctions. Mol Biol Cell. 2002 May;13(5):1449-61.

Lamouille S, Xu J, Derynck R. Molecular mechanisms of epithelial-mesenchymal transition. Nat Rev Mol Cell Biol. 2014 Mar;15(3):178-96.

Le Bras GF, Taubenslag KJ, Andl CD. The regulation of cell-cell adhesion during epithelial-mesenchymal transition, motility and tumor progression. Cell Adh Migr. 2012 Jul-Aug;6(4):365-73.

Lee JS, Heo J, Libbrecht L, Chu IS, Kaposi-Novak P, Calvisi DF, et al. A novel prognostic subtype of human hepatocellular carcinoma derived from hepatic progenitor cells. Nat Med. 2006 Apr;12(4):410-6.

Lewis DM, Park KM, Tang V, Xu Y, Pak K, Eisinger-Mathason TS, et al. Intratumoral oxygen gradients mediate sarcoma cell invasion. Proc Natl Acad Sci U S A. 2016 Aug 16;113(33):9292-7.

Li R, Knight JF, Park M, Pendergast AM. Abl Kinases Regulate HGF/Met Signaling Required for Epithelial Cell Scattering, Tubulogenesis and Motility. PLoS One. 2015 May 6;10(5):e0124960.

Lin Y, Mettling C, Chou C. Rap1-suppressed tumorigenesis is concomitant with the interference in ras effector signaling. FEBS Lett. 2000 Feb 11;467(2-3):184-8.

Ling L, Zhu T, Lobie PE. Src-CrkII-C3G-dependent activation of Rap1 switches growth hormone-stimulated p44/42 MAP kinase and JNK/SAPK activities. J Biol Chem. 2003 Jul 18;278(29):27301-11.

Liu WT, Jing YY, Yu GF, Chen H, Han ZP, Yu DD, et al. Hepatic stellate cell promoted hepatoma cell invasion via the HGF/c-Met signaling pathway regulated by p53. Cell Cycle. 2016;15(7):886-94.

Lleo A, de Boer YS, Liberal R, Colombo M. The risk of liver cancer in autoimmune liver diseases. Ther Adv Med Oncol. 2019 Jul 12;11:1758835919861914

Llovet JM, Montal R, Sia D, Finn RS. Molecular therapies and precision medicine for hepatocellular carcinoma. Nat Rev Clin Oncol. 2018 Oct;15(10):599-616.

Llovet JM, Zucman-Rossi J, Pikarsky E, Sangro B, Schwartz M, Sherman M, et al. Hepatocellular carcinoma. Nat Rev Dis Primers. 2016 Apr 14;2:16018.

Luk ST, Ng KY, Zhou L, Tong M, Wong TL, Yu H, et al. Deficiency in embryonic stem cell marker REX1 activates MKK6-dependent p38 MAPK signaling to drive hepatocarcinogenesis. Hepatology. 2019 Nov 4.

Machida K. Existence of cancer stem cells in hepatocellular carcinoma: myth or reality? Hepatol Int. 2017 Mar;11(2):143-147.

Maestrini E, Tamagnone L, Longati P, Cremona O, Gulisano M, Bione S, et al. A family of transmembrane proteins with homology to the MET-hepatocyte growth factor receptor. Proc Natl Acad Sci U S A. 1996 Jan 23;93(2):674-8.

Maher JJ. Cell-specific expression of hepatocyte growth factor in liver. Upregulation in sinusoidal endothelial cells after carbon tetrachloride. J Clin Invest. 1993 May;91(5):2244-52.

Maia V, Ortiz-Rivero S, Sanz M, Gutierrez-Berzal J, Alvarez-Fernández I, Gutierrez-Herrero S, et al. C3G forms complexes with Bcr-Abl and p38α MAPK at the focal adhesions in chronic myeloid leukemia cells: implication in the regulation of leukemic cell adhesion. Cell Commun Signal. 2013 Jan 23;11(1):9.

Maia V, Sanz M, Gutierrez-Berzal J, de Luis A, Gutierrez-Uzquiza A, Porras A, et al. C3G silencing enhances STI-571-induced apoptosis in CML cells through p38 MAPK activation, but it antagonizes STI-571 inhibitory effect on survival. Cell Signal. 2009 Jul;21(7):1229-35.

Malarkey DE, Johnson K, Ryan L, Boorman G, Maronpot RR. New insights into functional aspects of liver morphology. Toxicol Pathol. 2005;33(1):27-34.

Marquardt JU, Andersen JB, Thorgeirsson SS. Functional and genetic deconstruction of the cellular origin in liver cancer. Nat Rev Cancer. 2015 Nov;15(11):653-67.

Marquardt JU, Galle PR, Teufel A. Molecular diagnosis and therapy of hepatocellular carcinoma (HCC): an emerging field for advanced technologies. J Hepatol. 2012 Jan;56(1):267-75

Martín-Encabo S, Santos E, Guerrero C. C3G mediated suppression of malignant transformation involves activation of PP2A phosphatases at the subcortical actin cytoskeleton. Exp Cell Res. 2007 Nov 1;313(18):3881-91.

Maruthamuthu V, Sabass B, Schwarz US, Gardel ML. Cell-ECM traction force modulates endogenous tension at cell-cell contacts. Proc Natl Acad Sci U S A. 2011 Mar 22;108(12):4708-13.

Matsumoto K and Nakamura T. Hepatocyte growth factor and the Met system as a mediator of tumor-stromal interactions. Int J Cancer. 2006 Aug 1;119(3):477-83.

Matteucci E, Ridolfi E, Desiderio MA. Hepatocyte growth factor differently influences Met-E-cadherin phosphorylation and downstream signaling pathway in two models of breast cells. Cell Mol Life Sci. 2006 Sep;63(17):2016-26.

Mescher AL. Junqueira's Basic Histology: Text and Atlas, 12th Edition, 2009. The McGraw-Hill companies, Inc.

Michalopoulos G. K. Liver regeneration. J Cell Physiol 2007;213(2): 286-300.

Michalopoulos GK. Liver regeneration after partial hepatectomy: critical analysis of mechanistic dilemmas. Am J Pathol. 2010 Jan;176(1):2-13.

Min J, Feng Q, Liao W, Liang Y, Gong C, Li E, et al. IFITM3 promotes hepatocellular carcinoma invasion and metastasis by regulating MMP9 through p38/MAPK signaling. FEBS Open Bio. 2018 Jun 28;8(8):1299-1311.

Min L, He B, Hui L. Mitogen-activated protein kinases in hepatocellular carcinoma development. Semin Cancer Biol. 2011 Feb;21(1):10-20.

Mitra A and Radha V. F-actin-binding domain of c-Abl regulates localized phosphorylation of C3G: role of C3G in c-Abl-mediated cell death. Oncogene. 2010 Aug 12;29(32):4528-42.

Miyoshi A, Kitajima Y, Sumi K, Sato K, Hagiwara A, Koga Y, et al. Snail and SIP1 increase cancer invasion by upregulating MMP family in hepatocellular carcinoma cells. Br J Cancer. 2004 Mar 22;90(6):1265-73.

Monga SP. β-Catenin Signaling and Roles in Liver Homeostasis, Injury, and Tumorigenesis. Gastroenterology. 2015 Jun;148(7):1294-310.

Moustakas A, Heldin CH. Non-Smad TGF-beta signals. J Cell Sci. 2005 Aug 15;118(Pt 16):3573-84.

Nakamura T, Mizuno S. The discovery of hepatocyte growth factor (HGF) and its significance for cell biology, life sciences and clinical medicine. Proc Jpn Acad Ser B Phys Biol Sci. 2010;86(6):588-610.

Nakamura T, Sakai K, Nakamura T, Matsumoto K. Hepatocyte growth factor twenty years on: Much more than a growth factor. J Gastroenterol Hepatol. 2011 Jan;26 Suppl 1:188-202.

Nakamura T. Growth factor and growth inhibitor for hepatocyte proliferation. Gan To Kagaku Ryoho. 1989 Mar;16(3 Pt 2):481-8.

Naldini L, Vigna E, Bardelli A, Follenzi A, Galimi F, Comoglio PM. Biological activation of pro-HGF (hepatocyte growth factor) by urokinase is controlled by a stoichiometric reaction. J Biol Chem. 1995 Jan 13;270(2):603-11.

Nayak SC and Radha V. C3G (RapGEF1) localizes to the mother centriole and regulates centriole division and primary cilia dynamics.

Nebreda AR and Porras A. p38 MAP kinases: beyond the stress response. Trends Biochem Sci. 2000 Jun;25(6):257-60.

Nieto MA, Huang RY, Jackson RA, Thiery JP. EMT: 2016. Cell. 2016 Jun 30;166(1):21-45.

Nieto MA. The ins and outs of the epithelial to mesenchymal transition in health and disease. Annu Rev Cell Dev Biol. 2011;27:347-76.

Nishida K, Hirano T. The role of Gab family scaffolding adapter proteins in the signal transduction of cytokine and growth factor receptors. Cancer Sci. 2003 Dec;94(12):1029-33.

Nobre AR, Entenberg D, Wang Y, Condeelis J, Aguirre-Ghiso JA. The Different Routes to Metastasis via Hypoxia-Regulated Programs. Trends Cell Biol. 2018 Nov;28(11):941-956.

Nolz JC, Nacusi LP, Segovis CM, Medeiros RB, Mitchell JS, Shimizu Y, et al. The WAVE2 complex regulates T cell receptor signaling to integrins via Abl- and CrkL-C3G-mediated activation of Rap1. J Cell Biol. 2008 Sep 22;182(6):1231-44.

Novikova MV, Khromova NV, Kopnin PB. Components of the Hepatocellular Carcinoma Microenvironment and Their Role in Tumor Progression. Biochemistry (Mosc). 2017 Aug;82(8):861-873.

Noy R and Pollard JW.Tumor-associated macrophages: from mechanisms to therapy. Immunity. 2014 Jul 17;41(1):49-61.

O'Connor JW and Gomez EW. Biomechanics of TGFβ-induced epithelial-mesenchymal transition: implications for fibrosis and cancer. Clin Transl Med. 2014 Jul 15;3:23.

Odero-Marah V, Hawsawi O, Henderson V, Sweeney J. Epithelial-Mesenchymal Transition (EMT) and Prostate Cancer. Adv Exp Med Biol. 2018;1095:101-110.

Ohba Y, Ikuta K, Ogura A, Matsuda J, Mochizuki N, Nagashima K, et al. Requirement for C3G-dependent Rap1 activation for cell adhesion and embryogenesis. EMBO J. 2001 Jul 2;20(13):3333-41.

Okino K, Nagai H, Nakayama H, Doi D, Yoneyama K, Konishi H, et al. Inactivation of Crk SH3 domain-binding guanine nucleotide-releasing factor (C3G) in cervical squamous cell carcinoma. Int J Gynecol Cancer. 2006 Mar-Apr;16(2):763-71.

Okuma HS and Kondo S. Trends in the development of MET inhibitors for hepatocellular carcinoma. Future Oncol. 2016 May;12(10):1275-86.

Organ SL and Tsao MS. An overview of the c-MET signaling pathway. her Adv Med Oncol. 2011 Nov;3(1 Suppl):S7-S19.

Ortiz-Rivero S, Baquero C, Hernández-Cano L, Roldán-Etcheverry JJ, Gutiérrez-Herrero S, Fernández-Infante C, et al. C3G, through its GEF activity, induces megakaryocytic differentiation and proplatelet formation. Cell Commun Signal. 2018 Dec 19;16(1):101.

Pannekoek WJ, Kooistra MR, Zwartkruis FJ, Bos JL. Cell-cell junction formation: the role of Rap1 and Rap1 guanine nucleotide exchange factors. Biochim Biophys Acta. 2009 Apr;1788(4):790-6.

Paolillo M and Schinelli S. Extracellular Matrix Alterations in Metastatic Processes. Int J Mol Sci. 2019 Oct 7;20(19).

Park SY, Jeong KJ, Panupinthu N, Yu S, Lee J, Han JW et al. Lysophosphatidic acid augments human hepatocellular carcinoma cell invasion through LPA1 receptor and MMP-9 expression. Oncogene. 2011 Mar 17;30(11):1351-9.

Parsons JT, Horwitz AR, Schwartz MA. Cell adhesion: integrating cytoskeletal dynamics and cellular tension. Nat Rev Mol Cell Biol. 2010 Sep;11(9):633-43.

Patthy L, Trexler M, Váli Z, Bányai L, Váradi A. Kringles: modules specialized for protein binding. Homology of the gelatin-binding region of fibronectin with the kringle structures of proteases. FEBS Lett. 1984 Jun 4;171(1):131-6.

Pavlovic N, Rani B, Gerwins P, Heindryckx F. Platelets as Key Factors in Hepatocellular Carcinoma. Cancers (Basel). 2019 Jul 20;11(7).

Pearson GW. Control of Invasion by Epithelial-to-Mesenchymal Transition Programs during Metastasis. J Clin Med. 2019 May 10;8(5). pii: E646.

Peinado H, Zhang H, Matei IR, Costa-Silva B, Hoshino A, Rodrigues G, et al. Pre-metastatic niches: organ-specific homes for metastases. Nat Rev Cancer. 2017 May;17(5):302-317

Pepper MS. Lymphangiogenesis and tumor metastasis: myth or reality? Clin Cancer Res. 2001 Mar;7(3):462-8.

Pereira L, Mariadason JM, Hannan RD, Dhillon AS. Implications of epithelial-mesenchymal plasticity for heterogeneity in colorectal cancer. Front Oncol. 2015 Feb 2;5:13.

Perugorria MJ, Olaizola P, Labiano I, Esparza-Baquer A, Marzioni M, Marin JJG, et al. Wnt-β-catenin signalling in liver development, health and disease. Nat Rev Gastroenterol Hepatol. 2019 Feb;16(2):121-136.

Phaneuf D, Moscioni AD, LeClair C, Raper SE, Wilson JM. Generation of a mouse expressing a conditional knockout of the hepatocyte growth factor gene: demonstration of impaired liver regeneration. DNA Cell Biol. 2004 Sep;23(9):592-603.

Piedra J, Martinez D, Castano J, Miravet S, Dunach M, de Herreros AG. Regulation of beta-catenin structure and activity by tyrosine phosphorylation. J Biol Chem. 2001 Jun 8;276(23):20436-43.

Popper HH. Progression and metastasis of lung cancer. Cancer Metastasis Rev. 2016 Mar;35(1):75-91.

Porras A, Zuluaga S, Black E, Valladares A, Alvarez AM, Ambrosino C, et al. P38 alpha mitogen-activated protein kinase sensitizes cells to apoptosis induced by different stimuli. Mol Biol Cell. 2004 Feb;15(2):922-33.

Priego N, Arechederra M, Sequera C, Bragado P, Vázquez-Carballo A, Gutiérrez-Uzquiza Á, et al. C3G knock-down enhances migration and invasion by increasing Rap1-mediated p38α activation, while it impairs tumor growth through p38α-independent mechanisms. Oncotarget. 2016 Jul 19;7(29):45060-45078.

Radha V, Mitra A, Dayma K, Sasikumar K. Signalling to actin: role of C3G, a multitasking guanine-nucleotide-exchange factor. Biosci Rep. 2011 Aug;31(4):231-44.

Radha V, Rajanna A, Gupta RK, Dayma K, Raman T. The guanine nucleotide exchange factor, C3G regulates differentiation and survival of human neuroblastoma cells. J Neurochem. 2008 Dec;107(5):1424-35.

Radha V, Rajanna A, Mitra A, Rangaraj N, Swarup G. C3G is required for c-Abl-induced filopodia and its overexpression promotes filopodia formation. Exp Cell Res. 2007 Jul 1;313(11):2476-92.

Radha V, Rajanna A, Swarup G. Phosphorylated guanine nucleotide exchange factor C3G, induced by pervanadate and Src family kinases localizes to the Golgi and subcortical actin cytoskeleton. BMC Cell Biol. 2004 Aug 20;5:31.

Radisky ES, Radisky DC. Matrix metalloproteinase-induced epithelial-mesenchymal transition in breast cancer. J Mammary Gland Biol Neoplasia. 2010 Jun;15(2):201-12.

Rangarajan S, Enserink JM, Kuiperij HB, de Rooij J, Price LS, Schwede F, et al. Cyclic AMP induces integrin-mediated cell adhesion through Epac and Rap1 upon stimulation of the beta 2-adrenergic receptor. J Cell Biol. 2003 Feb 17;160(4):487-93.

Reedquist KA, Fukazawa T, Panchamoorthy G, Langdon WY, Shoelson SE, Druker BJ, et al. Stimulation through the T cell receptor induces Cbl association with Crk proteins and the guanine nucleotide exchange protein C3G. J Biol Chem. 1996 Apr 5;271(14):8435-42.

Ridley AJ, Schwartz MA, Burridge K, Firtel RA, Ginsberg MH, Borisy G, et al. Cell migration: integrating signals from front to back. Science. 2003 Dec 5;302(5651):1704-9.

Rombouts K and Carloni V. The fibrotic microenvironment as a heterogeneity facet of hepatocellular carcinoma. Fibrogenesis Tissue Repair. 2013 Sep 16;6(1):17.

Ronsin C, Muscatelli F, Mattei MG, Breathnach R. A novel putative receptor protein tyrosine kinase of the met family. Oncogene. 1993 May;8(5):1195-202.

Rørth P. Collective cell migration. Annu Rev Cell Dev Biol. 2009;25:407-29

Roura S, Miravet S, Piedra J, García de Herreros A, Duñach M. Regulation of E-cadherin/Catenin association by tyrosine phosphorylation. J Biol Chem. 1999 Dec 17;274(51):36734-40.

Rufanova VA, Lianos E, Alexanian A, Sorokina E, Sharma M, McGinty A, et al. C3G overexpression in glomerular epithelial cells during anti-GBM-induced glomerulonephritis. Kidney Int. 2009 Jan;75(1):31-40.

Sachs M, Brohmann H, Zechner D, Müller T, Hülsken J, Walther I, et al. Essential role of Gab1 for signaling by the c-Met receptor in vivo. J Cell Biol. 2000 Sep 18;150(6):1375-84.

Sakkab D, Lewitzky M, Posern G, Schaeper U, Sachs M, Birchmeier W, et al. Signaling of hepatocyte growth factor/scatter factor (HGF) to the small GTPase Rap1 via the large docking protein Gab1 and the adapter protein CRKL. J Biol Chem. 2000 Apr 14;275(15):10772-8.

Sameni M, Dosescu J, Moin K, Sloane BF. Functional imaging of proteolysis: stromal and inflammatory cells increase tumor proteolysis. Mol Imaging. 2003 Jul;2(3):159-75.

Sánchez-Tilló E, Siles L, de Barrios O, Cuatrecasas M, Vaquero EC, Castells A, et al. Expanding roles of ZEB factors in tumorigenesis and tumor progression. Am J Cancer Res. 2011;1(7):897-912.

Sanz-Moreno V, Gadea G, Ahn J, Paterson H, Marra P, Pinner S, et al. Rac activation and inactivation control plasticity of tumor cell movement. Cell. 2008 Oct 31;135(3):510-23.

Sármay G, Angyal A, Kertész A, Maus M, Medgyesi D. The multiple function of Grb2 associated binder (Gab) adaptor/scaffolding protein in immune cell signaling. Immunol Lett. 2006 Apr 15;104(1-2):76-82.

Sasi Kumar K, Ramadhas A, Nayak SC, Kaniyappan S, Dayma K, Radha V. C3G (RapGEF1), a regulator of actin dynamics promotes survival and myogenic differentiation of mouse mesenchymal cells. Biochim Biophys Acta. 2015 Oct;1853(10 Pt A):2629-39

Scallan J, Huxley VH, Korthuis RJ. Capillary Fluid Exchange: Regulation, Functions, and Pathology. San Rafael (CA): Morgan & Claypool Life Sciences; 2010.

Scheau C, Badarau IA, Costache R, Caruntu C, Mihai GL, Didilescu AC, et al. The Role of Matrix Metalloproteinases in the Epithelial-Mesenchymal Transition of Hepatocellular Carcinoma. Anal Cell Pathol (Amst). 2019 Nov 26;2019:9423907.

Schindelin J, Arganda-Carreras I, Frise E, Kaynig V, Longair M, Pietzsch T, et al. Fiji: an open-source platform for biological-image analysis. Nat Methods. 2012 Jun 28;9(7):676-82.

Schmidt C, Bladt F, Goedecke S, Brinkmann V, Zschiesche W, Sharpe M, et al. Scatter factor/hepatocyte growth factor is essential for liver development. Nature. 1995 Feb 23;373(6516):699-702.

Schuppan D, Ruehl M, Somasundaram R, Hahn EG. Matrix as a modulator of hepatic fibrogenesis. Semin Liver Dis. 2001 Aug;21(3):351-72.

Sciarratta V, Sohn K, Burger-Kentischer A, Brunner H, Oehr C. Controlled Cell Attachment, Using Plasma Deposited Polymer Microstructures: A Novel Study of Cells-Substrate Interactions. Plasma Process. Polym. 2006, 3, 532–539

Seiden-Long I1, Navab R, Shih W, Li M, Chow J, Zhu CQ, et al. Gab1 but not Grb2 mediates tumor progression in Met overexpressing colorectal cancer cells. Carcinogenesis. 2008 Mar;29(3):647-55.

Senoo H, Kojima N, Sato M. Vitamin A-storing cells (stellate cells). Vitam Horm. 2007;75:131-59.

Sequera C, Manzano S, Guerrero C, Porras A. How Rap and its GEFs control liver physiology and cancer development. C3G alterations in human hepatocarcinoma. Hepat Oncol. 2018 Apr 16;5(1):HEP05.

Shah B, Lutter D, Bochenek ML, Kato K, Tsytsyura Y, Glyvuk N, et al. C3G/Rapgef1 Is Required in Multipolar Neurons for the Transition to a Bipolar Morphology during Cortical Development. PLoS One. 2016 Apr 25;11(4):e0154174.

Shakyawar DK, Dayma K, Ramadhas A, Varalakshmi C, Radha V. C3G shows regulated nucleocytoplasmic exchange and represses histone modifications associated with euchromatin. Mol Biol Cell. 2017 Apr 1;28(7):984-995.

Shakyawar DK, Muralikrishna B, Radha V. C3G dynamically associates with nuclear speckles and regulates mRNA splicing. Mol Biol Cell. 2018 May 1;29(9):1111-1124.

Shang N, Wang H, Bank T, Perera A, Joyce C, Kuffel G, et al. Focal Adhesion Kinase and β-Catenin Cooperate to Induce Hepatocellular Carcinoma. Hepatology. 2019 Nov;70(5):1631-1645.

Shay G, Lynch CC, Fingleton B. Moving targets: Emerging roles for MMPs in cancer progression and metastasis. Matrix Biol. 2015 May-Jul;44-46:200-6.

Shayan R, Achen MG, Stacker SA. Lymphatic vessels in cancer metastasis: bridging the gaps. Carcinogenesis. 2006 Sep;27(9):1729-38.

Sheng Y, Ding S, Chen K, Chen J, Wang S, Zou C, et al. Functional analysis of miR-101-3p and Rap1b involved in hepatitis B virus-related hepatocellular carcinoma pathogenesis. Biochem Cell Biol. 2014 Apr;92(2):152-62.

Shiota G, Wang TC, Nakamura T, Schmidt EV. Hepatocyte growth factor in transgenic mice: effects on hepatocyte growth, liver regeneration and gene expression. Hepatology. 1994 Apr;19(4):962-72.

Shivakrupa R, Radha V, Sudhakar Ch, Swarup G. Physical and functional interaction between Hck tyrosine kinase and guanine nucleotide exchange factor C3G results in apoptosis, which is independent of C3G catalytic domain. J Biol Chem. 2003 Dec 26;278(52):52188-94.

Simister PC and Feller SM. Order and disorder in large multi-site docking proteins of the Gab family--implications for signalling complex formation and inhibitor design strategies. Mol Biosyst. 2012 Jan;8(1):33-46.

Smit L, van der Horst G, Borst J. Sos, Vav, and C3G participate in B cell receptor-induced signaling pathways and differentially associate with Shc-Grb2, Crk, and Crk-L adaptors. J Biol Chem. 1996 Apr 12;271(15):8564-9.

Soini Y. Tight junctions in lung cancer and lung metastasis: a review. Int J Clin Exp Pathol. 2012;5(2):126-36.

Sonnenberg E, Meyer D, Weidner KM, Birchmeier C. Scatter factor/hepatocyte growth factor and its receptor, the c-met tyrosine kinase, can mediate a signal exchange between mesenchyme and epithelia during mouse development. J Cell Biol. 1993 Oct;123(1):223-35.

Sternlicht MD, and Werb Z. How matrix metalloproteinases regulate cell behavior. Annu Rev Cell Dev Biol. 2001;17:463-516.

Stoker M, Gherardi E, Perryman M, Gray J. Scatter factor is a fibroblast-derived modulator of epithelial cell mobility. Nature. 1987 May 21-27;327(6119):239-42.

Su H, Yang JR, Xu T, Huang J, Xu L, Yuan, et al. MicroRNA-101, down-regulated in hepatocellular carcinoma, promotes apoptosis and suppresses tumorigenicity. Cancer Res. 2009 Feb 1;69(3):1135-42

Swartz MA and Skobe M. Lymphatic function, lymphangiogenesis, and cancer metastasis. Microsc Res Tech. 2001 Oct 15;55(2):92-9.

Tahmasebi Birgani M, and Carloni V. Tumor Microenvironment, a Paradigm in Hepatocellular Carcinoma Progression and Therapy. Int J Mol Sci. 2017 Feb 14;18(2).

Takai S, Tanaka M, Sugimura H, Yamada K, Naito Y, Kino I, et al. Mapping of the human C3G gene coding a guanine nucleotide releasing protein for Ras family to 9q34.3 by fluorescence in situ hybridization. Hum Genet. 1994 Nov;94(5):549-50.

Tanaka S, Morishita T, Hashimoto Y, Hattori S, Nakamura S, Shibuya M, et al. C3G, a guanine nucleotide-releasing protein expressed ubiquitously, binds to the Src homology 3 domains of CRK and GRB2/ASH proteins. Proc Natl Acad Sci U S A. 1994 Apr 12;91(8):3443-7.

Tang Z, Peng H, Chen J, Liu Y, Yan S, Yu G, et al. Rap1b enhances the invasion and migration of hepatocellular carcinoma cells by up-regulating Twist 1. Exp Cell Res. 2018 Jun 1;367(1):56-64.

Thiery JP, Acloque H, Huang RY, Nieto MA. Epithelial-mesenchymal transitions in development and disease. Cell. 2009 Nov 25;139(5):871-90

Tian Z, Hou X, Liu W, Han Z, Wei L. Macrophages and hepatocellular carcinoma. Cell Biosci. 2019 Sep 26;9:79

Tian Z, Hou X, Liu W, Han Z, Wei L. Macrophages and hepatocellular carcinoma. Cell Biosci. 2019 Sep 26;9:79.

Tomar A, and Schlaepfer DD. Focal adhesion kinase: switching between GAPs and GEFs in the regulation of cell motility. Curr Opin Cell Biol. 2009 Oct;21(5):676-83.

Trefts E, Gannon M, Wasserman DH. The liver. Curr Biol. 2017 Nov 6;27(21):R1147-R1151.

Trusolino L, Bertotti A, Comoglio PM. MET signalling: principles and functions in development, organ regeneration and cancer. Nat Rev Mol Cell Biol. 2010 Dec;11(12):834-48.

Tsanou E, Peschos D, Batistatou A, Charalabopoulos A, Charalabopoulos K. The E-cadherin adhesion molecule and colorectal cancer. A global literature approach. Anticancer Res. 2008 Nov-Dec;28(6A):3815-26.

Tse JC and Kalluri R. Mechanisms of metastasis: epithelial-to-mesenchymal transition and contribution of tumor microenvironment. J Cell Biochem. 2007 Jul 1;101(4):816-29.

Tulasne D, Foveau B. The shadow of death on the MET tyrosine kinase receptor. Cell Death Differ. 2008 Mar;15(3):427-34.

Uehara Y, Minowa O, Mori C, Shiota K, Kuno J, Noda T, et al. Placental defect and embryonic lethality in mice lacking hepatocyte growth factor/scatter factor. Nature. 1995 Feb 23;373(6516):702-5.

Ueki T, Kaneda Y, Tsutsui H, Nakanishi K, Sawa Y, Morishita R, et al. Hepatocyte growth factor gene therapy of liver cirrhosis in rats. Nat Med. 1999 Feb;5(2):226-30.

Utreras E, Henriquez D, Contreras-Vallejos E, Olmos C, Di Genova A, Maass A, et al. Cdk5 regulates Rap1 activity. Neurochem Int. 2013 May;62(6):848-53.

van den Berghe N, Cool RH, Horn G, Wittinghofer A. Biochemical characterization of C3G: an exchange factor that discriminates between Rap1 and Rap2 and is not inhibited by Rap1A(S17N). Oncogene. 1997 Aug 14;15(7):845-50.

Van Haele M, Roskams T. Hepatic Progenitor Cells: An Update. Gastroenterol Clin North Am. 2017 Jun;46(2):409-420.

van Veelen W, Le NH, Helvensteijn W, Blonden L, Theeuwes M, Bakker ER, et al. β-catenin tyrosine 654 phosphorylation increases Wnt signalling and intestinal tumorigenesis. Gut. 2011 Sep;60(9):1204-12.

van Zijl F, Zulehner G, Petz M, Schneller D, Kornauth C, Hau M, et al. Epithelial-mesenchymal transition in hepatocellular carcinoma. Future Oncol. 2009 Oct;5(8):1169-79.

Venepalli NK and Goff L. Targeting the HGF-cMET Axis in Hepatocellular Carcinoma. Int J Hepatol. 2013;2013:341636.

Voss AK, Britto JM, Dixon MP, Sheikh BN, Collin C, Tan SS, et al. C3G regulates cortical neuron migration, preplate splitting and radial glial cell attachment. Development. 2008 Jun;135(12):2139-49.

Voss AK, Gruss P, Thomas T. The guanine nucleotide exchange factor C3G is necessary for the formation of focal adhesions and vascular maturation. Development. 2003 Jan;130(2):355-67.

Voss AK, Krebs DL, Thomas T. C3G regulates the size of the cerebral cortex neural precursor population. EMBO J. 2006 Aug 9;25(15):3652-63.

Wagner EF and Nebreda AR. Signal integration by JNK and p38 MAPK pathways in cancer development. Nat Rev Cancer. 2009 Aug;9(8):537-49.

Wang K, Qin S, Liang Z, Zhang Y, Xu Y, Chen A, et al. Epithelial disruption of Gab1 perturbs surfactant homeostasis and predisposes mice to lung injuries. Am J Physiol Lung Cell Mol Physiol. 2016 Dec 1;311(6):L1149-L1159.

Wang W, Xu S, Yin M, Jin ZG. Essential roles of Gab1 tyrosine phosphorylation in growth factor-mediated signaling and angiogenesis. Int J Cardiol. 2015 Feb 15;181:180-4.

Watanabe T, Tsuda M, Makino Y, Konstantinou T, Nishihara H, Majima T, et al. Crk adaptor protein-induced phosphorylation of Gab1 on tyrosine 307 via Src is important for organization of focal adhesions and enhanced cell migration. Cell Res. 2009 May;19(5):638-50.

Wells RG. Cellular sources of extracellular matrix in hepatic fibrosis. Clin Liver Dis. 2008 Nov;12(4):759-68, viii.

Wendt MK, Tian M, Schiemann WP. Deconstructing the mechanisms and consequences of TGF-β-induced EMT during cancer progression. Cell Tissue Res. 2012 Jan;347(1):85-101.

Windmeier C and Gressner AM. Pharmacological aspects of pentoxifylline with emphasis on its inhibitory actions on hepatic fibrogenesis. Gen Pharmacol. 1997 Aug;29(2):181-96.

Wu Q, Zhou L, Lv D, Zhu X, Tang H. Exosome-mediated communication in the tumor microenvironment contributes to hepatocellular carcinoma development and progression. J Hematol Oncol. 2019 May 29;12(1):53.

Wu Z, Wang L, Li J, Wang L, Wu Z, Sun X. Extracellular Vesicle-Mediated Communication Within Host-Parasite Interactions. Front Immunol. 2019 Jan 15;9:3066.

Xia JL, Dai C, Michalopoulos GK, Liu Y. Hepatocyte growth factor attenuates liver fibrosis induced by bile duct ligation. Am J Pathol. 2006 May;168(5):1500-12.

Xie Q, Liu KD, HU MY, Zhou K. SF/HGF-c-Met autocrine and paracrine promote metastasis of hepatocellular carcinoma. World J Gastroenterol. 2001 Dec;7(6):816-20.

Xu L, Li J, Kuang Z, Kuang Y, Wu H. Knockdown of Gab1 Inhibits Cellular Proliferation, Migration, and Invasion in Human Oral Squamous Carcinoma Cells. Oncol Res. 2018 May 7;26(4):617-624.

Yang Y, Yang F, Wu X, Lv X, Li J. EPAC activation inhibits acetaldehyde-induced activation and proliferation of hepatic stellate cell via Rap1. Can J Physiol Pharmacol. 2016 May;94(5):498-507.

Yart A, Mayeux P, Raynal P. Gab1, SHP-2 and other novel regulators of Ras: targets for anticancer drug discovery? Curr Cancer Drug Targets. 2003 Jun;3(3):177-92.

Yin Z, Dong C, Jiang K, Xu Z, Li R, Guo K, et al. Heterogeneity of cancer-associated fibroblasts and roles in the progression, prognosis, and therapy of hepatocellular carcinoma. J Hematol Oncol. 2019 Sep 23;12(1):101.

Yip YP, Thomas T, Voss AK, Yip JW. Migration of sympathetic preganglionic neurons in the spinal cord of a C3G-deficient mouse suggests that C3G acts in the reelin signaling pathway. J Comp Neurol. 2012 Oct 1;520(14):3194-202.

Yokote K, Hellman U, Ekman S, Saito Y, Rönnstrand L, Saito Y, et al. Identification of Tyr-762 in the platelet-derived growth factor alpha-receptor as the binding site for Crk proteins.

Yokoyama U, Patel HH, Lai NC, Aroonsakool N, Roth DM, Insel PA. The cyclic AMP effector Epac integrates pro- and anti-fibrotic signals. Proc Natl Acad Sci U S A. 2008 Apr 29;105(17):6386-91

York RD, Yao H, Dillon T, Ellig CL, Eckert SP, McCleskey EW, et al. Rap1 mediates sustained MAP kinase activation induced by nerve growth factor. Nature. 1998 Apr 9;392(6676):622-6.

You H, Ding W, Dang H, Jiang Y, Rountree CB. c-Met represents a potential therapeutic target for personalized treatment in hepatocellular carcinoma. Hepatology. 2011 Sep 2;54(3):879-89.

Zarnegar R. Regulation of HGF and HGFR gene expression. EXS. 1995;74:33-49.

Zeisberg M, and Neilson EG. Biomarkers for epithelial-mesenchymal transitions. J Clin Invest. 2009 Jun;119(6):1429-37.

Zhai B, Huo H, Liao K. C3G, a guanine nucleotide exchange factor bound to adapter molecule c-Crk, has two alternative splicing forms. Biochem Biophys Res Commun. 2001 Aug 10;286(1):61-6.

Zhang YW and Vande Woude GF. HGF/SF-met signaling in the control of branching morphogenesis and invasion. J Cell Biochem. 2003 Feb1;88(2):408-17.

Zhang L, Duan HB, Yang YS. Knockdown of Rap2B Inhibits the Proliferation and Invasion in Hepatocellular Carcinoma Cells. Oncol Res. 2017 Jan 2;25(1):19-27.

Zhao W, Zhang L, Xu Y, Zhang Z, Ren G, Tang K, et al. Hepatic stellate cells promote tumor progression by enhancement of immunosuppressive cells in an orthotopic liver tumor mouse model. Lab Invest. 2014 Feb;94(2):182-91.

Zhao Y, He D, Stern R, Usatyuk PV, Spannhake EW, Salgia R, et al. Lysophosphatidic acid modulates c-Met redistribution and hepatocyte growth factor/c-Met signaling in human bronchial epithelial cells through PKC delta and E-cadherin. Cell Signal. 2007 Nov;19(11):2329-38.

Zheng G, Ma Y, Zou Y, Yin A, Li W, Dong D. HCMDB: the human cancer metastasis database. Nucleic Acids Res. 2018 Jan 4;46(D1):D950-D955.

Zheng LY1, Zhou DX, Lu J, Zhang WJ, Zou DJ. Down-regulated expression of the protein-tyrosine phosphatase 1B (PTP1B) is associated with aggressive clinicopathologic features and poor prognosis in hepatocellular carcinoma. Biochem Biophys Res Commun. 2012 Apr 13;420(3):680-4.

Zhuang PY, Shen J, Zhu XD, Zhang JB, Tang ZY, Qin LX, et al. Direct transformation of lung microenvironment by interferon-α treatment counteracts growth of lung metastasis of hepatocellular carcinoma. PLoS One. 2013;8(3):e58913.

Zihni C, Mills C, Matter K, Balda MS. Tight junctions: from simple barriers to multifunctional molecular gates. Nat Rev Mol Cell Biol. 2016 Sep;17(9):564-80.

Zucman-Rossi J, Villanueva A, Nault JC, Llovet JM. Genetic Landscape and Biomarkers of Hepatocellular Carcinoma. Gastroenterology. 2015 Oct;149(5):1226-1239.e4.

Zuluaga S, Alvarez-Barrientos A, Gutierrez-Uzquiza A, Benito M, Nebreda AR and Porras A. Negative regulation of Akt activity by p38alpha MAP kinase in cardiomyocytes involves membrane localization of PP2A through interaction with caveolin-1. Cell Signal 2007;19(1): 62-74.

Zuluaga S, Gutierrez-Uzquiza A, Bragado P, Alvarez-Barrientos A, Benito M, Nebreda AR et al. p38alpha MAPK can positively or negatively regulate Rac-1 activity depending on the presence of serum. FEBS Lett 2007;581(20): 3819-3825.

13. APPENDIX

Review

For reprint orders, please contact: reprints@futuremedicine.com

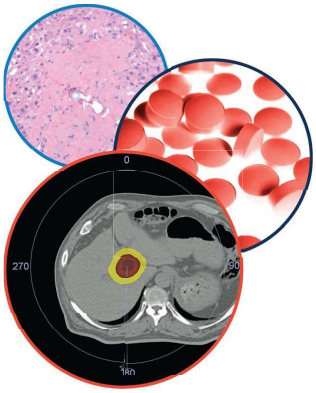

Hepatic Oncology

How Rap and its GEFs control liver physiology and cancer development. C3G alterations in human hepatocarcinoma

Celia Sequera*[,1,2], Sara Manzano[1,2], Carmen Guerrero[3,4,5] & Almudena Porras**[,1,2]

[1]Departamento de Bioquímica y Biología Molecular, Facultad de Farmacia, Universidad Complutense de Madrid, Madrid, Spain
[2]Instituto de Investigación Sanitaria del Hospital Clínico San Carlos (IdISSC), Madrid, Spain
[3]Instituto de Biología Molecular y Celular del Cáncer, USAL-CSIC, Salamanca, Spain
[4]Instituto de Investigación Biomédica de Salamanca (IBSAL), Salamanca, Spain
[5]Departamento de Medicina, Universidad de Salamanca, Salamanca, Spain
*Author for correspondence: Tel.: +34 913941785; celiasequera@ucm.es
**Author for correspondence: Tel.: +34 913941627; maporras@ucm.es

Rap proteins regulate liver physiopathology. For example, Rap2B promotes hepatocarcinoma (HCC) growth, while Rap1 might play a dual role. The RapGEF, Epac1, activates Rap upon cAMP binding, regulating metabolism, survival, and liver regeneration. A liver specific Epac2 isoform lacking cAMP-binding domain also activates Rap1, promoting fibrosis in alcoholic liver disease. C3G (RapGEF1) is also present in the liver, but mainly as shorter isoforms. Its function in the liver remains unknown. Information from different public genetic databases revealed that C3G mRNA levels increase in HCC, although they decrease in metastatic stages. In addition, several mutations in RapGEF1 gene are present, associated with a reduced patient survival. Based on this, C3G might represent a new HCC diagnostic and prognostic marker, and a therapeutic target.

First draft submitted: 19 December 2017; Accepted for publication: 20 March 2018; Published online: 16 April 2018

Keywords: C3G • Epac • hepatocarcinoma • liver • liver diseases • Rap

Rap & C3G

Rap is a member of the Ras family of small GTPases, with five different isoforms: Rap1A, Rap1B, Rap2A, Rap2B and Rap2C expressed in mammalian cells [1]. Rap proteins play a relevant role in cell adhesion [2,3], junction formation [4–6], migration, invasion [7], cell polarity [8,9], exocytosis [10], apoptosis [11] and proliferation [12]. As a consequence, they are important for carcinogenesis [13,14] and cardiovascular function [15]. Rap switches from an inactive conformation, bound to GDP, to an active conformation, bound to GTP. This activation is regulated by different GEFs that mediate the dissociation of GDP from Rap, favoring the binding of GTP, which is much more abundant than GDP within the cell. On the other hand, GAPs activate Rap GTPase activity, promoting GTP hydrolysis leading to the inactive, GDP-bound, form [1]. Therefore, the activation and inactivation of Rap proteins by specific GEFs and GAPs regulates the duration of Rap activation and its localization (Figure 1).

The main GEF for Rap1 is C3G, also known as RapGEF1 [2]. C3G is a 140 kDa protein, although several other isoforms, generated by alternative splicing, has been described in human and other species [16]. In particular, a truncated isoform, called p87C3G, that lacks the first 305 amino acids from the N-terminus, has been associated with myeloid leukemia [17]. C3G structure is composed by three well differentiated modules. A GEF-catalytic unit at the C-terminal region that includes the Ras exchange motif domain and a Cdc25 homologous domain [16]. A central proline rich (or SH3-binding) domain that interacts with SH3 domains from other proteins, such as Crk, p130Cas, Grb2, c-Abl or Hck, and harbors a tyrosine residue (Tyr504) susceptible of being phosphorylated by different kinases, leading to C3G activation [18]. Finally, an N-terminal region with an E-cadherin binding domain, which negatively regulates the GEF activity (Figure 2B) [6,19]. C3G is ubiquitously expressed, although there are some tissue-specific differences. In humans, C3G levels are higher in adult skeletal muscle, brain, heart, kidney,

Future Medicine